Summer 2019

LIMITATIONS TO PHOTOSYNTHESIS IN SILVER BOW AND BLACKTAIL CREEKS

Isaiah Robertson

LIMITATIONS TO PHOTOSYNTHESIS IN SILVER BOW AND BLACKTAIL CREEKS

by

Isaiah James Robertson

A thesis submitted in partial fulfillment of the

requirements for the degree of

Master of Science Geoscience

Geochemistry Option

Montana Tech

2019

Abstract

Throughout Silver Bow Creek's history, consideration of the photosynthetic communities that make heterotrophic life possible have often been overlooked since macroinvertebrates made up a majority of ecosystem health assessments. Silver Bow Creek has had minimal biological research outside of macroinvertebrate surveys, especially as it pertains to photosynthetic organisms. This study assessed the photosynthetic communities of Silver Bow Creek and their limitations by limiting available light and comparing uptake of nutrients during a 23-day incubation experiment conducted at four sites along the flow of Silver Bow Creek and Blacktail Creek. At each site, nine one-liter microcosms, filled with creek water and divided evenly into three acrylic boxes, remained in the creek for 23 days. One of the boxes allowed 100% transmittance of visible light. The other two boxes restricted visible light to 54% transmittance and 6% transmittance. The boxes incubated in the creek for 23 days with samples withdrawn periodically to monitor for extracted chlorophyll *a*. Analysis of major anions and cations at the beginning and end of the experiment showed typical nutrient uptake. Despite anticipated light limitations, nutrient limitations, specifically phosphorus, had a stronger impact on total photosynthetic growth. Light did not limit total chlorophyll growth, instead light limited the chlorophyll growth rate. Together light and phosphorus created a biochemically dependent colimitation. At Slag Canyon, severe light limitation prevented oxygenation of microcosms and chemoautotrophic metabolisms took over reducing nitrate and sulfate. This experiment concluded that in Sliver Bow and Blacktail Creeks, light limited the primary production growth rate and phosphorus limited total possible photosynthesis.

Keywords: Colimitation, biogeochemistry, light, light exclusion, nutrients, phosphorus, nitrogen, microbial processes, nitrate reduction, sulfate reduction

Dedication

To my first teachers, my associate engineer, and my editor-in-chief. To my parents Todd and Sally. I wouldn't be here if it weren't for you.

Acknowledgments

Table of Contents

List of Tables

List of Figures

List of Equations

Glossary of Abbreviations

Abbreviation	Definition
BTC	Blacktail Creek
IC	Ion chromatography
ICP-MS	Inductively coupled plasma-mass spectrometry
ICP-OES	Inductively coupled plasma-optical emission spectrometry
LEGEND	Laboratory Exploring Geobiochemical Engineering and Natural Dynamics
MBMG	Montana Bureau of Mines and Geology
PAR	Photosynthetically available radiation
SBC	Silver Bow Creek

1. Introduction

Photosynthesis provides heterotrophic life on Earth with carbon dioxide uptake and oxygen production (Oakes, 2018). Furthermore, most of the Earth's known ecosystems depend on primary producers for conversion of energy and inorganic nutrients (Christian et al., 1995). Without photosynthetic autotrophs, the higher trophic life humans rely on for food and recreation could not exist, yet when they become too numerous, these autotrophs can cripple the very ecosystems they once sustained (Ansari et al., 2011). As a body of water ages, it naturally accumulates nutrients, and plant and algal life expand in a process known as eutrophication (Ansari et al., 2011). When eutrophication becomes extreme, it can often cause toxic algal blooms and hypoxic zones, with significant impacts on drinking water and recreation (McLellan et al., 2015; Wolf et al., 2017). Such extremes usually only happen after humans have accelerated this process with nutrient pollution, and as improvements have been made to control point source pollutants, such as municipal wastewater, management processes shifted to address more diffuse pollution sources (Sas, 1989; Thornton et al., 1999). This shift created a need to explore new creative methods of management, in part controls and limitations to photosynthetic organisms.

Like all chemical reactions, the least available reactant limits photosynthesis. At its most fundamental level photosynthesis follows the reaction outlined in equation one, and must be limited by water, carbon dioxide, or light (Eq. 1). Since carbon dioxide concentrations in Earth's atmosphere increase continuously, carbon dioxide limitations become unlikely (Lemon, 2018). Water limitation is a possibility in ephemeral streams, but when continuously inundated with water, an aquatic ecosystem will not show a water limitation, leaving light as the most plausible limiting reactant (Lawlor, 2002). Yet, this reaction does not occur spontaneously in the

environment, instead it requires organisms that possess photosystems that facilitate the reaction. Such organisms and photosystems often have other physical and chemical limitations. For instance, nucleic acids, membranes, and ATP species require phosphorus as a major structural element, and the many proteins utilized by these organisms require nitrogen. Collectively, these biomolecules make up the photosystems, organelles, and organisms that facilitate photosynthesis (O'Kelley, 1968). Although more than a dozen essential elements exist for primary producers, nitrogen and phosphorus typically cause nutrient limitations in surface waters, making light, nitrogen, and phosphorus the most anticipated limitations to photosynthetic communities (O'Kelley, 1968).

Photosynthesis
$$H_2O + CO_2 + Light \rightarrow O_2 + CH_2O$$

$$(1)$$
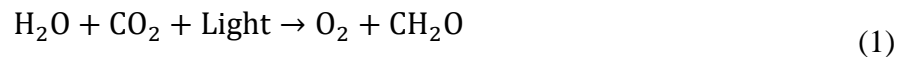
Blacktail Creek (BTC) and Silver Bow Creek (SBC) flow through the city of Butte, Montana, until SBC flows through the Warm Spring Ponds to form the headwaters for the Clark Fork River. Such headwater streams form the catchments that influence the larger rivers, lakes, and oceans throughout a watershed, and failure to control eutrophication within watersheds creates hypoxic or dead zones like that in the Gulf of Mexico (McLellan et al., 2015). Butte has a history of mining over 150 years old, and throughout that time numerous mining companies heavily manipulated SBC to accommodate mining needs (Gammons and Madison, 2006). Additionally, BTC and SBC served as the primary method for removing mining and municipal wastes from the Butte area, and poorly managed mining wastes and regular flooding of the creek ultimately led to the 1995 decision to remediate the stream banks as a US Superfund Site (DEQ and EPA, 1995; Gammons and Madison, 2006). Subsequent efforts to restore the creek banks have begun to shape portions the creek into a healthier environment (NRDP, 2005; EPA, 2011).

SBC and BTC provide an environment bearing many opportunities for unique limitations to photosynthesis. In rocky, low-order, headwater streams, such as BTC and SBC, plants and benthic algae dominate primary production, and any planktonic algae present are likely to have been scoured from the benthos and can be 50% or more diatoms (Wehr and Sheath, 2003). Nutrients usually cause the most predominant limitations to these communities in fresh water, with phosphorus and/or nitrogen limiting most surface waters (Sanches et al., 2010). In small to medium sized headwater streams, however, light is often one of the most limiting factors due to stream bed shading from plant growth in the riparian zone, and this limitation often surpasses that of nutrients (Hill, 1996; Hutchin et al., 2010). The restoration efforts in the creek banks have altered the riparian communities and therefore the shading to the stream bed (NRDP, 2005; EPA, 2011). Furthermore, many metals still contaminate the creeks with arsenic, cadmium, lead, iron, mercury, and zinc generating the most concern (EPA, 2018). Although all heavy metals have a certain degree of lethality and are known to limit photosynthetic growth, copper is a known algicide, and cadmium is lethal to most life, and both present possible limitations to photosynthesis (Adamson and Sommerfeld, 1980; Cox. 2011; Dao and Beardall, 2016). Many factors control the limits of photosynthetic communities including temperature, pH, and the availability of light and nutrients, all of which have been altered in the creeks by restoration efforts (Stevenson, 1996; EPA, 2011). Human influences can affect these variables and occurrence of the fundamental process of photosynthesis (Cox, 2011). Therefore, due to a combination of pollutants and restoration efforts, SBC and BTC present an environment with the potential for unique limitations to photosynthesis.

Historically, SBC and BTC have had similar geochemistry to other creeks with a few notable, mining-related exceptions (Stumm and Morgan, 1996; Langmuir, 1997; Plumb 2009).

SBC and BTC showed some mining-related damages and had a lower pH than most creeks (Stumm and Morgan, 1996; Langmuir, 1997; Plumb 2009). Similarly, metals, particularly magnesium, copper, and zinc, have been elevated in SBC and BTC sometimes as much as five times mean creek water (Stumm and Morgan, 1996; Langmuir, 1997; Plumb 2009). Despite these noticeable damages, dissolved oxygen, temperature, and dissolved silicon in SBC and BTC have been consistent with a typical creek (Stumm and Morgan, 1996; Langmuir, 1997; Plumb 2009). Historically BTC differs from a typical creek since it is likely limited by nitrogen rather than phosphorus, but SBC is typical in this regard (Stumm and Morgan, 1996; Plumb 2009). Many of the atypical parameters, such as elevated metals and decreased pH, have shown "significant improvement" with recent restoration efforts (EPA, 2011). More recent historical data from the Laboratory Exploring Geobiochemical Engineering and Natural Dynamics (LEGEND) also show some improvement to fundamental parameters in the creeks.

SBC and BTC received a typical amount of light. Photosynthetically available radiation (PAR), a measure of light, typically varies from tens to hundreds of micromoles of photons per square meter per second. Since this is an average number, Oakland National Laboratories controls an indoor simulated stream at PAR at 110 μmols photons m^{-2} sec^{-1} (Hill et al., 2011). Light varies greatly with time of day latitude, cloud cover, and water surface making PAR a difficult parameter to accurately characterize. Studies from this stream showed changes in benthic primary producers with light and are useful because they used similar values to those found in BTC and SBC (Hill et al., 2011).

Since the 1950s culturing has been taken into the field in the form of *in situ* bottle incubations (Neilsen, 1952). Such bottle experiments have led to the discovery of new species of algae and provided further insights into the water column of aqueous environments (Johnson and

Seiburth, 1979; Waterbury, 1979; Cushing and Horwood, 1998). Bottle experiments have been primarily used to observe planktonic algae as these experiments allow a single unit of water to be repeatedly sampled without any unplanned additions while maintaining consistent temperature and light exposure to the natural condition, allowing resulting changes in community and chemistry (Nielsen 1952; Cushing and Horwood, 1998). Bottle incubation experiments have typically been used in ocean and lake environments with very few riverine experiments.

Bottle experiments often reveal metabolism that cannot be abundantly observed in the environment (Cushing and Horwood, 1998). Since nitrate and sulfate reduction are not thermodynamically favorable metabolisms in oxygenated waters, such metabolism cannot be found in typical creek waters (Grundl et al., 2011). Finding such metabolisms in SBC and BTC contribute to the unique potential in these creeks.

Mining related metal contamination in SBC has forced remediation efforts to focus on metal concentrations leaving the microbial and photosynthetic communities of SBC and BTC understudied. While a plethora of unique limitations to such communities may occur, a fundamental understanding of the basic nutrient and light limitations must first be established. Restoration efforts on the banks of SBC have left it with a diversity of riparian regimens allowing the streambed varying light access at different sites. Light is a predominant limit on photosynthesis, and likely affects the photosynthetic intensity down the stream path (Roberts et al., 2004; EPA, 2011). Wastewater treatment and discharge of storm waters have altered the nutrient regimens within SBC creating further enhancement to photosynthetic communities (Plumb, 2009). Nitrogen and phosphorus often have limiting effects if light is saturated (Konopka, 1983).

This study set out to characterize what limits photosynthetic communities in Silver Bow and Blacktail Creeks. Dissolved chemistry – major cations, major anions, and trace elements – analyzed before and after this bottle experiment, provided an understanding of how photosynthetic organisms interact with the geochemistry and helped discern which of the many essential nutrients limit photosynthetic communities. Chlorophyll *a* concentrations analyzed throughout the experiment provided insight into how light and geochemistry affect photosynthetic growth. We hypothesized that reductions in photosynthetic growth would correlate with an increase in light exclusion, and light limitation would exceed any nutrient limitations by prohibiting full nutrient use. If a nutrient limitation limited photosynthetic growth, phosphorus would be the limiting nutrient.

2. Methods

An *in situ* incubation, light exclusion bottle experiment was conducted at four locations in SBC and BTC from August 16th to September 8th, 2018. Samples for dissolved chemistry were taken at the beginning and end of the experiment. Filters extracted for chlorophyll *a* were collected nine times throughout the experiment according to an escalating schedule designed to capture the most rapid growth periods (Appendix A). A lotic plant survey was also conducted at all four sites in the weeks leading up to the experiment (Appendix D).

2.1.   Study Area

Blacktail Creek and Silver Bow Creek are two streams located near Butte, Montana in the northwest United States. BTC originates in the Beaverhead-Deerlodge National Forest and runs through Thompson Park into the city of Butte where it joins SBC. In the mid-1950s, mining in the Berkley Pit cut off SBC. Now SBC starts as an ephemeral stream, and its irregular flow is made up of municipal, residential, and industrial drainage rather than waters drained from heavily forested land. Once SBC is joined by BTC, near the center of Butte, it becomes a perennial stream. Two sample sites were selected from each creek and unofficially named Thompson, KOA, Slag Canyon, and Santa (Fig. 1). These sites have been sampled every three months by the Laboratory Exploring Geobiochemical Engineering and Natural Dynamics (LEGEND) since 2015 and unpublished data from LEGEND provides context to this study. Sites were selected to represent a gradient of available light and account for the state of the creek above, below, and throughout the city of Butte.

Nitrogen and phosphorus often limit growth in an ecosystem. Although it is difficult to determine actual limitation without experimentation, since 1958 the Redfield ratio has proved useful in predicting nutrient limitations based on available nutrient concentrations (Redfield,

1958; Schindler, 1974). The Redfield ratio outlines the rate that phytoplankton utilize carbon and nitrogen relative to phosphorus – 106 moles of carbon to 16 moles nitrogen to every mole of phosphorus (Redfield, 1958). Consequently, a limiting nutrient can be predicted by comparing the ratio of available nitrogen to available phosphorus present in an ecosystem to the Redfield Ratio (Fig. 2).

Thompson, the furthest upstream site, is situated within Thompson Park and serves as a control above major residential and mining influences (Fig. 1a). Thompson is situated in a mountain valley where dense tree and shrub riparian cover shade most of the light from the creek bed. These conditions cause Thompson to be the coldest site with the lowest specific conductivity and dissolved ion concentrations (Figs. 3,4). In addition, Thompson has the highest pH and dissolved oxygen of all sampled sites (Figs. 5,6). If a nutrient is limiting growth, nitrogen likely would be limiting (Fig. 2).

KOA is located within the city of Butte just before BTC joins SBC. Its riparian zone contains forbs and various willows (*Salix spp.*) providing sparse cover, and the wider stream channel allows more light access to the streambed (Fig. 1b). Increased light access made KOA one of the warmest sites, up to 15 °C (Fig. 3). It also had moderate dissolved ions with conductivity and dissolved oxygen generally falling in the middle of the sample sites (Figs. 4,6). Also, KOA had a pH that is often the nearest neutral of all the sample sites (Fig. 5). The expected nutrient limitation would be phosphorus (Fig. 2).

Slag Canyon is also located in the city of Butte just after BTC joins SBC and had similar chemistry to KOA The most significant differences between Slag Canyon and KOA are the Montana street bridge, three-meter slag walls, and various trees and shrubs that dominate the riparian zones at Slag Canyon (Fig. 1c) (Kaplan, 2016). Combined, the bridge, slag walls, and

numerous plants provided significant creek bed shading and made it a slightly cooler site, only

reaching 13 °C during the study period (Fig. 1,3). Similar to KOA, Slag Canyon had a middle

Figure 1: Sample Site Map. (a) Thompson, (b) KOA, (c) Slag Canyon, and (d) Santa.
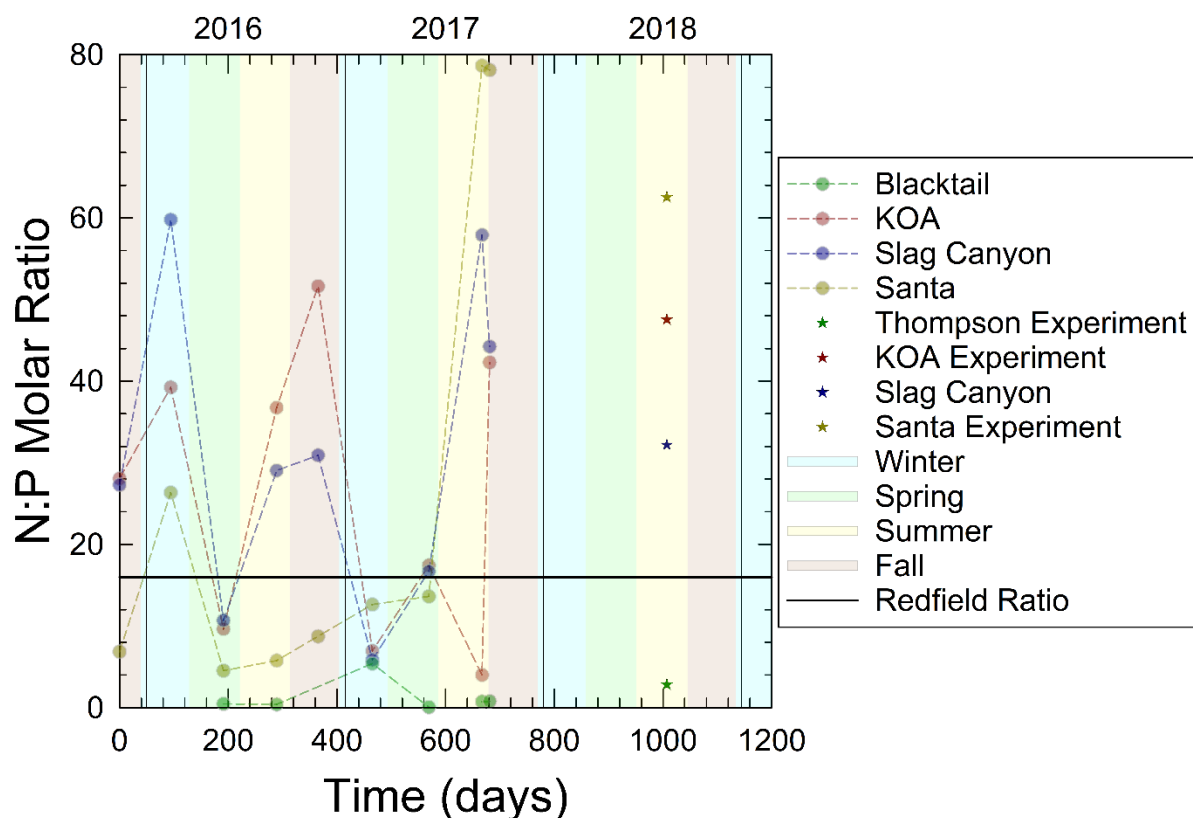
Figure 2: Historical dissolved phosphate and nitrate, both analyzed by IC (Cox et al., unpublished). Points below the Redfield ratio line are likely limited by nitrogen, whereas those above the line are likely limited by phosphorus. Instrumental error is within symbol size.

range conductivity, dissolved oxygen, and pH, although pH was usually slightly higher than

KOA at Slag Canyon (Figs. 4,5,6). In the event of nutrient limitation, phosphorus would likely

limit growth at Slag Canyon (Fig. 2).

Santa is located just outside of the Butte city limits and runs through a constructed sedge

Meadow (Fig. 1d). Here the riparian zone is dominated by sandbar willows (*Salix exigua*), and

once again demonstrates a wider stream channel providing little shading to the stream bed. This

made Santa the warmest site studied, reaching temperatures as high 17 °C (Fig. 3). Even though,

historically, KOA was warmer than Santa, more often Santa was warmer than KOA (Fig. 3).

Santa generally has a higher pH and conductivity likely from the Lower Area One Treatment

Plant, which is just over a kilometer upstream (Figs. 4,5). Similarly, Santa often had the highest

dissolved oxygen of all sample sites (Fig. 6). Historically, nutrient limitations at Santa could

have been from nitrogen or phosphorus (Fig. 2). Most recently, this site has most likely been

limited by phosphorus (Fig. 2).

2.1. *In Situ* Incubation Experiment

The *in situ* incubation experiment took place in late summer – August-September

– 2018 and lasted 23 days. Boxes were constructed of one quarter inch acrylic (Midland Plastics,

New Berlin, Wisconsin, USA) and designed to hold three one-liter polycarbonate bottles (Fisher

Scientific), as well as allow water to freely flow through the boxes (Appendix C). Two boxes for

each site were then tinted with window film (Buy Decorative Film, Buena Park, California,

USA), one to 6% visible light transmittance, and one to 54% visible light transmittance, and one

box at each site was left clear for 100% visible light transmittance (Appendix C).
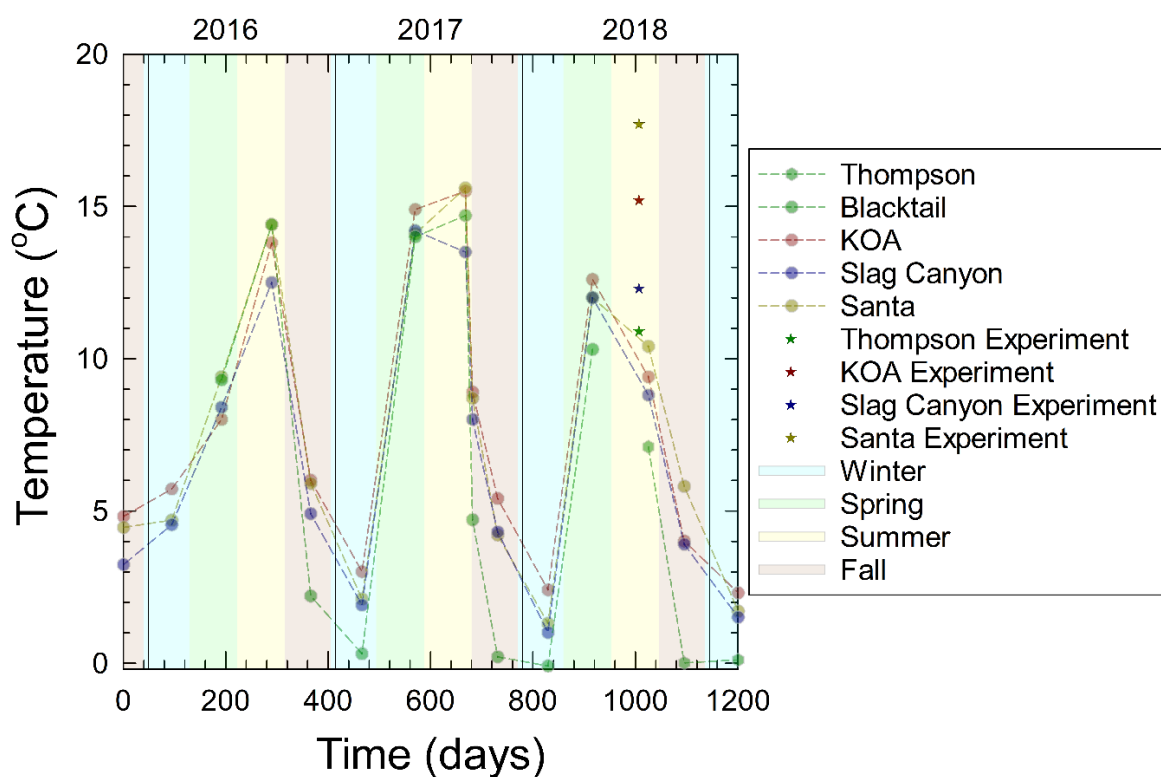
Figure 3: Historical temperature in creeks (Cox et al., unpublished). Stars indicate experiment. Error, variation in meter readings, is within symbol size.
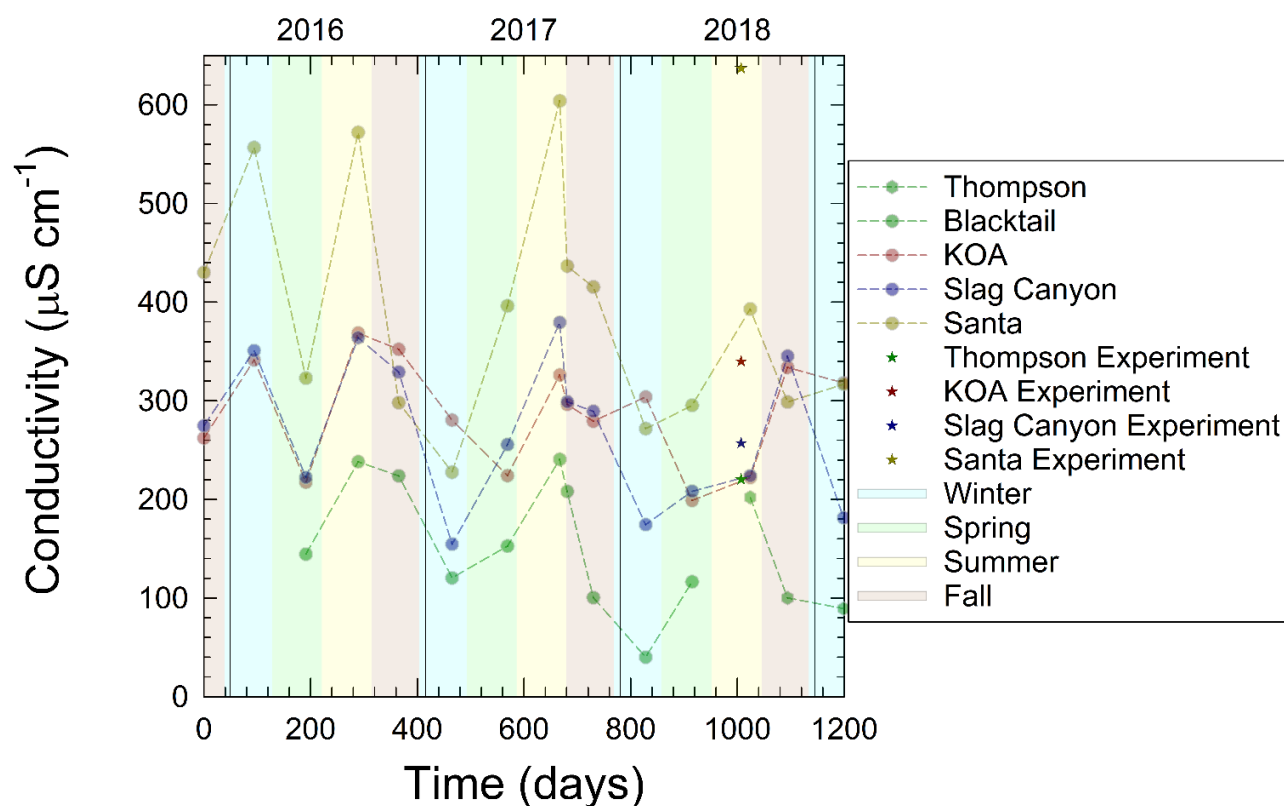
Figure 4: Historical conductivity in creeks (Cox et al., unpublished). Stars indicate experiment starting time. Error, variation in meter readings, is within symbol size.

Microcosms were created from new, clear, trace metal cleaned, one-liter polycarbonate bottles. Trace metal cleaned indicates three rinses of 18.2 MΩ-cm water (Q water) before soaking in 1% citranox (Alconox Inc, White Plains, New York, USA) for six days, three upright and three inverted. The bottles then received seven additional Q water rinses and soaked in pH zero trace metal grade hydrochloric acid (JT Baker, Center Valley, Pennsylvania, USA) for six days, three upright and three inverted. The bottles received another seven Q water rinses, and soaked for six days, three upright and three inverted, in pH two trace metal grade hydrochloric acid. Finally, the bottles received a final seven Q water rinses (Law, 2018).

A five-gallon bucket was rinsed with pH zero hydrochloric acid, then rinsed seven times with Q water. Upon deployment, a five-gallon grab sample was taken at each sample site, after rinsing the bucket with 70% ethanol, and then rinsed three times with sample water, and partitioned into nine microcosms which were fastened into one box of each light treatment. The microcosms were numbered one through three in each box starting with microcosm one at the most upstream position. The boxes were then staked into the creek bed.

The microcosms incubated in the creek for 23 days. This time frame was chosen after a 500 mL microcosm was staked to the bottom of the creek and observed visually for two weeks. No further growth occurred after two weeks. Throughout the experiment, samples were taken on days zero – the same day as deployment – four, twelve, fifteen, eighteen, twenty, twenty-one, and twenty-three. This plan was developed to ensure the most frequent sampling occurred during
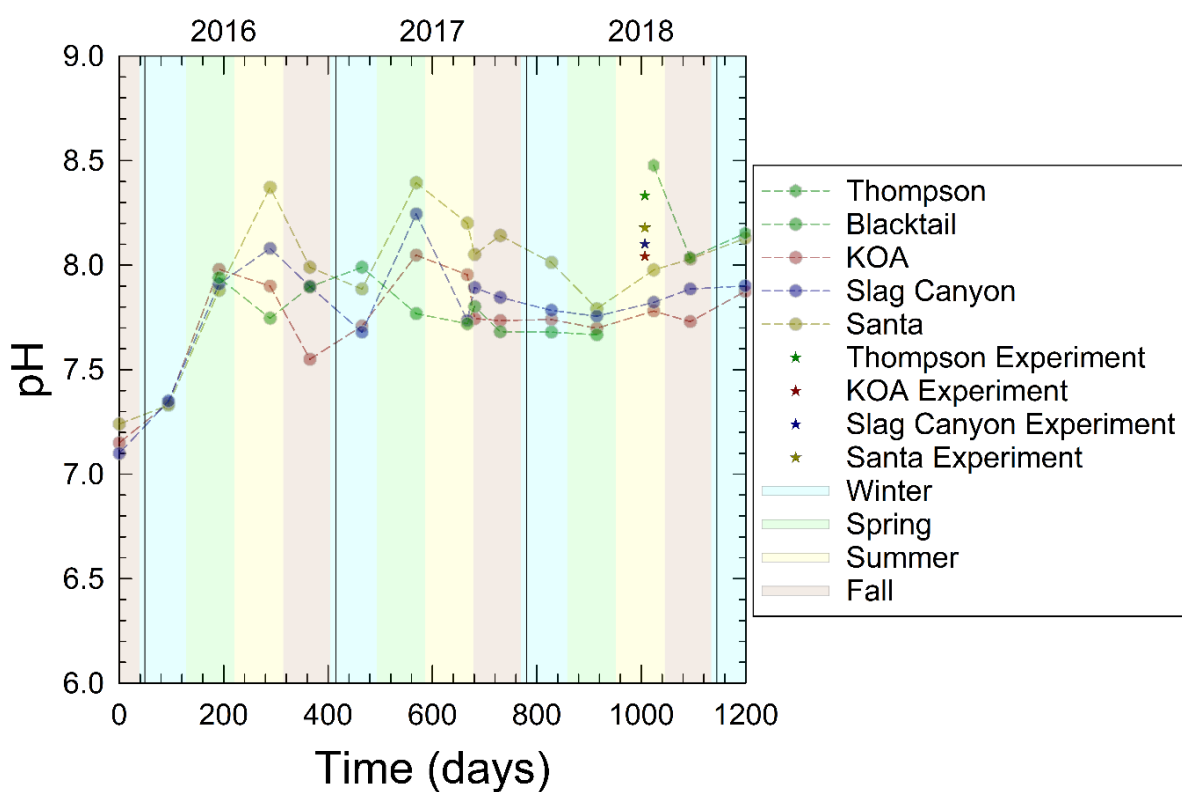
Figure 5: Historical pH in creeks (Cox et al., unpublished). Stars indicate experiment starting time. Error, variation in meter readings, is within symbol size.
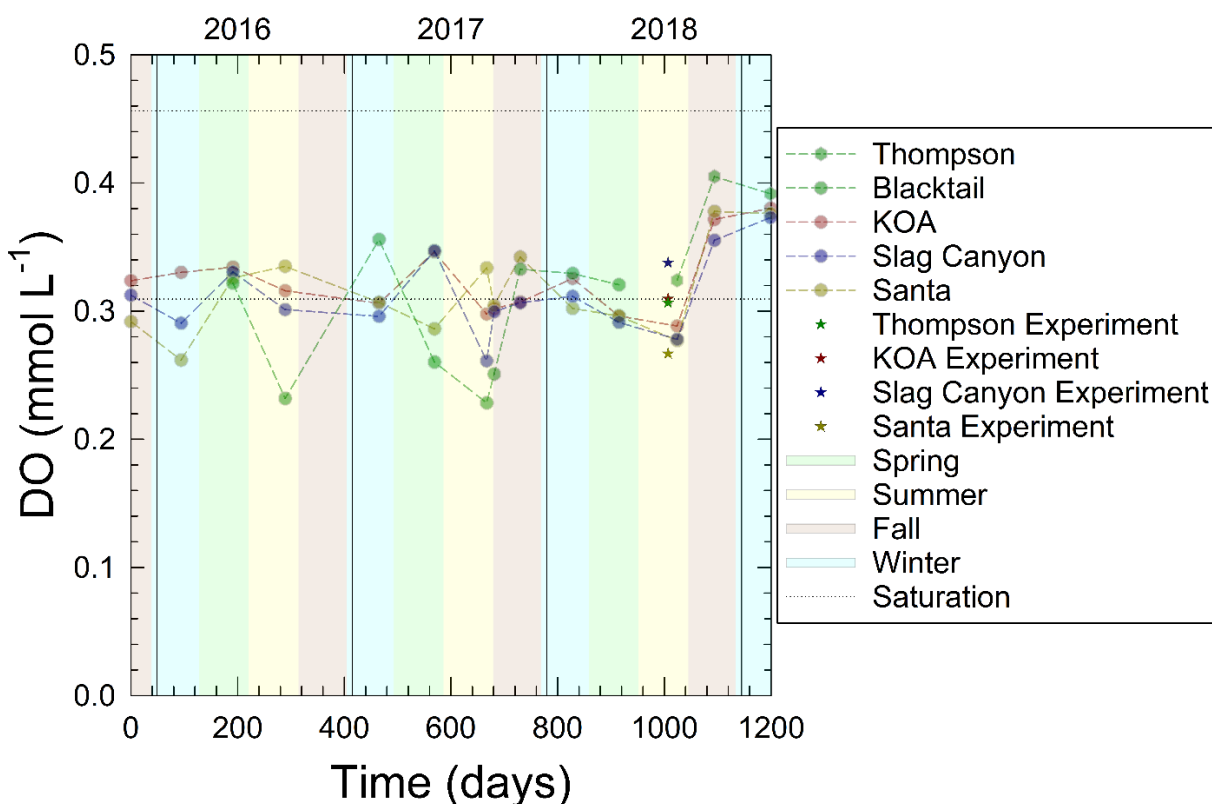
Figure 6: Historical dissolved oxygen in creeks (Cox et al., unpublished). Stars indicate experiment starting time. Saturation calculated for highest and lowest temperatures plotted. Error, variation in meter readings, is within symbol size.

the most rapid growth period. Microcosms remained sealed in the creek and were briefly

exposed to atmospheric gasses during sampling.

2.2. Dissolved Chemistry

Upon deployment and withdrawal, water was filtered across 25mm, 1.2 and 0.8/0.2 μm

polyethersulfone syringe filters (Acrodisc, vwr.com) and collected for major anions, major

cations, and metals. All sample were stored in trace metal clean 30 mL high-density polyethylene

(HDPE) Nalgene bottles (Law, 2018). The filtration apparatus that consisted of a 1 L HDPE

Nalgene bottle, a 140 mL polypropylene syringe, a polycarbonate stop cock, and Tygon tubing

were also cleaned with this method (Law, 2018). Bottles to be analyzed for trace elements were

pre-acidified with 300 μL trace metal grade concentrated nitric acid (Fisher Scientific). Samples

for major cations (Li^+, Na^+, K^+, Ca^{+2}, Mg^{+2}, and Si^{+4}) were frozen until analyzed by the Montana

Bureau of Mines and Geology (MBMG) on a Thermo Scientific iCAP 6000 Series inductively

coupled plasma optical emission spectrometer (ICP-OES) using EPA method 200.7 (Law, 2018).

Prior to analysis, major cation samples were thawed and acidified with extra pure,

methanesulfonic acid (MSA) (Acros Organics, New Jersey, USA) (St. Clair et al., 2019). Major

cations generally had measurable micromolal concentrations with errors ranging from 1.1% to

7.6%. Major anions (F^-, Cl^-, NO_2^-, NO_3^-, Br^-, PO_4^{-3}, SO_4^{-2}) were also stored frozen until analyzed

by the MBMG on a Metrohm Compact Ion Chromatograph (IC) Plus using EPA method 300.1

(Schmidt, 2017). Major anions also had micromolal concentrations. Major anions had errors

from 1.7% to 5.8%. Samples for trace elements (Be, B, Al, Ti, V, Cr, Mn, Fe, Co, Ni, Cu, Zn,

Ga, As, Se, Rb, Sr, Zr, Nb, Mo, Pd, Ag, Cd, Sn, Sb, Cs, Ba, La, Ce, Pr, Nd, W, Tl, Pb, Th, and

U) were kept at room temperature until analyzed by the MBMG on a Thermo Scientific iCAP Q

inductively coupled plasma-mass spectrometer (ICP-MS) by EPA method 200.8 (Dahlquist,

2017). Metals were present at nanomolal and low micromolal concentrations with errors from

0.9% to 5.7%. Samples were run from the middle microcosm, bottle two, in each box except in

one case in which the upstream microcosm was analyzed. Due to unexpected results from the

dark microcosms at Slag Canyon, all three replicates were analyzed.

2.3.   Field Parameters

On each sample day, including deployment and withdrawal, *in situ* parameters were

measured at each site. Temperature and pH were measured using a WTW pH 3110 meter

calibrated daily with pH 4, 7, and 10 buffers and error of $\pm$ 0.01. Conductivity and temperature

were measured using a YSI 30 meter that has an error of 0.5% for conductivity and 1% for temperature. PAR was measured with a LI-Cor LI1400 meter that had a typical error of 3%. Dissolved oxygen and temperature were measured with a PreSens Fibox 4 Trace meter with a detection limit of 0.94 µmol kg^{-1} and an error of 0.4%. For all meters, error was recorded as measurement variability at the time of reading if variability exceeded instrumental error. Due to limited amounts of water, pH was the only parameter measured at the end of the experiment and was measured in the major anion bottle after analysis.

2.4. Extracted Chlorophyll *a*

On each sample day, including withdrawal, samples were taken for in vitro chlorophyll *a* analysis. 80 milliliters of water were filtered across a 25 mm, 1.0 µm glass fiber filter (Pall Corp. New York City, New York, USA) and a 25mm, 0.2 µm nylon membrane filter (Advanced Microdevices PVT. LTD, Ambala Cantt, Haryana, India.). An inline filter setup was made with two single-stage 25 mm Teflon filter casings (Savillex, Corp. Eden Prairie, Minnesota, USA), thereby separating the majority of prokaryotic and eukaryotic organisms. 1.0 µm filters filter out the majority of diatoms, and 0.2 µm should remove most, other active life (Litchman et al., 2009). Filters were then frozen on dry ice for transport to storage at -80° C. Filters were extracted using the non-acidification method, an accepted modification to EPA Method 445.0 rev. 1.2. (Welschmeyer, 1994; Arar and Collins, 1997). Samples were stored at -80°C, and extracted with HPLC grade acetone (Fisher Chemical, Fair Lawn, NJ, USA) within 19 weeks of collection. Extracts were then analyzed on a TD Aquafluor (Turner Designs, Sunnyvale, CA, USA) configured for extracted chlorophyll *a* with 395/130 nm excitation filters and 685 nm emission filters. Growth rates were than calculated by taking the slope from the linear regression of the natural log of the growth portion of the chlorophyll *a* curve (Eq. 2).

Growth rate where g=growth rate, T=time, and chl a=chlorophyll *a* concentration

$$g = \frac{T + \ln(\text{chl a}_o)}{\ln(\text{chl a})}$$

(2)

3. Results

This experiment generated the following data. Field parameters characterized the environment for this experiment. Chlorophyll *a* concentrations analyzed provided a surrogate measurement for the growth and reproduction of photosynthetic organisms. Starting and ending chemistry showed changes in the water condition over 23 days. All raw data can be found in Appendix B.

3.1. Field Parameters

The field parameters measured at box deployment defined the water that went into the microcosms. Dissolved oxygen measured highest at Slag Canyon at 338 μmol L^{-1} and lowest at Santa at 267 μmol L^{-1} (Fig. 7a). Specific conductivity appeared highest at Santa at 637 μS cm^{-1}, the farthest downstream site, where it was nearly double the specific conductivity of all other sites (Fig. 7b); pH remained consistent for all sites ranging from 8.04 to 8.33 (Fig. 7c).

Unlike the other parameters, PAR defined the conditions of each treatment. PAR generally reflected the tinting of the boxes, with the light treatment PAR nearly identical to the site PAR, with each site ranging from 180 to 260 μE at the site and 220 to 590 μE in the clear boxes. Further tinting resulted in decreasing PAR with medium boxes ranging from 130 to 160 μE and dark boxes ranging from 20 to 340 μE (Fig. 8). The only exception to this occurred at the brightest site, KOA. Here the dark box appears brighter than the medium with PAR being 340 μE in the dark box's and 160 μE in the medium box.

3.2. Extracted Chlorophyll a

All four sites started with chlorophyll *a* concentrations around 1 μg L^{-1}, with the highest starting concentration of 1.6 μg L^{-1} at KOA and the lowest concentration of 0.5 μg L^{-1} at Thompson. The highest chlorophyll concentration of 157 μg L^{-1} occurred in the light microcosm
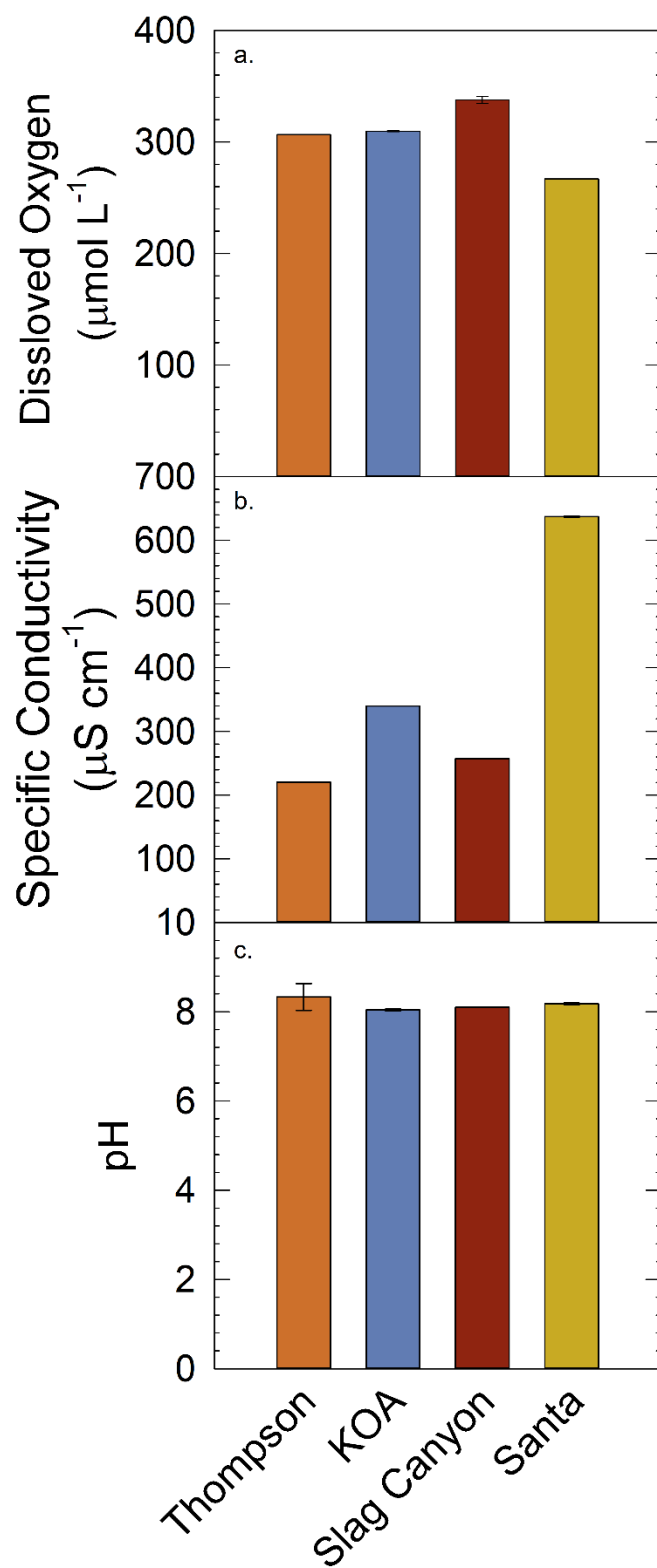
Figure 7: Field parameters. (a) Dissolved Oxygen, (b) Specific Conductivity, and (c) pH box deployment. Error bars shown as variability in meter readings.
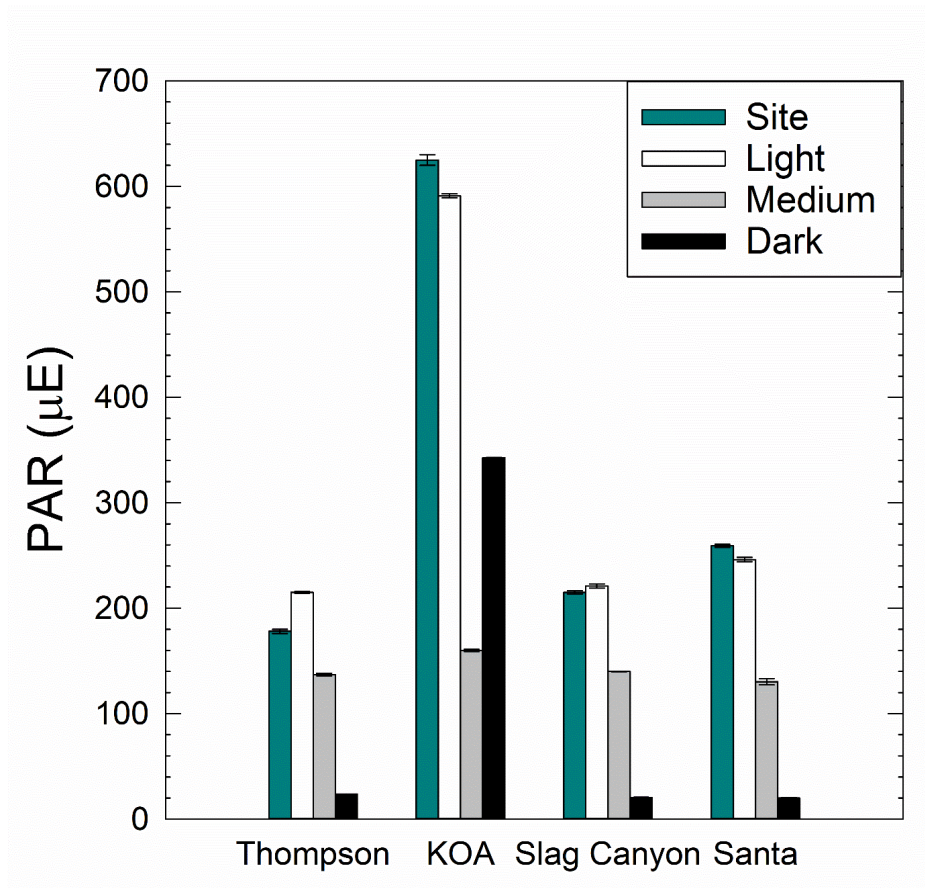
Figure 8: PAR at the streambed and under the tinted lid for each treatment. Error shown as variability in the meter reading.

at Slag Canyon and displayed a similar magnitude to medium and dark microcosms at KOA. The highest concentrations at KOA and Slag Canyon had grown to at least twice the concentrations of any sample at Thompson or Santa.

Thompson's larger fraction reached maximum concentrations of 22 and 180 μg L^{-1} at day 21 for the light and medium treatments, respectively, and then declined (Fig. 9a). The dark treatment's larger fraction increased in concentration continuously into the 23rd day reaching a concentration of 34 μg L^{-1}. The smaller size fraction at Thompson fell to its lowest concentration
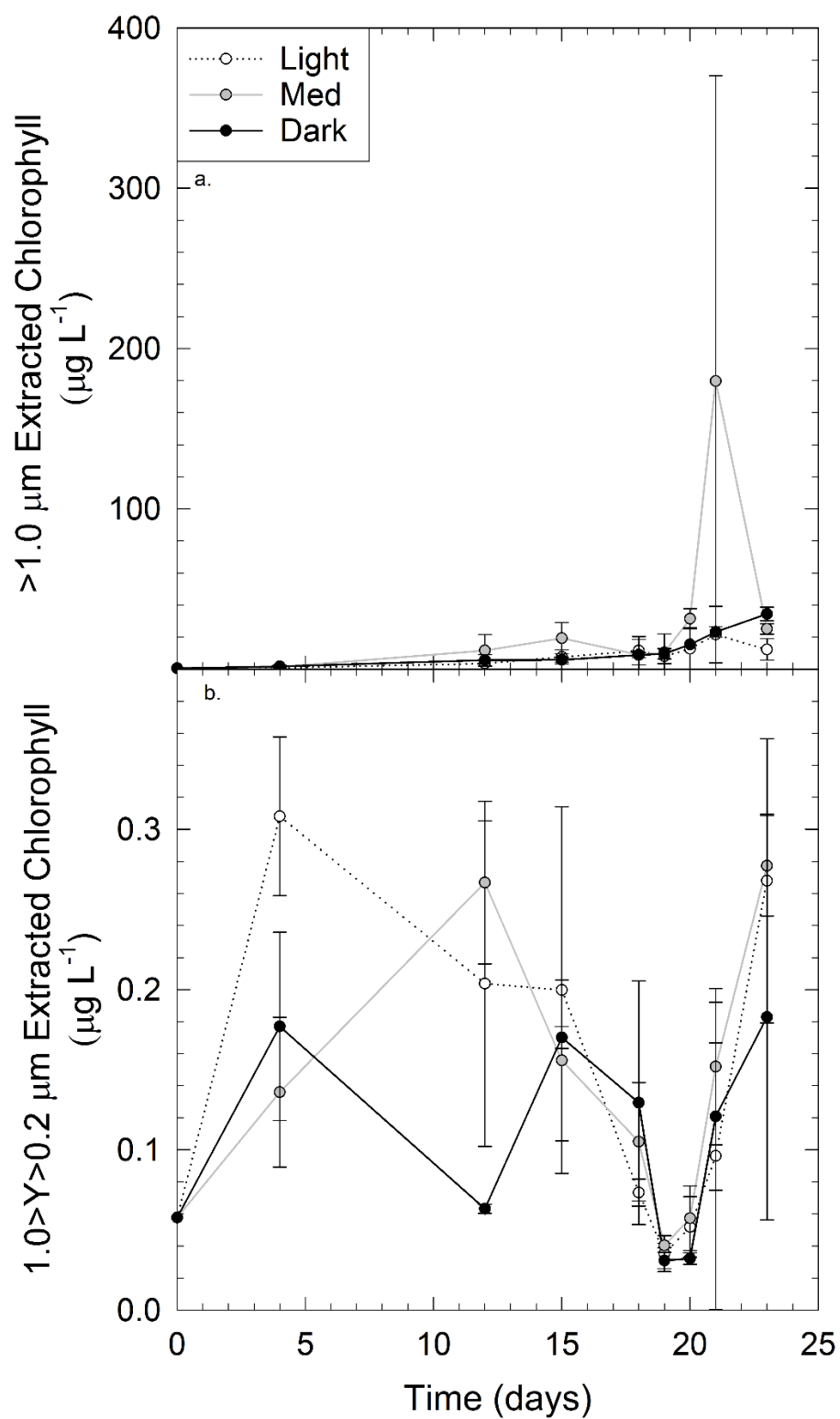
Figure 9: Size fractionated extracted chlorophyll at Thompson from planktonic material. (a) 1.0-micron fraction and (b) 0.2-micron fraction. The average of triplicates shown as values with standard deviation of triplicates shown as error.

in all treatments on day 19 ranging from 0.03 to 0.04 µg L^{-1} (Fig. 9b). Maximum concentrations ranging from 0.2 to 0.3 µg L^{-1} occurred at day 4 in the light box and day 23 in the medium and dark boxes (Fig. 9b).

Extracts from the larger size fraction at KOA increased in concentration until days 12, 15, and 20 for the medium, light, and dark treatments respectively, until their maximum concentrations of 130, 80, and 130 µg L^{-1} and then declined (Fig. 10a). The smaller size fraction showed three concentration spikes at days 4, 15, and 21, with day four as the maximum concentration of 0.4 µg L^{-1} for the medium treatment, day 15 as the maximum of 0.3 µg L^{-1} for the light treatment, and day 21 the maximum of 0.6 µg L^{-1} for the dark treatment (Fig. 10b).

At Slag Canyon, the larger size fraction increased in concentration to values from 22 to 160 µg L^{-1} on day 19 and then declined until the end of the experiment (Fig. 11a). The smaller size fraction remained mostly stable until a spike in concentration at day 21 that reached values from 0.08 to 0.5 µg L^{-1} (Fig. 11b). Chlorophyll *a* concentrations, for the larger size fraction, reached a maximum of 160 µg L^{-1} at day 15 for the light treatment, 105 µg L^{-1} at day 19 for the medium treatment, and 20 µg L^{-1} at day 19 for the dark treatment, whereas the smaller size fraction showed maximum chlorophyll *a* concentrations of 0.5 µg L^{-1} at day 21 for the light treatment, 0.5 µg L^{-1} at day 23 for the medium treatment and, 0.2 µg L^{-1} at day 23 for the dark treatments (Fig. 11).

The larger size fraction chlorophyll *a* concentrations at Santa increased into day 18 to values from 42 to 60 µg L^{-1} and decreased into day 23, whereas the smaller size fraction remained fairly stable around 0.1 µg L^{-1} until day 15 when greater day-to-day fluctuation
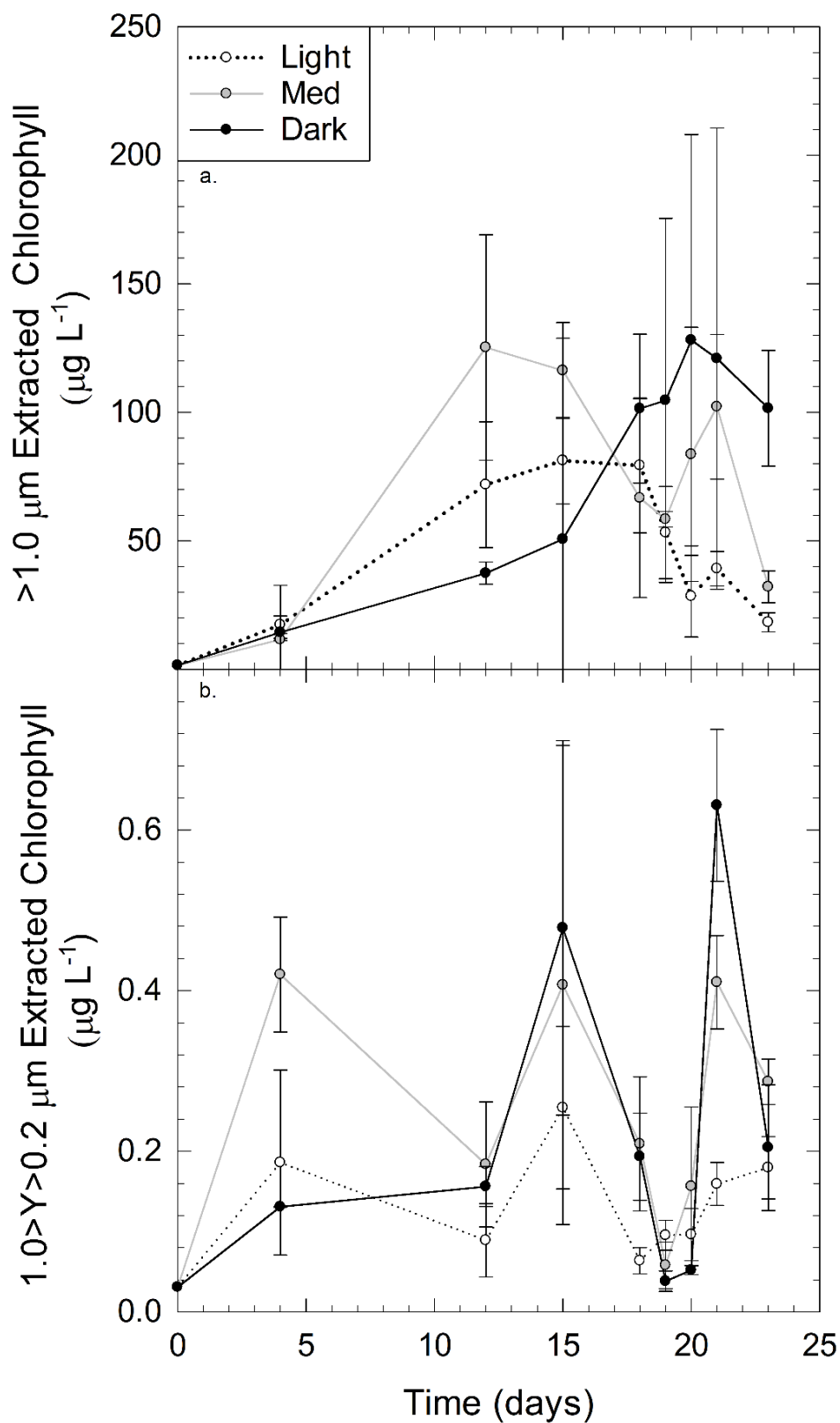
Figure 10: Size fractionated extracted chlorophyll at KOA from planktonic material. (a) 1.0-micron fraction and (b) 0.2-micron fraction. The average of triplicates shown as values with standard deviation of triplicates shown as error.
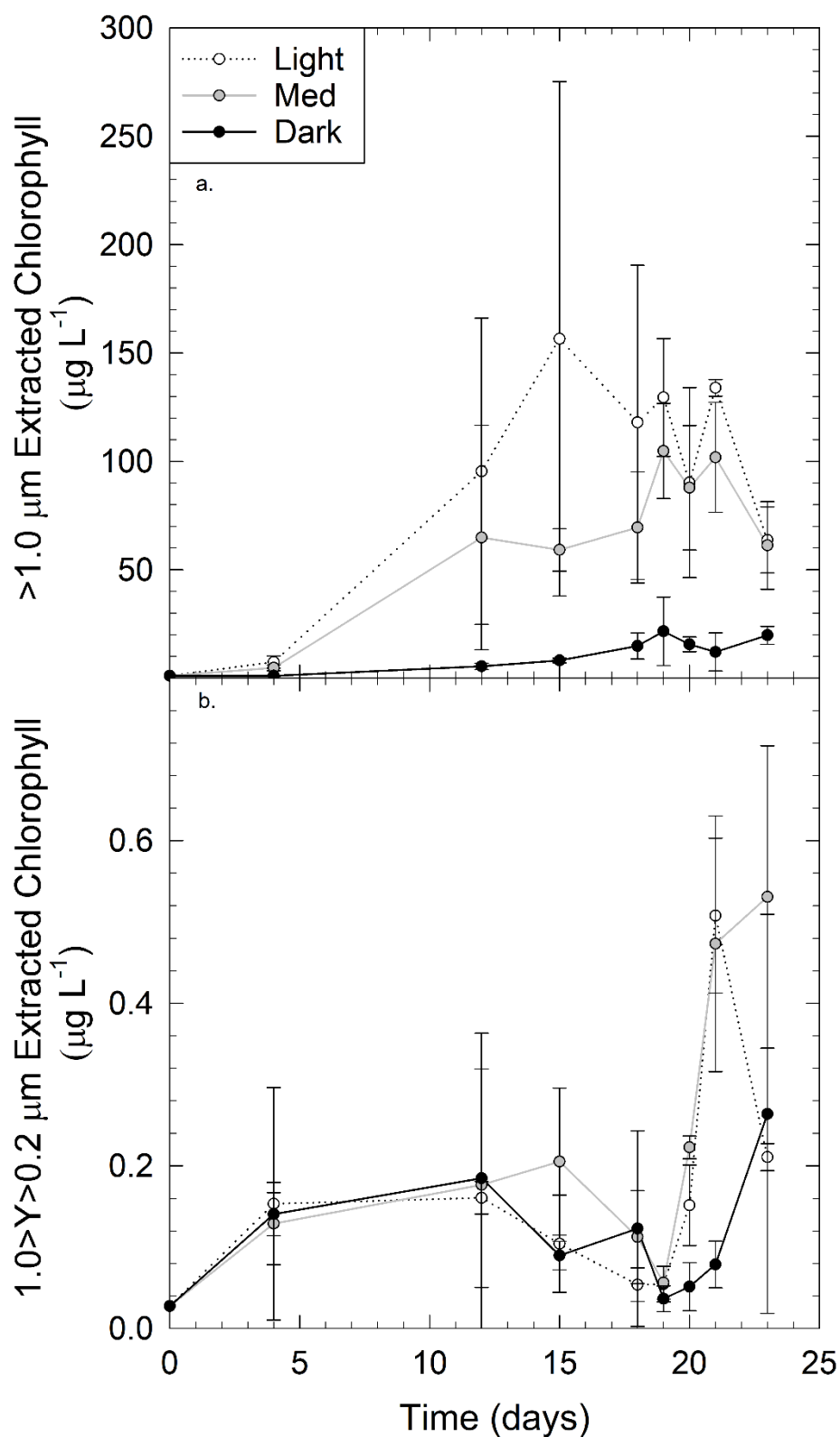
Figure 11: Size fractionated extracted chlorophyll at Slag Canyon from planktonic material. (a) 1.0-micron fraction and (b) 0.2-micron fraction. The average of triplicates shown as values with standard deviation of triplicates shown as error

for both the light and medium treatments respectively, whereas the dark treatment peaked at 42 $\mu g\ L^{-1}$ on day 21 (Fig. 12a). The smaller size fraction peaked on days 15, 21, and 18 for the light, medium, and dark treatments with concentrations of 0.2, 0.1, and 0.1 $\mu g\ L^{-1}$, respectively (Fig. 12b).

Santa, Slag Canyon, and KOA showed the larger size fraction's chlorophyll *a* had two orders of magnitude more chlorophyll *a* in the larger size fraction than the smaller fraction (Figs. 10,11,12). Thompson, however, had an order of magnitude more chlorophyll *a* in the larger fraction than the smaller fraction, except at the highest points where the larger fraction had two orders of magnitude more chlorophyll *a* (Fig. 9).

3.3.   Changes in Water Chemistry During Incubation

Throughout the experiment, elements demonstrated multiple types of behavior. Most elements showed depletions. A few elements became enriched, and a few did both. Many analyzed elements showed no change and those elements are not included in this section. All the elements that demonstrated a change have been organized according to behavior.

Macronutrient concentrations fell during the incubation. Initial phosphate concentrations ranged from 0.26 to 0.50 $mmol\ kg^{-1}$ and fell below the detection limit of 0.21 $mmol\ kg^{-1}$ in the water of all treatments, except the dark microcosm at Thompson which dropped to 0.23 $mmol\ kg^{-1}$ (Fig. 15c). Nitrate decreased at all sites from initial concentrations between 0.74 to 24 $mmol\ kg^{-1}$ to ending concentrations between the detection limit of 0.16 and 19 $mmol\ kg^{-1}$ (Fig. 15a). Nitrate dropped below detection after incubation only in the light and medium treatments at KOA, and the medium microcosm at Thompson (Fig. 15a). In two of the three dark microcosms at Slag Canyon, a loss of nitrate coincided with an increase in nitrite (Fig. 15a,b).
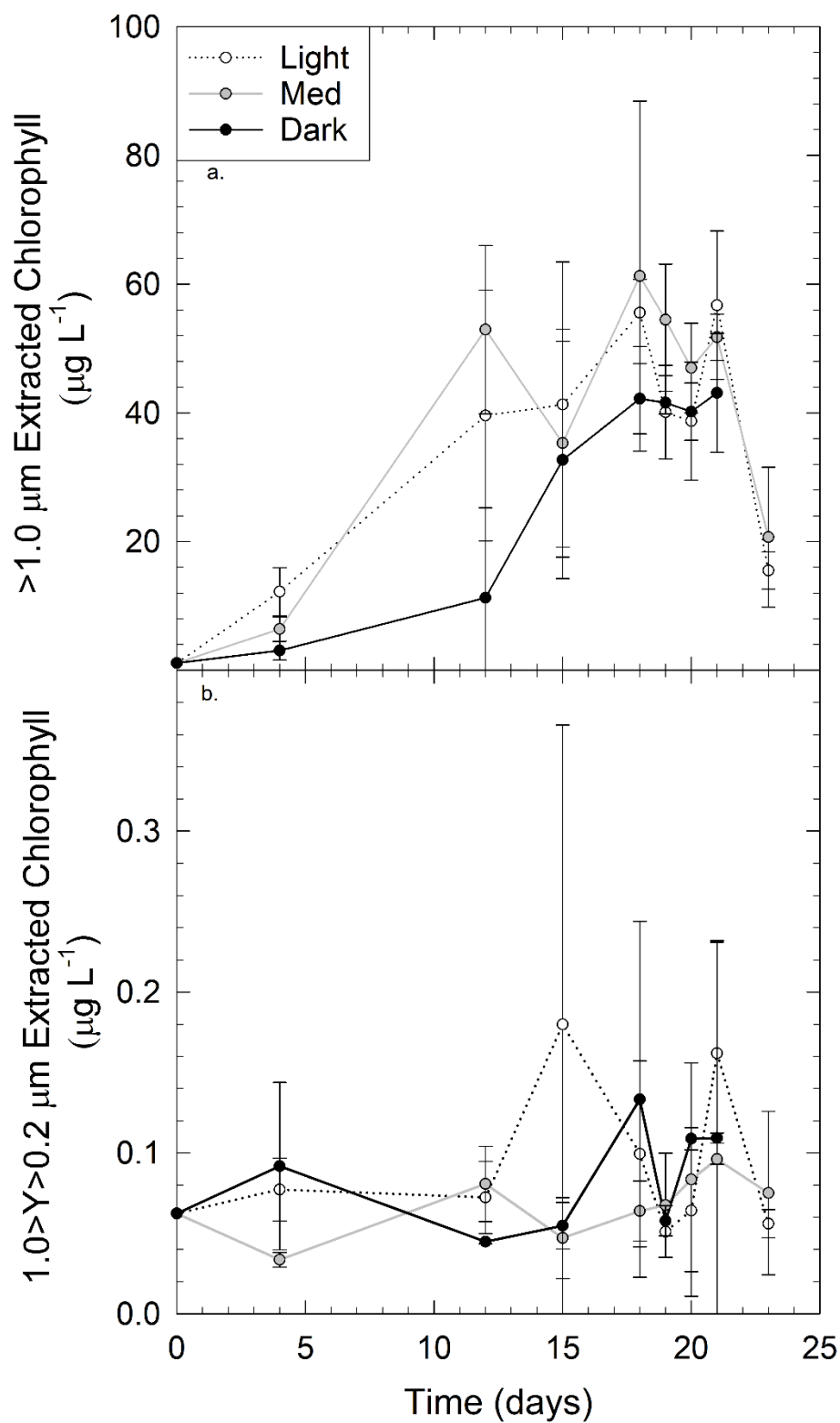
Figure 12: Size fractionated extracted chlorophyll at Santa from planktonic material. (a) 1.0-micron fraction and (b) 0.2-micron fraction. The average of triplicates shown as values with standard deviation of triplicates shown as error.
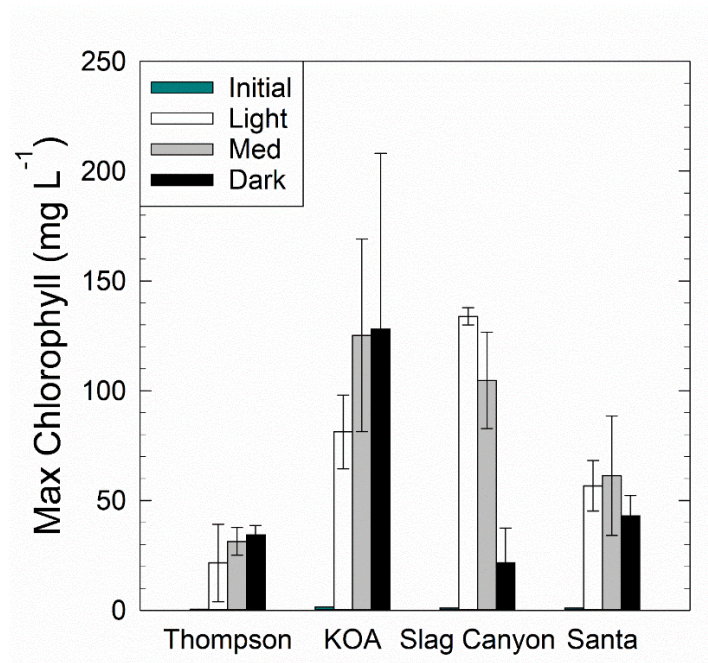
Figure 13. Initial extracted chlorophyll and maximum extracted chlorophyll. Standard deviation of triplicates shown as error.
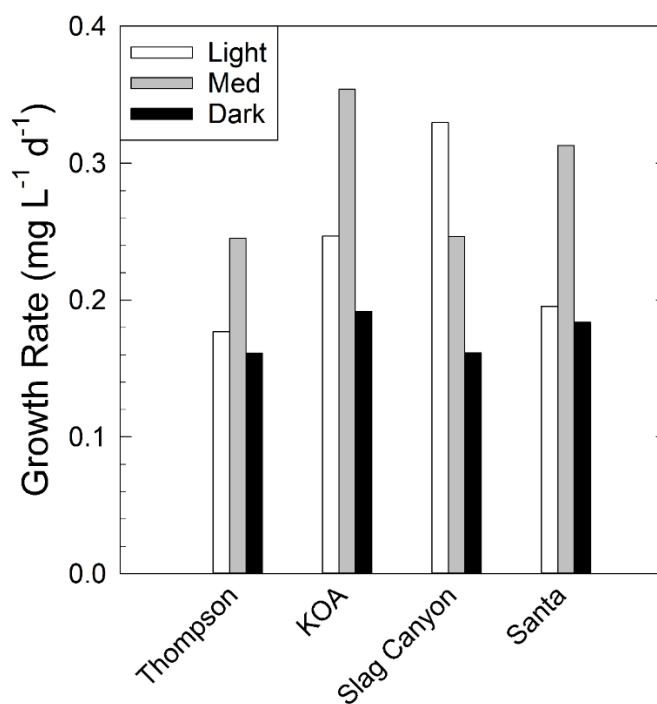
Figure 14: Growth rate calculated from extracted chlorophyll concentrations.
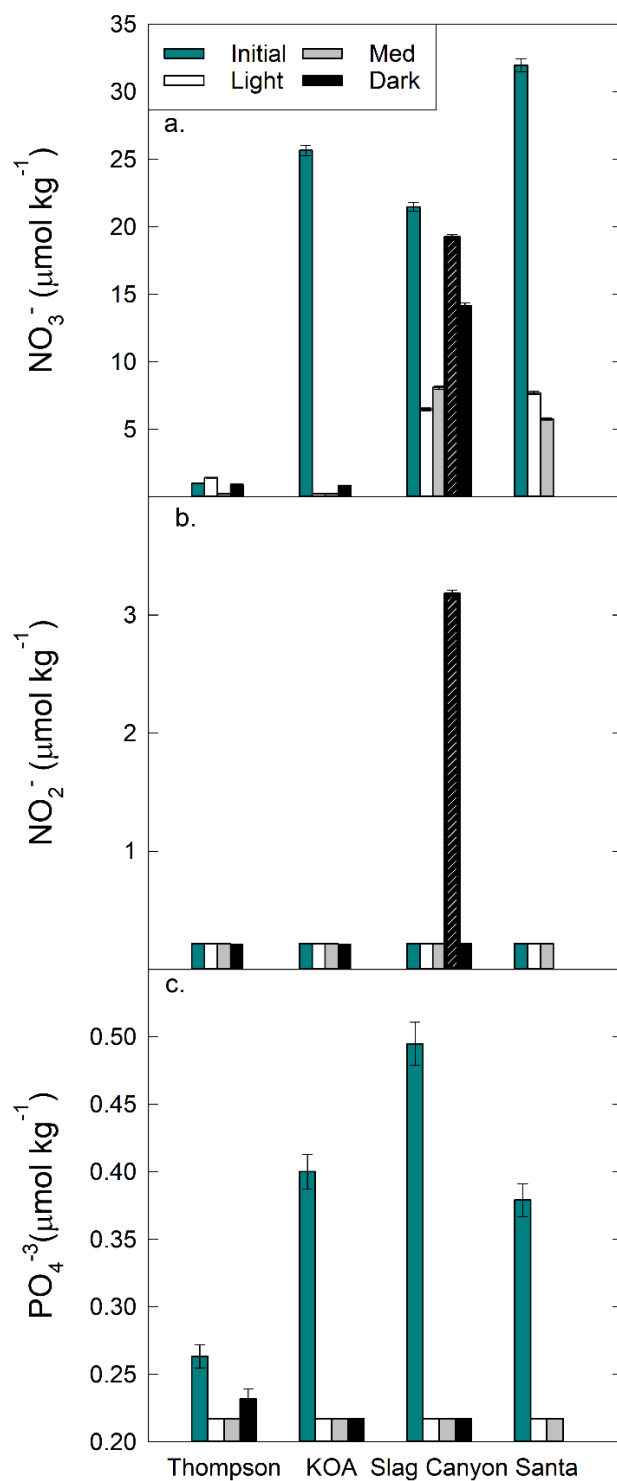
Figure 15: Macronutrient concentrations at deployment and after incubation. (a) Nitrate, (b) nitrite, and (c) phosphate, all analyzed by IC. Error bars show instrumental error calculated from standards and range from 1.1% to 3.2%. Patterned bars represent dark microcosm one at Slag Canyon where metabolisms appeared to diverge from microcosm two (solid bar).

Selenium, an essential micronutrient known for its toxicity, decreased in most treatments (Lenz and Lens, 2009; Kazamia et al., 2016). It dropped from 64 to 60 nmol kg^{-1} in the light box and 59 nmol kg^{-1} in the medium box at KOA (Fig. 16a). At Santa, selenium dropped from 88 nmol kg^{-1} to 85 nmol kg^{-1} in the light box and 81 nmol kg^{-1} in the medium box, and at Slag Canyon selenium dropped from 70 nmol kg^{-1} to below the 29 nmol kg^{-1} detection limit in the light box, to 59 nmol kg^{-1} in the medium box (Fig. 16a). Two of the three microcosms at Slag Canyon showed selenium loss to 65 nmol kg^{-1} (Fig. 16a). The light box at Slag Canyon and all treatments at Thompson did not contain detectable selenium, and the dark boxes at Slag Canyon and KOA did not change in selenium concentration.

Silicon, another micronutrient, started out reasonably consistent at all sites with concentrations between 0.395 and 0.466 µmol kg^{-1} and displayed a very distinct drawdown in most treatments with ending concentrations between 0.198 and 0.445 µmol kg^{-1} (Fig. 16b). Silicon showed the most drawdown in the dark box at KOA and had similar drawdowns in the medium and light boxes at KOA and Santa, as well as the medium microcosm at Slag Canyon (Fig. 16b). The three Thompson treatments and the light box at Slag Canyon presented milder drawdowns, and Slag Canyon's dark microcosm showed the least silicon loss (Fig. 16b).

Alkaline earth metals, essential for growth, dropped through the experiment. Magnesium dropped by approximately 5% from starting concentrations between 380 and 620 µmol kg^{-1} in the light and medium boxes at KOA, Slag Canyon, and Santa, and remained approximately the same in all other treatments (Fig. 17a). Calcium concentrations fell by approximately 60% from starting concentrations between 540 and 810 µmol kg^{-1} in all three treatments at KOA and the light and medium boxes at Slag Canyon and Santa (Fig. 17b). Calcium did not change in the other treatments (Fig. 17b). Strontium concentrations fell by approximately 25% from starting
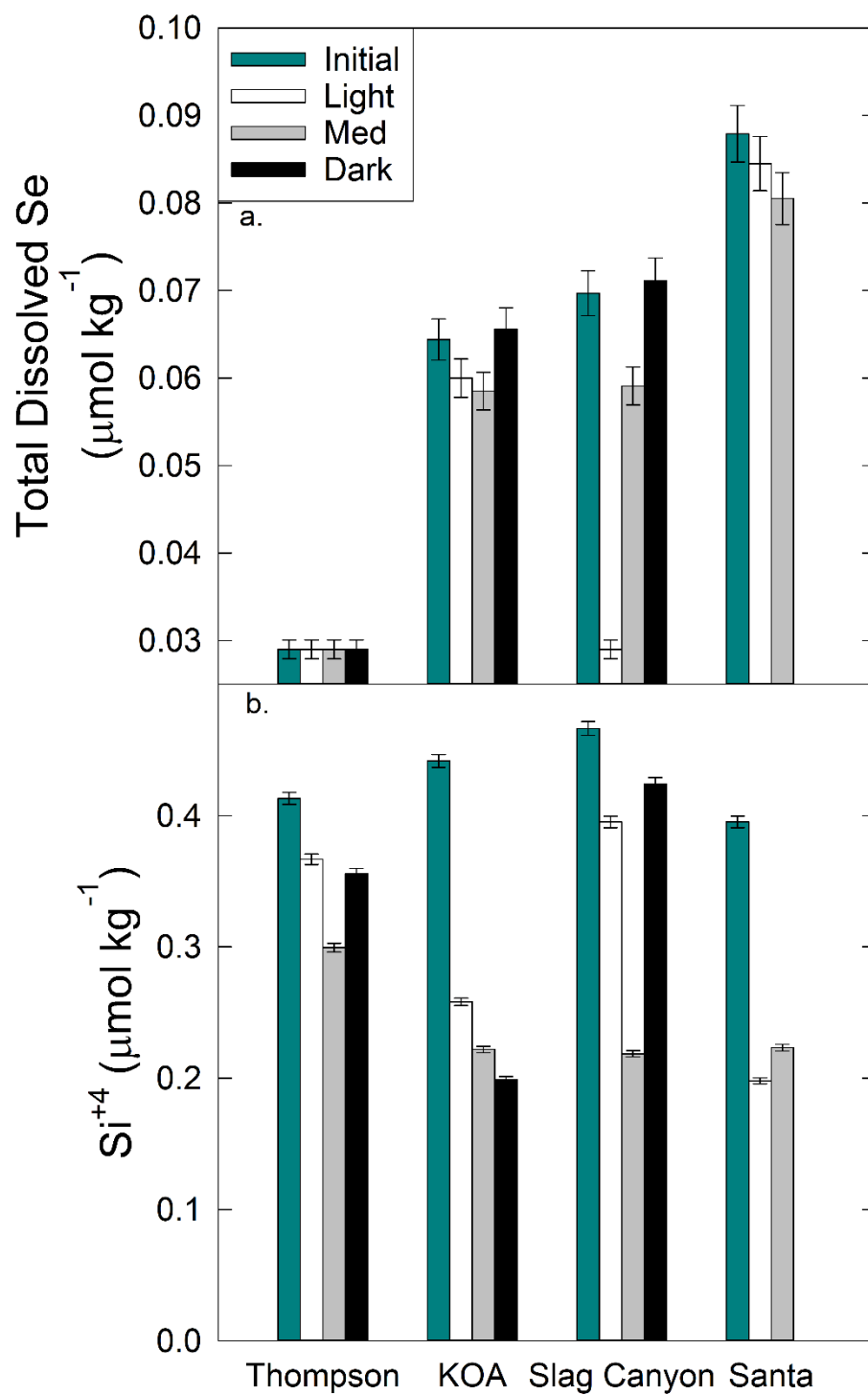
Figure 16: Metalloid nutrient concentrations at deployment and after incubation. (a) Selenium, analyzed by ICP-MS, and (b) silicon, analyzed by ICP-OES. Error bars show instrumental error calculated from standards and range from 1.1% to 3.7%.
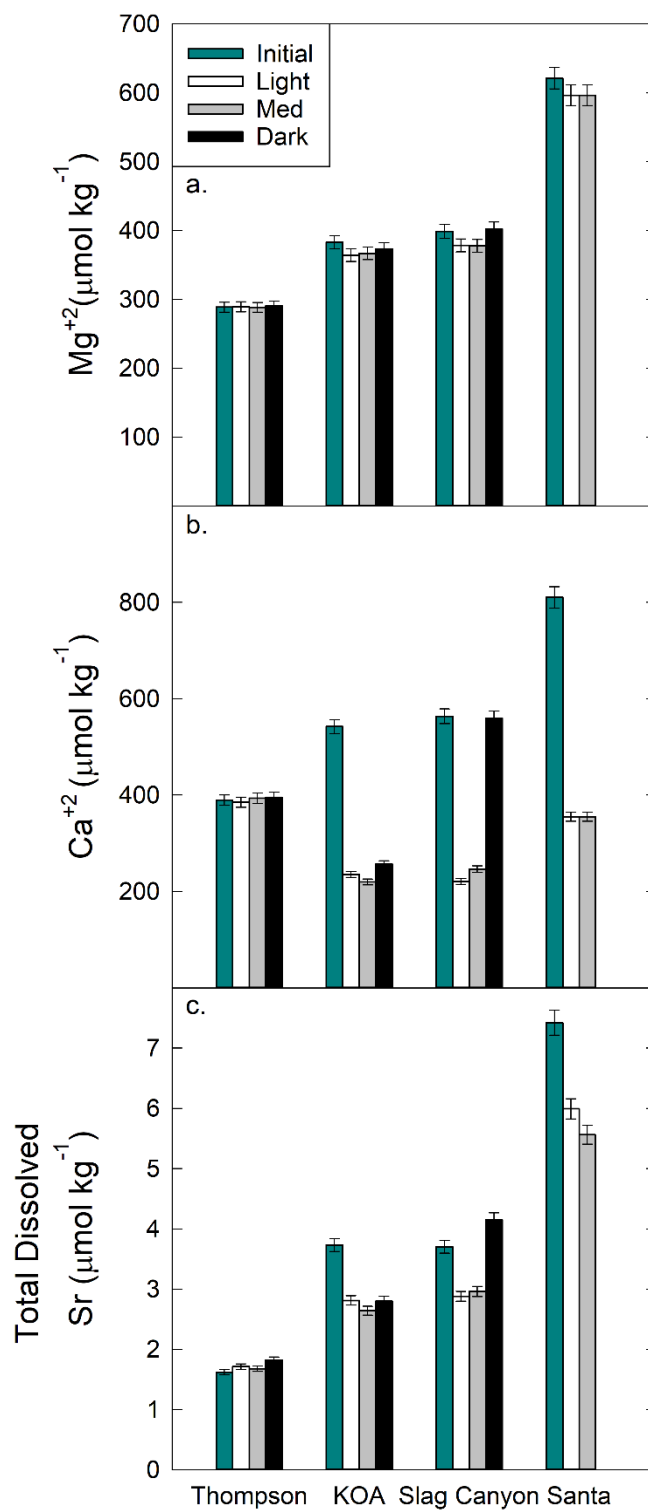
Figure 17: Alkaline earth metal concentrations at deployment and after incubation. (a) Magnesium, analyzed by ICP-OES, (b) calcium, analyzed by ICP-OES, and (c) strontium, analyzed by ICP-MS. Error bars show instrumental error calculated from standards and range from 2.5% to 2.8%.

concentrations between 395 and 466 µmol kg^{-1} in all three treatments at KOA and the light and medium boxes at Slag Canyon and Santa (Fig. 17c). Strontium did not change in the other treatments (Fig. 17c).

Barium and gallium showed nutrient like behavior. Both element's concentrations displayed values approximately 55% lower than starting concentrations between 0.1 and 4.7 µmol kg^{-1}, in light, medium, and dark boxes at KOA and the after incubation, in light, medium, and dark boxes at KOA and the light and medium boxes at Santa and Slag Canyon (Fig. 18). No other treatment showed changes in barium and gallium (Fig. 18).

Essential nutrients, iron and manganese, play similar cellular roles to each other and have caused limitations in oceans (Entsch et al., 1983; Stumm and Morgan, 1996; Borsetti et al., 2018). Manganese decreased from initial concentrations between 338 and 1620 nmol kg^{-1} during the incubation at all sites and all treatments, and only the dark treatments at Thompson and Slag Canyon remained above the detection limit of 36 nmol kg^{-1} (Fig. 19a). The dark treatments maintained manganese concentrations around 72 nmol kg^{-1} (Fig. 19a). Iron decreased like manganese at Slag Canyon and KOA but only dark microcosms and the light microcosm at Slag Canyon fell below its 98 nmol kg^{-1} detection limit (Fig. 19b). The other microcosms dropped from 1480 and 1580 nmol kg^{-1} ending the experiment ranging from 11 to 45 nmol kg^{-1} (Fig. 19b). At Thompson, iron started the experiment at 4300 nmol kg^{-1}, and the light and medium microcosms drop, whereas the dark microcosm increased to ending concentrations between 2800 and 5100 nmol kg^{-1} (Fig. 19b). Ending iron concentrations at Thompson increased concurrently with light reduction (Fig. 19b). Iron never existed at a detectable level at Santa (Fig. 19b).
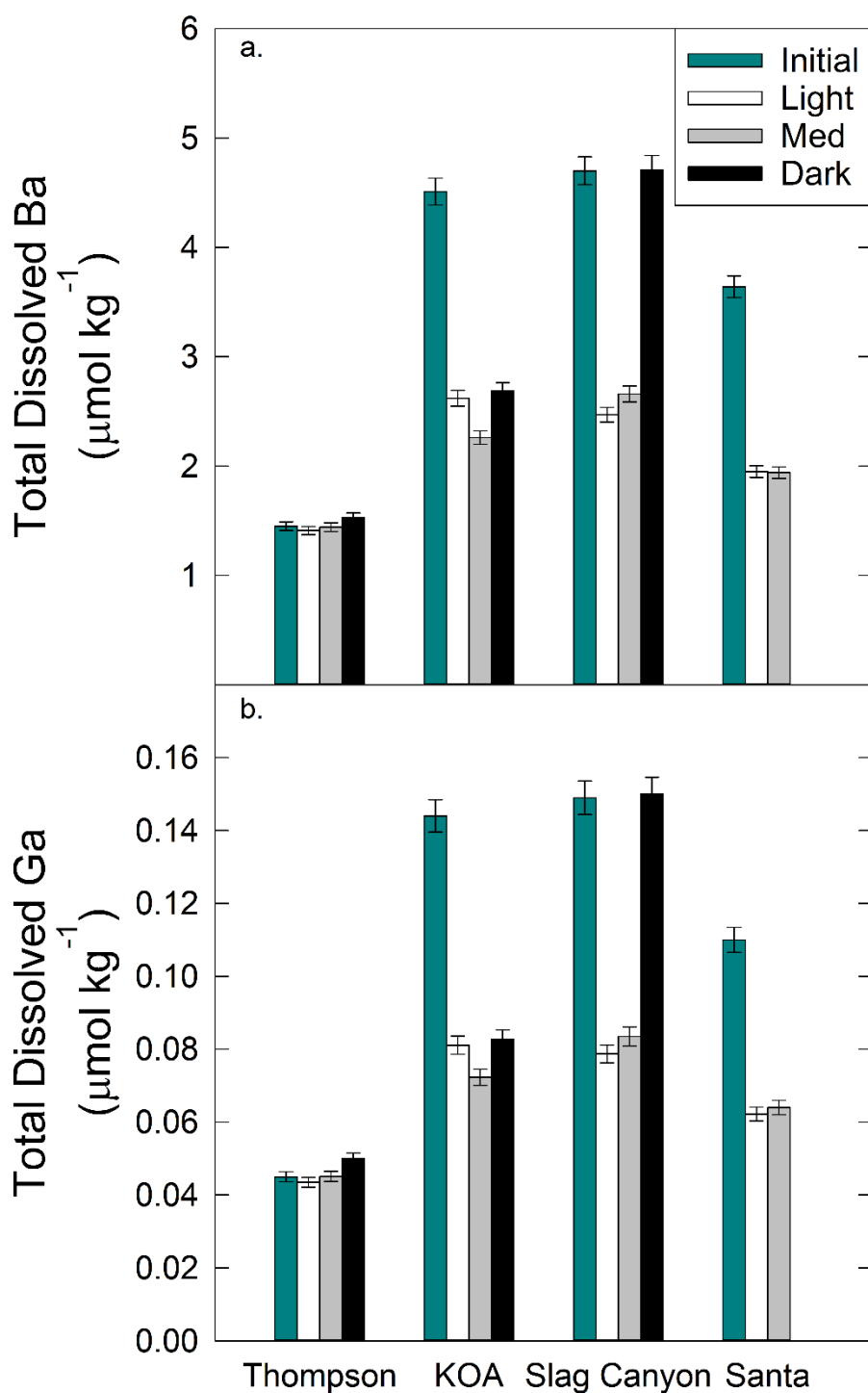
Figure 18: Nutrient-like metal concentrations at deployment and after incubation. (a) Barium and (b) gallium, both analyzed by ICP-MS. Error bars show instrumental error calculated from standards and range from 2.7% to 3.1%.
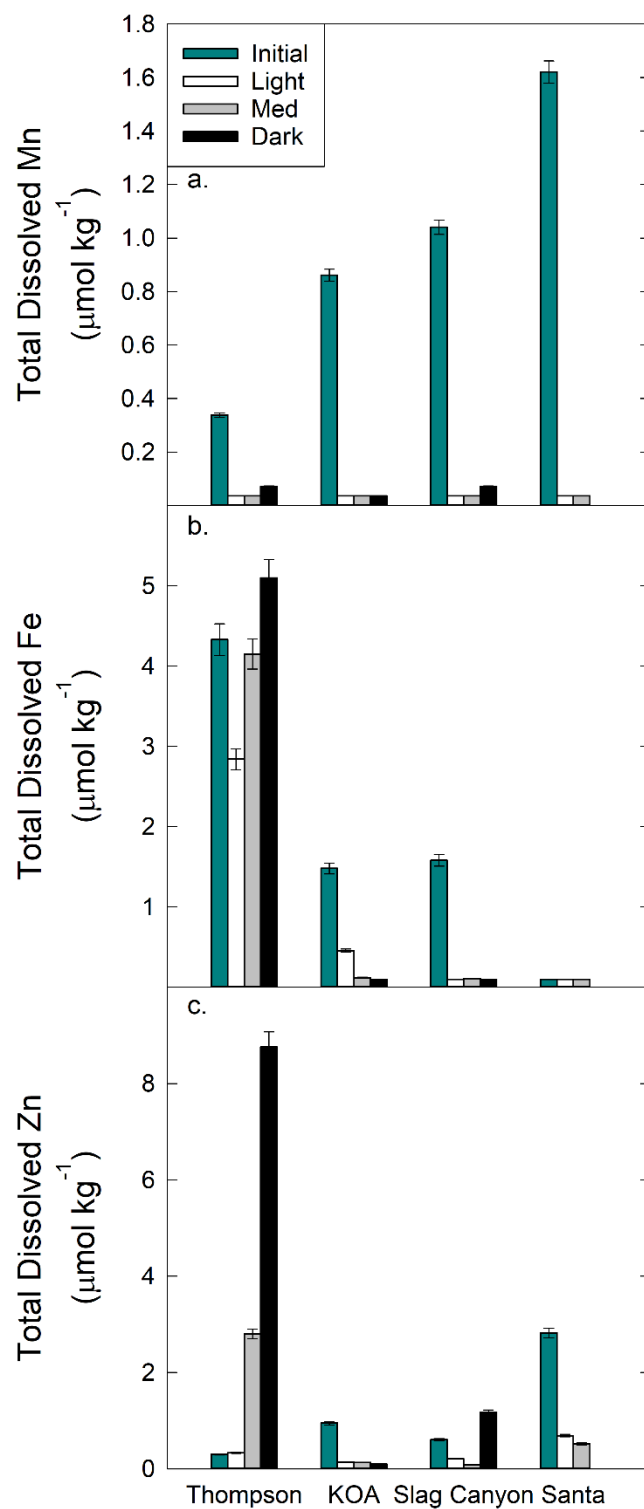
Figure 19: Metal nutrient concentrations at deployment and after incubation. (a) Manganese, (b) iron, and (c) zinc, all analyzed by ICP-MS. Error bars show instrumental error calculated from standards and range from 2.6% to 4.5%.

Zinc and copper serve as essential structural elements (Fraústo da Silva and Williams,

1991). Additionally, copper is a known algicide (Adamson and Sommerfeld, 1980). Zinc also

showed similar decreases to manganese but had detectable levels after incubation at Santa and,

therefore, showed losses at Santa, Slag Canyon, and KOA (Fig. 19c). Zinc concentrations start

the experiment between 2800 and 3000 nmol kg^{-1} (Fig. 19c). All treatments at KOA and Santa,

and the light and medium boxes at Slag Canyon decreased to a range from 84 to 690 nmol kg^{-1}

(Fig. 19c). Similar to iron, zinc increased in the dark box at Thompson, but it also increased in

the medium box ending at a range between 1180 and 8800 nmol kg^{-1} (Fig. 19c). In a similar

fashion to zinc and iron at Thompson, copper increased in every treatment at every site with an

initial range between 60 and 140 nmol kg^{-1} and ending between 74 and 230 nmol kg^{-1} (Fig. 20).
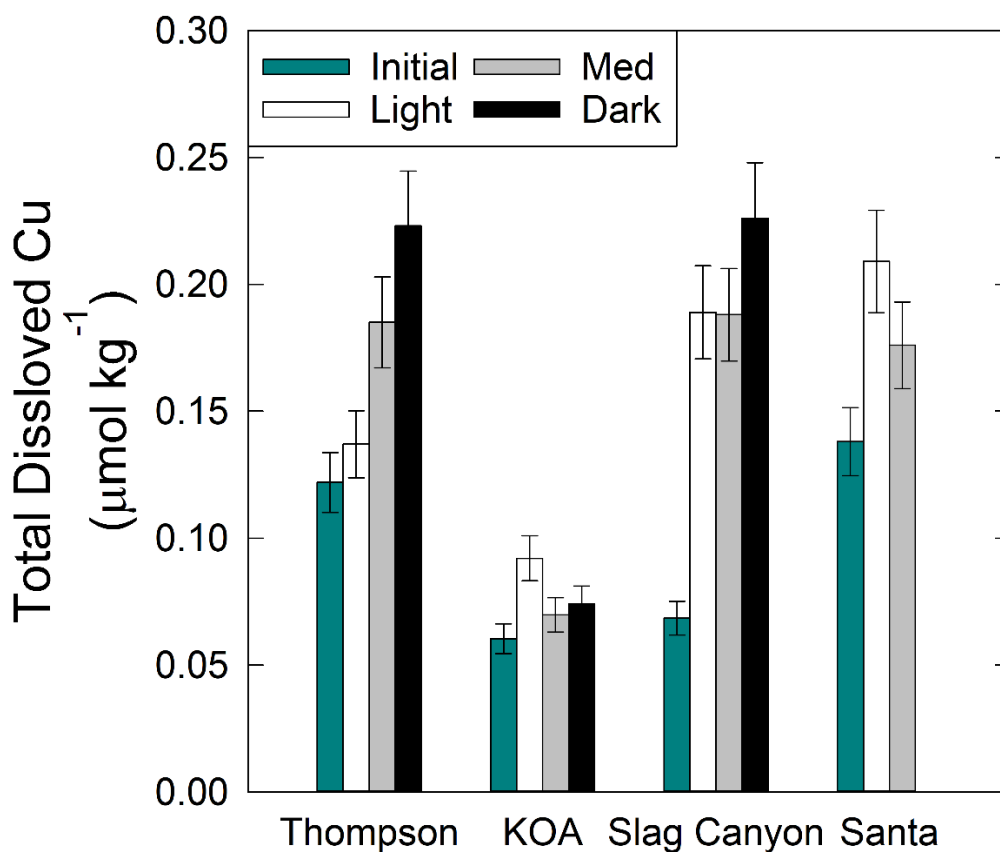
Figure 20: Copper concertation, analyzed by ICP-MS, at deployment and after incubation. Error bars show 9.7% instrumental error calculated from standards.

Halogens cause toxicity to all life, yet all life requires chloride (Fraústo da Silva and Williams, 1991). Halogens started the experiment ranging from 0.7 to 1240 μmol kg^{-1} with chloride being the most abundant and bromide being the least (Fig. 21). All measured halogens – fluoride, chloride, and bromide – showed substantial losses in the dark box at Slag Canyon ending the experiment with bromide below its detection limit of 0.125 μmol kg^{-1} and fluoride and chloride at 4.0 and 14.2 μmol kg^{-1}, respectively (Fig. 21). Fluoride showed some other small losses throughout the other sites and treatments with final concentrations between 180 and 8.5 μmol kg^{-1} (Fig. 21a). Unidentified overlapping peaks during analysis likely exaggerated fluoride depletion in the dark-two microcosm (Fig. 21a). Chloride showed a similar loss in the dark box at KOA which ended at 403 μmol kg^{-1} (Fig. 21b). Chloride showed no other losses and some small gains (Fig. 21b). Bromide showed losses at Santa, Slag Canyon, and KOA, with losses at Slag Canyon and KOA dropping below the lower detection limit of 0.125 μmol kg^{-1} (Fig. 21c). Thompson never had detectable bromide (Fig. 21c). Sulfate also decreased in the dark box of Slag Canyon, where it fell from 290 to 18 μmol kg^{-1} (Fig. 22). Sulfate showed a similar decrease in the dark box of KOA, where it fell from 320 to 270 μmol kg^{-1} (Fig. 22).

Several small changes and one major change in pH occurred during the experiment (Fig. 23). All but one treatment demonstrated an increase in pH from starting pH values around eight to ending pH values around nine (Fig. 23). The only exception was the middle dark microcosm at Slag Canyon which decreased in pH to a value of 4.45 (Fig. 23).

Many elements changed during this experiment. Alkaline earth metals, halogens, selenium, silicon, gallium, manganese, iron, zinc, nitrate, phosphate, and sulfate became depleted resembling nutrient like behavior. Iron, zinc, and copper became enriched, and several others exhibited both behaviors. Lithium, sodium, potassium, beryllium, boron, aluminum, titanium,

vanadium, chromium, cobalt, nickel, arsenic, rubidium, zirconium, niobium, molybdenum, palladium, sliver, cadmium, tin, antimony, cesium, lanthanum, cerium, praseodymium, neodymium, tungsten, tantalum, lead, thorium, and uranium showed no major changes (Appendix B).
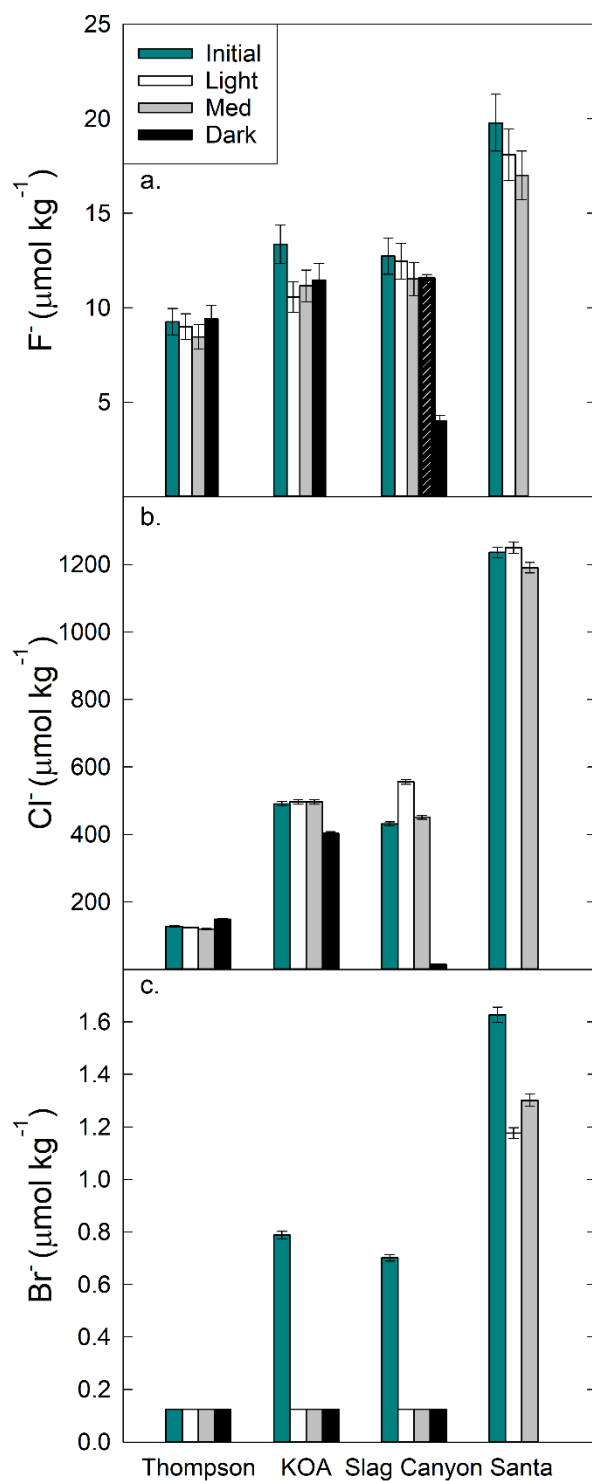
Figure 21: Halogen concentrations at deployment and after incubation. (a) Fluoride, (b) chloride, and (c) bromide, all analyzed by IC. Error bars show instrumental error calculated from standards and range from 1.8% to 7.6%. Patterned bar represents dark microcosm one at Slag Canyon where metabolisms appear to diverge from microcosm two (solid bar).
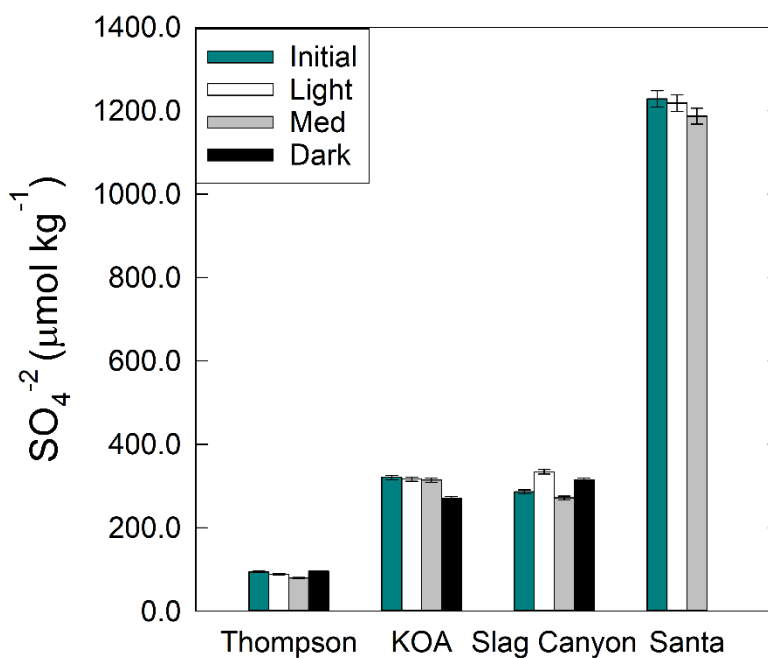
Figure 22: Sulfate concentrations, analyzed by IC, at deployment and after incubation. Error bars show instrumental error calculated from standards and range from 1.6% to 1.7%. Patterned bar represents dark microcosm one at Slag Canyon where metabolisms appear to diverge from microcosm two (solid bar).
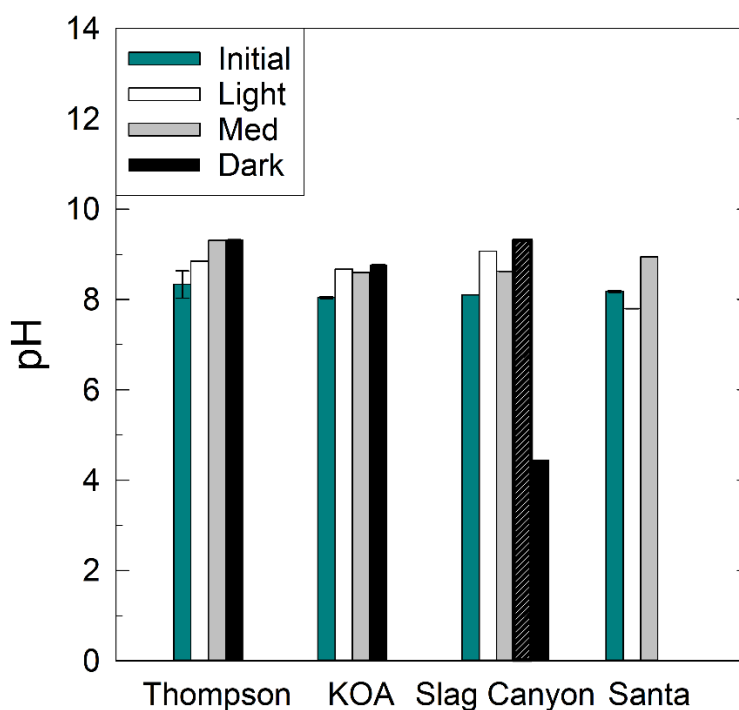
Figure 23: pH at deployment and after incubation. Error bars variability in meter reading and are typically <1%. Patterned bar represents dark microcosm one at Slag Canyon where metabolisms appear to diverge from microcosm two (solid bar).

4. Discussion

4.1. Creeks' Basal State

Historically, Silver Bow and Blacktail Creeks demonstrated seasonal trends in temperature, pH, and conductivity (Figs. 3,4,5). Seasonal trends in temperature are directly caused by warmer atmospheric temperatures in the spring and summer months and colder atmospheric temperatures during the fall and winter months, and Thompson and Blacktail sample sites even demonstrated super-cooling during winter 2018 and 0°C during fall 2018 (Fig. 3). During the spring thaw, pH converges just below eight at all sites (Fig. 5). This trend occurred most noticeably in the springs of 2016 and 2018 (Fig. 5). Later sampling that missed the spring thaw explains the lack of this phenomenon in spring 2017 (Fig. 5). Photosynthetic carbon dioxide consumption explains the increase in pH during the warmer months as carbon dioxide makes waters more acidic. Solute concentration caused by increases in evaporation in the summer and ice formation in the winter likely drive correlating increases in conductivity (Fig. 4). Dilution from atmospheric precipitation likely caused dips in conductivity (Fig. 4).

Seasonal variations also influence dissolved oxygen, but different processes can create increases at different times, making these changes less noticeable (Fig. 6). Warm temperatures with abundant light encourage photosynthetic organisms to produce oxygen, causing dissolved oxygen spikes in the summer. High biological oxygen demand and corresponding respiration of decomposers outweighs photosynthesis, causing net oxygen use and a dip in dissolved oxygen. In spring, after most dead material has decomposed, new primary producers rapidly grow, and net oxygen production occurs from metabolic processes. As a high light site, KOA most consistently showed this trend, especially in 2017 (Fig. 6). Water can dissolve more oxygen at lower temperatures, making dissolved oxygen higher in colder months. The best evidence of this

reverse solubility occurred at the Blacktail and Thompson sample sites where low light limited

the impact of photosynthetic organisms. Other processes, like turbulence, ice cover, and

precipitation, can also have a significant impact on dissolved oxygen as they influence how

water interacts with the atmosphere, and increasing atmospheric interactions result in more

dissolved oxygen.

Nitrogen and phosphorus can also be significantly impacted by thaw and precipitation.

Phosphorus typically moves with soil particles and is often related to runoff, and nitrogen

typically moves with water and tends to be related to groundwater flow. A spike in nitrogen to

phosphorus ratio can therefore be attributed to an increase in groundwater inputs, and a decrease

in this ratio can be attributed to an increase in surface runoff (Fig. 2) (Yan et al., 2016). Being

that fertilizing and wastewater primarily source these essential nutrients, discerning specific

reasons for changes in this ratio get increasingly complicated with changes in surrounding land

use management and urbanization (Ansari and Gill, 2011). Historical spikes or drops in the

nitrogen to phosphorus ratio therefore become difficult to explain (Fig. 2). When compared to

the Redfield ratio – the average ratio that a community uses nitrogen and phosphorus – nutrient

limitations become predictable, and phosphorus likely limited at all but one study site.

4.2. Limitations to Photosynthesis

Photosynthesis requires carbon dioxide, water, and light, as well as the organisms needed

to facilitate the process. SBC and BTC contain an abundance of water, the surrounding

atmosphere contains plenty of carbon dioxide, but shading to the riverbed limits available light.

In addition, nitrogen and phosphorus are necessary structural elements for all organisms

including photosynthesizers. Phosphorus makes up the backbone of DNA and is present as a

major component of membranes, and all proteins require nitrogen as an essential component of

amino acids (Fraústo da Silva and Williams, 1991). These elements also specifically apply to photosynthesis, because the membranes needed for chloroplasts require phosphorus, and chlorophyll requires nitrogen in its porphyrin ring (Fraústo da Silva and Williams, 1991). More commonly in oceans, micronutrients can also have limiting effects (Bertrand et al, 2015). In fresh surface waters, nutrient and/or light limitations typically prevail. In small, headwater, low-order streams light is typically the more significant limitation.

4.2.1. Nutrient Limitations

Nutrients often pose one of the most significant limitations to photosynthetic communities, a principle observed as early as 1840 (Leibig, 1840). Liebig's law of the minimum established the principle that the lowest necessary nutrient limits potential growth. This does not apply directly to environmental concentrations of nutrients, because as organisms need different amounts of different nutrients (Redfield, 1958). Redfield established a ratio between macronutrients carbon, nitrogen, and phosphorus of 106:16:1 (Redfield, 1958). Nitrogen and phosphorus often limit photosynthesis as they are in such high demand relative to other nutrients (Twining et al., 2004). Furthermore, nitrogen tends to be more limiting near coastal environments and phosphorus is typically limiting in inland waters (Stumm and Morgan, 1996). The inland waters assessed in this experiment demonstrated similar limitations.

Macronutrients (N, P) caused limitations to photosynthetic communities in all treatments. Despite the expectation that light would be most limiting, nutrient limitations exceeded light limitations in the microcosms. After incubation, all macronutrients showed measurable concentration decreases (Fig. 15). Nitrate showed measurable losses from starting concentrations between 0.74 and 24 μmol kg^{-1} and was consumed below a 0.16 μmol kg^{-1} detection limit in the light and medium microcosms at KOA, and the medium microcosm at Thompson and between

0.63 and 17 µmol kg^{-1} at all other sites (Fig. 15a). Nitrite can be an important nitrogen source as many primary producers are capable of nitrite uptake, but chemoautotrophic bacteria usually convert nitrite to nitrate before the nitrite can be consumed (Baah, 2018). At deployment, nitrite in the creeks existed in concentrations below the detection limit of 22 µmol kg^{-1}, if at all, so any contributions to nutrient use could not be observed (Fig 15b).

Phosphate showed similar relative losses to nitrate (Fig. 15c). All treatments except the dark box at Thompson demonstrated a loss below the detection limit of 0.211 µmol kg^{-1} from starting concentrations of 0.263 and 0.495 µmol kg^{-1} (Fig. 15c). The dark box at Thompson fell to 0.232 µmol kg^{-1} (Fig 15c). These losses suggest that the microbial communities formed in eight of the nine treatments displayed phosphorus limitation. These limitations developed as expected since phosphorus more commonly limits growth in inland waters, and the nitrogen to phosphorus ratios suggest phosphorus should be limiting at most study sites (Fig. 2). Nutrient limitations did not exceed light limitations, as expected.

4.2.2. Light Limitations

Although light limited chlorophyll growth, it did not limit growth as anticipated. Instead, in most treatments, light allowed full nutrient use, unless 95% of light was restricted at the darkest site. Unlike the nutrients, that had a finite starting value, everyday light penetrated the boxes at a rate controlled by the tinting. Growth rate decreases, therefore, better represented light limitations, because they also accounted for time (Riebesell et al., 1993). Throughout the experiment, decreases in light and growth rate occurred concurrently (Fig. 14). Similarly, Warner and Madden found that in vitro algal growth rate increased with higher irradiance given sufficient time to adjust to the increased light (2006). Based on the relationship between light and

growth rate, light is also likely a significant limiting factor in photosynthetic growth in SBC and BTC.

4.2.3. Colimitations

Two prevailing theories on limitation exist, Liebig's law of the minimum, in which the lowest available nutrient limits total biomass, and Blackman limitation, where the slowest process limits growth rate (Saito et al., 2008). Both theories only consider a single limiting factor, but in practice multiple factors often limit growth, a situation now known as colimitation. In 2008, Saito *et al*. characterized these colimitations into three types. The first type, independent nutrient colimitation, occurs if two or more nutrients are equally scarce, and an increase in both nutrients is necessary to see a significant increase in growth. The second type, biochemical substitution colimitation, occurs if certain metalloenzymes that function ideally with two or more different metals and those metals are lacking. The third type, biochemically dependent colimitations, occurs if one limiting factor slows the uptake of a second limiting factor. The first type is most commonly considered a typical colimitation and can be observed in the medium microcosm at Thompson and the light and medium microcosms at KOA that had both nitrogen and phosphorus drawn down below detection limits. Type three occurred at every site if light slowed growth rate and complete drawdown of one or more macronutrients occurred.

Such a change in growth rate suggests that available light limits the rate at which phytoplankton grow, and therefore, the rate at which they can assimilate nutrients. Still, light does not limit the maximum possible growth. Available nutrients, especially phosphorus, limited maximum growth. A similar study conducted in a simulated stream, also found a synergistic relationship between light and phosphorus (Hill, *et al*. 2012). Hill *et al.* also suggest that in the presence of light, periphyton surpasses bacteria in growth rate. Since both light and nutrients

appear to have limiting effects in this experiment, a colimitation likely existed between light and nutrients. Such a limitation exemplifies a biochemically dependent colimitation, observable in treatments with lower light exposure that also have lowered growth rates (Saito et al., 2008).

The medium microcosm at Thompson and the light and medium microcosms at KOA demonstrated independent nutrient colimitation by nitrogen and phosphorus. These microcosms had nitrite, nitrate, or phosphate levels below detection after incubation (Fig. 15) (Saito et al., 2008). The pivotal study conducted by Redfield in 1958 suggests this is highly unlikely, however, as the biological community in the lightest two KOA treatments used nitrogen at a rate of 64 moles of nitrogen for every one mole of phosphorus, far greater than the idealized Redfield ratio of 16 moles nitrogen for every one mole of phosphorus. This suggests the microbial communities in these microcosms are especially unusual in the ratios at which they used nitrogen and phosphorus, or another process, such as denitrification, removed nitrogen from the water in the microcosms.

4.3. Element Depletions

This experiment used 0.22 micron filters to process samples for dissolved chemical analysis, meaning an element that showed a depletion had to be taken up by microbes or form a complex larger than 0.22 microns during the 23-day incubation. Microbes, minerals, and organic matter make up these particles, and these three types of particles can all complex elements (Cox, 2011). Organisms usually take up elements for use as nutrients, but an organism can take up non-nutrient elements unintentionally. Uptake of non-nutrient elements occurs when charge and size are similar to a nutrient element (Rensing and Rosen, 2009). Element depletion could happen via organismal uptake, or complexation with inorganic particles or organic matter.

4.3.1. Metal Depletion

Most of the alkaline earth and transition metals drawdown can be attributed to nutrient type behavior (Figs. 17,18,19). Magnesium, calcium, and strontium are micronutrients, and microbes should have drawn down these elements (Fraústo da Silva and Williams, 1991). Treatments that showed little to no drawdown also did not exhibit much chlorophyll growth (Figs. 9,10,11,12,17). Magnesium is essential for all life as a necessary structural component of cell walls and membranes, where it serves as a cross-link between proteins. Moreover, photosynthetic organisms especially require magnesium as the sole ion that can associate with chlorophyll's porphyrin ring and maintain optimal pigment function (Fraústo da Silva and Williams, 1991). Calcium serves a similar structural role, in addition to most metabolisms containing at least one calcium-dependent step (Fraústo da Silva and Williams, 1991). Since strontium is also an alkaline metal, it is also logical to see a drawdown, since it may substitute for calcium in small amounts.

Microbes also need the micronutrients manganese, iron, zinc, and selenium for growth (Kazamia et al., 2016). As a divalent ion, zinc performs a similar cellular role as magnesium and calcium by cross-linking proteins (Frastúso da Silva & Williams, 1991). In addition, evidence exists suggesting photosynthetic organisms take up zinc in the light and release it in the dark (Moris et al., 2006). Compared to Moris *et al.,* this experiment also showed evidence of this zinc trend, because microcosms with more light showed more zinc drawdown than darker microcosms. Iron often limits primary producers in oceans, but such limitations rarely occur in inland waters (Fig. 19b) (Entsch et al. 1983; Stumm and Morgan, 1996). Similarly, manganese would not be expected to be limiting in inland waters but has been found to have a limiting effect *in vitro* (Stumm and Morgan, 1996; Borsetti et al., 2018). At sites where iron and manganese

appear to be completely drawn down, they may even form a biochemical substitution

colimitation (Fig. 19a,19b) (Saito et al., 2008). Although toxic at high enough levels, selenium is

an essential nutrient as it replaces sulphur in cystine allowing for new protein functions (Fraústo

da Silva and Williams, 1991; Lenz and Lens, 2009). Selenium also showed nutrient depletion

(Fig 16a).

Barium and gallium are the only metals drawn down with no known history as nutrients

(Fig 18) (Waldron et al., 2009). In extreme environments such as mudpots, many metals with no

known uses have proven to be essential to some organisms, and a similar situation may be

present here for barium and gallium (Pol et al., 2013). Similar trends are present in oceans, where

barium has a nutrient-like vertical profile where it is mostly depleted near the surface (Bruland

and Lohan, 2003). Therefore, microbes either use barium as a nutrient in a way not yet known or

take up barium due to its similarity to other alkaline earths. In the ocean, gallium behaves like

the other group 13 metal aluminum and likely gets scavenged onto high-affinity particles

(Bruland and Lohan, 2003). Although barium and gallium are not essential nutrients, algae are

still able to take up these elements, sometimes with enough efficiency to be used for remediative

purposes (Vetrivel et al., 2017).

4.3.2. Nonmetal Depletions

4.3.2.1. Silicon Depletion

Silicon is a necessary structural element in diatoms, single cellular algae that secrete a

siliceous cell wall (Fraústo da Silva and Williams, 1991). The drawdown of silicon showed a

direct, opposite relationship with photosynthetic growth, where larger growth treatments showed

greater silicon depletion (Figs. 9,10,11,12,16b). Silicon drawdown suggested that diatoms

contribute to chlorophyll *a* concentration more than other photosynthetic organisms. Since this

experiment used filters that kept the majority of diatoms in the larger size fraction and the larger

size fraction controlled the chlorophyll *a* concentrations, diatoms likely make up the majority of

microbial chlorophyll (Figs. 9,10,11,12). Diatoms in low order creeks tend to be benthic

organisms scoured into the water column (Wehr and Sheath, 2003). Such benthic organisms have

not evolved the necessary mechanisms to quench excess light present in the water column, which

further explains why high light seems to slow the growth rate of photosynthetic organisms

(Laviale et al., 2016).

4.3.2.2. Halogen Depletion

All halogens are toxic to microbes in high enough concentrations, and although chloride

is an essential nutrient for life, all three domains of life have found different ways to utilize

halogens (Fig. 21). These compounds often make up toxins used to help compete with other

microbes or as hormones in some eukaryotes (Fraústo da Silva and Williams, 1991). The

demonstrated decrease in bromide may be related to several processes (Fig 21c). Microbes have

been known to take up bromide when they lack sufficient chloride; however, with an abundance

of chloride present, there should be no need to take up bromide in its place (Stewart, 1967). It is

also possible that a bacterial community exists, similar to that observed by Weigold et al., and

microbes converted the dissolved halogens into gaseous halogenated organic compounds such as

chloroform and bromoform (2016). A similar study also showed that similar processes could

happen in moderately acidic salt lakes, verifying that such halogenation is possible in aquatic

environments (Ruecker et al., 2015). Further evidence of halogenation occurring in aquatic

environments can be found in the ocean, where chloride is the most abundant ion (Ekdahl et al.,

1998; Liu et al., 2013). Furthermore, in the oceans, a strong correlation has been found between

halogenation and photosynthetic microbes (Carpenter and Liss, 2000; Quack et al., 2007; Karlson et al., 2008).

4.4. Element Enrichments

For an element to be enriched, it had to start the experiment as part of a complex larger than 0.22 microns, and end the experiment associated with smaller complex or completely dissolved, to fit through the 0.22 micron filters. This could happen if organisms died, and their cells broke to release elements, or if larger particles broke down during the experiment. Organisms, using parts of these particles such as organic carbon, likely cause the latter breakdown.

Although the majority of changes in dissolved chemistry consist of depletions caused by microbial uptake, iron, copper, and zinc showed increases throughout the experiment (Fig. 19b,19c,20). Iron and zinc only showed increases in the darkest treatments (Fig. 19b,19c). All three enriched elements are known to bind with organic ligands with as much as 99.8% of copper and 98% of zinc bound this way (Bruland and Lohan, 2003). Copper, iron, and zinc also all have nutrient-like vertical profiles in oceans (Bruland and Lohan, 2003). Copper has a "modified" profile however as it does not reach a mid-depth maximum like other nutrients (Boyle, 1977). Remineralization of particulate copper likely causes copper's continual increase with depth (Bruland, 1980). The light microcosms likely showed a decrease in iron and zinc because they had active primary production, and microbes took up these micronutrients. Since all of these elements have a strong affinity for carbon and non-photosynthetic organisms cannot utilize carbon dioxide, the observed enrichment likely resulted from non-photosynthetic microbes breaking down many of these particles as a source of organic carbon releasing the associated metals (Fig. 19b,19c,20). Furthermore, since microbes require all three elements for nutrient use,

it is also possible that the enrichment of these elements occurred as microbes died and broke down to release these nutrients (Fraústo da Silva and Williams, 1991; Bruland and Lohan, 2003).

4.5.   Anoxia at Slag Canyon

Microbial metabolisms vary greatly with oxygen availability (Broman et al., 2017). Gasses could only enter the microcosms when opened for sampling, and Slag Canyon had almost no chlorophyll *a* development in the dark box (Fig. 11). Therefore, primary producers likely failed to balance out oxygen losses due to the respiration of heterotrophic consumers and decomposers, and these microcosms did not likely remain oxygenated throughout the experiment. Several anaerobic processes can take over in the absence of oxygen; one of the first expected is nitrate reduction (Grundl et al., 2011). The next expected process is sulfate reduction (Grundl et al., 2011).

Nitrate reduction is a common process in anoxic environments and often occurs in sediments (Thamdrup and Dalsgaard, 2001). Also, in anoxic waters, nitrate reduction is known to cause a loss of available nutrient nitrogen and produce nitrogen gas (Dalsgaard et al., 2003; Lim et al., 2018). Two of the dark microcosms at Slag Canyon show nitrate reduction with a loss of nitrate and the presence of nitrite (Fig. 15 a,b). This completes the first step of denitrification, a major microbially mediated loss of nutrient nitrogen, and the microbes mediating this process leave a distinct isotopic signature (Martin and Casciotti, 2016; Lim et al., 2018).

Sulfate reduction is similarly microbially mediated, and the dark microcosms at Slag Canyon likely received slightly different microbial communities (Roesler et al., 2007). The third microcosm at Slag Canyon showed this process in the loss of sulfate (Fig. 22). Being that turbulent flow keeps the creek mostly oxygenated, it is likely that the bacteria necessary for this process are upwelling from the subsurface, and therefore, this light limited treatment may

provide more insight into subsurface processes than those of the water column. A thesis by Rader found a similar reduction of sulfate occurring in the subsurface of SBC in close proximity to this experiment (2019). Another thesis by Schmidt found sulfate reducing bacteria present in nearby flooded mines (2017).

Groundwater flows from these mines towards SBC, but this groundwater is supposed to be intercepted by the West Camp Extraction Well (Gammons et al., 2009). However, with the subsurface sulfur concentrations in Rader's thesis, the microbes found in Schmidt's, and the sulfur reduction seen in these microcosm experiments, it is incredibly likely that groundwater from flooded mines still enters SBC (Schmidt, 2017; Rader, 2019). Metagenomic analysis of the microbial communities, isotope analysis, and groundwater flow modeling could confirm this hypothesis.

Further water quality degradation occurred in the sulfate reducing microcosm in the form of a pH drop (Fig. 23). The expected behavior of a pH increase, correlating with carbon dioxide consumption, occurred in all other treatments (Fig. 23). The decrease in this bottle further indicates atypical metabolism took place in the middle dark microcosm at Slag Canyon (Fig. 23).

4.6. Caveats

Microcosm incubation did not account for the transient nature of a creek. Consequently, the actual limitation in the creek may not be the same as the limitation demonstrated in the microcosms. During the experiment, it took up to 20 days to see a nutrient limitation, and the water only remains at any place in the creeks for a few minutes. Flow carries much of the nutrient load downstream, making the impacts of light much more significant. A 24-hour experiment may be more representative of the immediate light effects in the creek, but 23 days based on the reconnaissance experiment likely represents total potential growth. In the 23-day

experiment, light limitations were still evident, but still allowed observation of potential nutrient limitations.

Variability in the atmosphere and water surfaces makes PAR a difficult parameter to measure accurately (Long et al., 2012). When deploying the boxes, most of the PAR measurements match the tinting of the boxes, but at KOA the tinting did not appear as functional. The possibility exists that unobstructed sunlight renders the tinting less useful at KOA. It is more likely that obstruction, such as clouds in the atmosphere or texture of the water surface, changed between these initial measurements and created this drastic change (Long et al., 2012).

Being designed and built in house, the light exclusion boxes suffer several design flaws which caused multiple periods where the boxes had broken up or flipped. In the process, the microcosms received more light than intended for a period of time no more than 72 hours (Appendix A). Several of these failures also resulted in the loss of microcosms (Appendix A). Although many microcosms potentially received additional light, and the additional light could accelerate photosynthetic growth beyond the parameters of the experiment, most of the exposures happened overnight or during heavy rainstorms, and natural attenuation of light should have limited the impacts from these exposures.

Originally, this experiment included a series of sandblasted slides to compare growth in the benthos. Silicone adhered these slides to the boxes, and the silicone held the slides too well, resulting in breakage of the slides upon removal. Freezing the slides at -80° C kept the microbial communities preserved and determining a precise surface area while keeping slides cold enough to maintain unaltered microbial communities prohibited accurate extraction.

5. Conclusions

The bulk of the microbial work on Silver Bow and Blacktail Creeks comes out of the Laboratory Exploring Geobiochemical Engineering and Natural Dynamics, making this 23-day light exclusion experiment one of the first full studies published on microbes in these creeks (Foster and Cox, 2016). Light often proved impactful on the rate of photosynthetic growth that occurred during this study at four sites in the creeks with variable light exposure. Phosphorus also appeared as a limitation to photosynthetic growth, and the impact of light did not outweigh the effects of phosphorus. Despite the limitation imposed by phosphorus, light often appeared more impactful in the creek since light most directly impacts the growth rate and streams are very transient. Instead, a synergistic colimitation between phosphorus and light together created the limiting factor in this ecosystem.

After 23 days, much of the aqueous chemistry within the 30 microcosms changed as expected. Atypical changes occurred, however. One major unexpected change occurred in the darkest microcosms at Slag Canyon. These microcosms contained the least amount of photosynthetic growth, and photosynthesis could not support oxygenation of the microcosm. Typical nitrate reduction occurred in two of the triplicates, but one showed sulfate reduction, which usually does not occur until most or all of the nitrogen has been reduced.

Much of the aqueous chemistry did follow predictable changes. For instance, alkaline earth metals, halogens, selenium, silicon, gallium, manganese, iron, zinc, nitrate, phosphate, and sulfate behaved like nutrients and became depleted, whereas, copper became enriched. Iron and zinc exhibited both behaviors. Nutrient use and particle behavior explain the bulk of these changes.

Remediation efforts have improved the fundamental parameters of the creek, such as pH. These parameters – pH, dissolved oxygen, temperature, and specific conductivity – reflect a typical, healthy creek. Additionally, light and phosphorus make up the predominant limitations in the study area, typical for inland waters. Many metal concentrations, notably copper, zinc, iron, arsenic, and mercury, in SBC remain at elevated levels, and incredible variability exists in nitrogen to phosphorus ratios. Therefore, even though future restoration efforts need to be focused on remediating metals, nutrient loading and light exposure to the creeks needs to be controlled to maintain creek health. Increasing shading will help reduce temperature and increase oxygen solubility. This could improve fish habitat, but since limiting light will in turn limit photosynthesis, it will increase nutrient loading to lower parts of the stream, including the warm spring ponds and possibly the Upper Clark Fork River. Additionally, anoxic conditions in microcosms raise concerns about contaminated groundwater flowing from flooded mines to the creek, which may be impeding progress of remediation efforts.

6. Future Work

If this experiment were to be repeated, measures would need to be taken to prevent the exposure and microcosm loss failures. This could include a simple pin system to lock the lids of boxes in place, and longer stakes or rebar for holding the boxes in place. Volumes in the microcosms limited the ability to conduct a full nutrient uptake experiment, with samples being taken for chemistry at each timepoint to observe temporal changes in uptake. Conducting such an experiment may confirm that light is limiting nutrient uptake.

Conducting genomic studies into the metabolic potential for halogenation and sulfate reduction would confirm microbes drive these processes. Sequencing 16S/18S rRNA genes for microbial diversity and comparing species to those in the thesis by Schmidt could find similar organisms to those found in the nearby West Camp Mines (2017). If similar species are found, metagenomic sequencing should be considered for the creek and mines to confirm any close ties between these communities. Microbial diversity could also be compared to the species in Weigold et al. looking for species known to halogenate organic compounds. Gene specific PCR could be conducted to analyze for key genes in related biochemical pathways.

Similarly, culturing experiments could be conducted to verify these processes, as well as discern if toxic, mining-related metals create limitations for which this experiment could not account. To determine toxicity, a medium similar to the creek could be constructed and varying the metal contents to simulate the creek as it is, and any possible changes in the creek that would either increase or decrease metal content, such as stormwater flow or remediation. This would also be an opportunity to test how federal and state standards may impact microbial communities. Culturing in a lab allows for more control, and conditions could be adjusted to

specifically select for organisms that partake in the proposed metabolism. Culturing could,

therefore, provide confirmation of the presence of these metabolisms.

7. References Cited

Adamson, R. P., Sommerfeld, M. R. 1980. Laboratory comparison of the effectiveness of several algicides on isolated swimming pool algae. *App.and Environ. Microbio.* 80(02): 348-356.

Agarwal, L., Prakash, A., Purohit, H. J. 2019. Expression of autotrophic genes under CO2 environment and genome mining of desert bacterium *Cupriavidus sp*. HPC(L). *Bior. Tech. Reports.* 7:100258

Ansari, A. A., Lanza, G. R., Gill, S. S., Rast, W. 2011. *Eutrophication: Causes, Consequences and Control.* Springer Science + Business Media, New York, 1-386.

Arar, E. J., Collins, G. B. 1997. In vitro determination of chlorophyll a and pheophytin a in marine and freshwater algae by fluorescence. *Method 44.5*. U.S. Environmental Protection Agency, Cincinnati, Ohio.

Baah, D. A. 2018. Using microalgae to remediate food and bio-digester effluents from western New York agro industries and prospecting harvested algae biomass for biofuel feedstocks. Masters Thesis, Rochester Institute of Technology, Rochester, New York, USA. 13425693.

Betrand, E. M., McCrow, J. P., Moustafa, A., Zheng, H., Mcquaid, J. B., Delmont, T. O., Post, A. F., Sipler, R., E., Spackeen, J. L., Xu, K., Bronk, D. A., Hutichins, D. A. 2015. Phytoplankton–bacterial interactions mediate micronutrient colimitation at the coastal Antarctic sea ice edge. *PNAS*. 112:9938-9943.

Borsetti, F., Pial, F. D., D'Alessio, F., Stefan, A., Brandimarti, R., Sarkar, A., Datta, A., Silva, A. M., den Blaauwen, T., Alberto, M., Spinsni, E., Hochkoeppler, A. 2018. Manganese is a *Deinococcus radiodurans* growth limiting factor in rich culture medium. *Microbio*. 164:1266-1275.

Boyle, E. A., Sclater, F. R., and Edmond, J. M. 1977. The distribution of dissolved copper in the Pacific. *Earth Planet. Sci*. Lett. 37: 38-54.

Broman, E., Sjöstedt, J., Pinhassi, J., Dopson, M. 2017. Shifts in coastal sediment oxygenation cause pronounced changes in microbial community composition and associated metabolism. *Microbiome*. 5:96.

Bruland, K. W. 1980. Oceanographic distributions of cadmium, zinc, nickel and copper in the North Pacific. *Earth Planet. Sci. Lett*. 47, 176-198.

Bruland, K.W., Lohan, M.C. 2003. Controls of trace metals in seawater. Treat. On Geochem. 6:23-47.

Carpenter, L. J., Liss, P.S. 2000. On temperate sources of bromoform and other reactive organic bromine gases. *J. Geophys. Res.* 105:20539-20547.

Cox, A. D. 2011. Interactions of cadmium, zinc, and phosphorus in marine *Synechococcus*: Field uptake, physiological and proteomic studies. Ph.D. Dissertation, Massachusetts Institute of Technology, Cambridge, Massachusetts.

Cristian, R. R., Forés, E., Comin, F., Viaroli, P., Naldi, M., Ferrari, I. 1995. Nitrogen cycling networks of coastal ecosystems: influence of trophic status and primary producer form. *Ecol. Mod.* 97:111-129.

Cushing, D. H., Horwood, J. W. 1998. Experiments on nutrient limitation in bottles. *J. Plank. Res.* 20:1527-1538.

Dahlquist, G. 2017. Foundations for geobiochemical characterization of mudpots in Yeallowstone National Park. Masters Thesis, Montana Tech of the University of Montana, Butte, Montana. Montana Tech Graduate Thesis 132.

Dalsgaard, T., Canfield, D. E., Petersen, J. Thamdrup, B., Acuna-Gonzalezm J. 2003. N2 production by the anammox reaction in the anoxic water column of Golfo Dulce, Costa Rica. *Nat.* 422:606-608.

Dao, H. T., Beardall, J. 2016. Effects of lead on growth, photosynthetic characteristics and production of reactive oxygen species of two freshwater green algae. *Chemosphere* 147:420-429.

Department of Environmental Quality, Environmental Protection Agency. 1995. Streamside tailings operable unit of the Silver Bow Creek / Butte area national priorities list site. *Record of Decision*. 1-36.

Ekdahl, A., Pedesrsén, M., Abrahamsson, K. 1998. A study of the diurnal variation of biogenic volatile halocarbons. *Mar. Chem.* 63:1-8.

Entsch, B., Sim, R. G., Hatcher, B. G. 1983. Indications from photosynthetic components that iron is a limiting nutrient in primary producers on coral reefs. *Mar. Bio.* 73:17-30.

Environmental Protection Agency. 2011. Third five-year review report for Silver Bow Creek/Butte area site. *Five-Year Review Report*. U.S. Environmental Protection Agency, Helena, Montana.

Environmental Protection Agency. 2018. Draft surface water technical impracticability evaluation, Butte Priority Soils Operable Unit. *Silver Bow Creek/Butte Area NPL Site*.

Foster, J., Cox, A., 2016. Storm water in Silver Bow and Blacktail Creeks: Implications for the microbial community. *Intermountain J. of Sci.* 22:133. Butte, Montana, p. 3038.

Fraústo da Silva, J.J.R., & Williams, R. J. P. 1991. *The Biological Chemistry of the Elements*. Oxford University Press, New York.

Greenwood, N. N., Earnshaw, A. 1997. *In Chemistry of the Elements*. Elsevier Ltd. Burlington, pp. 107-138.

Grundl, T. J., Haferlien, S., Nurmi, J. T., Tratnyek, P. G. 2011. Introduction to aquatic redox chemistry. *Aquatic Redox Chemistry*. ACS Symposium Series, 1071:1-14.

Harder, J., Probian, C. 1995. Microbial degradation of monoterpenes in the absence of molecular oxygen. *Applied Environmental Microbiology*. 61.11:3804-3808.

Hill, W. 1996. Effects of light. *In* Stevenson, R. J., Bothwell, M. L. & Lowe, R. L. [Eds.] *Algal Ecology.* Academic Press, San Diego, pp. 121–48.

Hill, W. R., Roberts, B.J., Francoeur, S. N., and Fanta, S. E. 2011. Resource synergy in stream periphyton communities. *J. of Ecol.* 99:454-463.

Hutchins, M. G., Johnson, A. C., De flandre-Vlandas, A., Comber, S., Posen, P., Boorman, D. 2010. Which offers more scope to suppress river phytoplankton blooms: Reducing nutrient pollution or riparian shading? *The Sci. of the Total Environ*. 408(21):5065-5077.

Johnson, P.W., and Sieburth J.M., 1979. Chroococcoid cyanobacteria in the sea: a ubiquitous and diverse phototrophic biomass. *L&O*. 24:925-935.

Kalrsson, A., Auer, N., Schulz-Bull, D., Abrahamsson, K. 2008. Cyanobacterial blooms in the Baltic – A source of halocarbons. *Mar. Chem.* 110:129-139.

Kaplan, J. 2016. Mineralogy and environmental geochemistry of Slag Canyon in Lower Area One, Butte, Montana. Masters Thesis, Montana Tech of the University of Montana, Butte, Montana. Montana Tech Graduate Thesis 79.

Karimi, R., Folt., Carol. 2006. Beyond macronutrients: element variability and multielement stoichiometry in freshwater invertebrates. *Ecol. Let.* 9:1273-1283.

Kazamia, E., Helliwell, K. E., Purton, S., Smith, A. G., 2016. How mutualisms arise in phytoplankton communities: building eco-evolutionary principles for aquatic microbes. *Ecol. Let.* 19:810-822.

Konopka, A. 1983. The effect of nutrient limitation and its interaction with light upon the products of photosynthesis in *Merismopedia tesnuissima* (cyanphyceae). *J. of Phycol.* 19:403-409.

Langmuir, D. 1997. *Aqueous Environmental Geochemitry.* Prentice Hall, Upper Saddle River, New Jersey, USA. 1-600.

Laviale, M., Frankenbach, S., Serôdio, J. 2016. The importance of being fast: comparative kinetics of vertical migration and non-photochemical quenching of benthic diatoms under light stress. *Mar. Biol.* 163:10.

Law, S. 2018. Hydrothermal water-rock reaction modeling with microbial considerations: Rabbit Creek Area, Yellowstone National Park, WY. Masters Thesis, Montana Technological University, Butte, Montana. Montana Tech Graduate Thesis 181.

Lawlor, D. W. 2002. Limitation to photosynthesis in water-stressed leaves: Stomata vs. metabolism and the role of ATP. *Anns. of Bot.* 89(7):871-885.

Lemon, E. R. 2018. *The Response of Plants to Rising Levels of Atmospheric Carbon Dioxide*. Routledge New York.

Lenz, M., Lens, P.N.L. 2009. The essential toxin: The changing perception of selenium in environmental sciences. *Sci. of the Total Environ.* 407:3620-3633.

Liebig, J. 1840. *Organic chemistry in its applications to agriculture and physiology.* Taylor and Walton, London, pp. 1-387.

Lim, N. Y. N., Frostegard, A., Bakken, L. R. 2018. Nitrite kinetics during anoxia: The role of abiotic reactions versus microbial reduction. *Soil Bio. And Biochem.* 119:203-209

Litchman, E., Klausmeier, C. A., Yoshiyama, K. 2009. Contrasting size evolution in marine and freshwater diatoms. *PNAS early Ed.* 106 (8): 2665-2670.

Liu, Y., Yvon-Lewis, S. A., Thornton, D. C. O., Campbell, L., Bianchi, T. S. 2013. Spatial distribution of brominated very short-lived substances in the eastern Pacific. *J. Geophys. Research.* 118:2318-2328.

Long, M. H., Rheuban, J. E., Berg, P., and Zieman, J. C. 2012. A comparison and correction of light intensity loggers to photosynthetically active radiation sensors. *L&O Methods.* 10:416-424.

Martin, T. S., Casciotti K. L. 2016. Nitrogen and oxygen isotopic fractionation during microbial nitrite reduction. *L&O*. 61.3:1134-1143.

McLellan, E., Robertson, D., Schilling, K., Tomer, M., Kostle, J., Smith, D., King, K. 2015. Reducing nitrogen export from the corn belt to the Gulf of Mexico: Agricultural strategies for remediating hypoxia. *JAWRA*. 51:263-289.

Moris J. M., Farag, A. M., Nimick, D. A., Meyer, J.S. 2006. Light-mediated Zn uptake in photosynthetic biofilms. *Hydrobio*. 571:361-371

Natural Resource Damage Program. 2005. *Silver Bow Creek Watershed Restoration Plan*. State of Montana Natural Resources Damages Program, Helena, Montana, United States.

O'Kelley, J. C. 1968. Mineral nutrition of algae. *Annu. Rev. Plant. Physiol.* 19:89-112.

Oakes, K. 2018. Lessons from early Earth. *New Scientist*. 239:39-41.

Pol, A., Barends, T. R. M., Dietl, A., Khadem, A. F., Eygensteyn, J., Jetten, M. S. M., Op den Camp, H. J. M. 2013. Rare earth metals are essential for methanotrophic life in volcanic mudpots. *Eniron. Micorbio*. 16(1):255-64.

Plumb, B. 2009. Geochemistry of nutrients in Silver Bow Creek, Butte, Montana. Masters Thesis, Montana Tech of the University of Montana, Butte, Montana. EP31090

Quack, B., Peeken, I., Petrick, G., Nachtigall, K. 2007. Oceanic distribution and sources of bromoform and dibromomethane in the Mauritanian upwelling. *J. Geophys. Res.* 112:C10006

Rader, R. M. 2019. Geochemistry of metals and nutrients in fine-sediment pore water in Blacktail and Silver Bow Creeks, Butte, Montana. Masters Thesis, Montana Technological University, Butte, Montana. Montana Tech Graduate Thesis 204.

Redfield, A.C. 1958. The biological control of chemical factors in the environment. *Amer. Sci.* 46:205-22.

Rensing C., Rosen, B. P. 2009. Heavy metals cycle (arsenic, mercury, selenium, others). *Encyclopedia of Microbiology.* Academic Press, Cambridge, Massachusetts, USA, pp. 205-219.

Riebesell, U., Wolf-Gladrow, D.A., Smetacek V. 1993. Carbon dioxide limitation of marine phytoplankton growth rates. *Nat.* 361:249-251.

Roberts, S., Sabater, S., & Beardall, J. 2004. Benthic microalgal colonization in streams of differing riparian cover and light availability. *J. Phycol.* 40:1004-1012

Roesler, A. J., Gammons, C.H., Druschel, G. K., Orudro, H., Poulson, S. R. 2007. Geochemistry of flooded underground mine workings influenced by bacterial sulfate reduction. *Aquat. Geochem.* 13:211-235

Ruecker, A., Weigold, P., Behrens, S., Jochmann, M., Osorio Barajas, X. L., Kappler, A. 2015. Halogenated hydrocarbon formation in a moderately acidic Salt Lake in Western Australia – role of abiotic and biotic processes. *Environ. Chem.* 12:406-414.

Saito, M. A., Goepfert, T. J., Ritt, J. T. 2008. Some thoughts on the concept of colimitation: Three definitions and the importance of bioavailability. *L&O.* 53:276-290.

Sanches, L. F., Guariento, R.D., Caliman, A., Bozelli, R. L., Esteves, F. A. 2011. Effects of nutrients and light on periphytic biomass and nutrient stoichiometry in a tropical black-water aquatic ecosystem. *Hydrobio.* 669:35-44.

Sas, H. 1989. *Lake Restoration by Reduction of Nutrient Loading. Expectation, Experiences, Extrapolation.* Academia, St Augustin, BRD

Schindler, D. W. 1974. Eutrophication and recovery in Experimental Lakes: Implications for Lake Manage. *Sci.* 184:897-899.

Schmidt, R. 2017. Biogeochemical interactions in flooded underground mines. Masters Thesis, Montana Tech of the University of Montana, Butte, Montana. Montana Tech graduate thesis 129.

St Clair, B., Pottenger, J., Debes, R., Hanselmann, K., Schock, E. 2019. Distinguishing Biotic and Abiotic Iron Oxidation at Low Temperatures. *ACS Earth Space Chem.* 10.1021.

Stanley, D. W., and J. E. Hobbie. 1981. Nitrogen cycling in a North Carolina coastal river. *L&O.* 26:30–42.

Stevenson, R. J. 1996. An introduction to algal ecology in freshwater benthic habitats. *In* Stevenson, R. J., Bothwell, M. L. & Lowe, R. L. [Eds.] *Algal Ecology*. Academic Press, San Diego, pp. 3–30.

Stewart, W. D. P. 1967. Bromide a substitute for chloride in a marine algal medium. *Nat.* 214:604-605.

Stumm, W., Morgan, J. J. 1996. *Aquatic Chemistry*. John Wiley and Sones, Inc, New York, USA. 1-1022.

Thamdrup, B., Dalsgaard, T. 2002. Production of N_2 through anaerobic ammonium oxidation coupled to nitrate reduction in marine sediments. *App. And Enviro. Microbio.* 68.3:1312-1318.

Thornton, J.A., Rast W, Holland, M.M., Jolankai, G., Ryding S.O. 1999. Assessment and control of nonpoint source pollution of aquatic ecosystems. A practical approach. MaBSeries. UNESCO, Paris, 23:1–466.

Vetrivel, S. A., Diptanghu, M., Ebhin, M. E., Sydavalli, S., Guarav, N., Tiger, K. P. 2017. Green algae of the genus *Spirogyra*: A potential absorbent for heavy metal from coal mine water. *Remediation.* 27:81-90.

Waldron, K. J., Rutherford, J.C., Ford, D., Robinson, N. J. 2009. Metalloproteins and metal sensing. *Nat.* 460:823-830.

Warner, M. E., Madden, M. L. 2006. The impact of shifts to elevated irradiance on the growth and photochemical activity of the harmful algae *Chattonella subsalsa* and *Prorocentrum minimum* from Delaware. *Harm. Alga.* 6:332-342.

Waterbury, J. B., Watson, S. W., Guillard. R. R. L., Brand, L. E. 1979. Widespread occurrence of a unicellular marine planktonic cyanobacterium. *Nat*. 277:293-294.

Wehr, J.D., Sheath, R. G. 2003. Freshwater Habitats of Algae. *Freshwater Algae of North America.* Elsevier Science, USA, pp 11-57.

Weigold, P., El-Hadidi, M., Ruecker, A., Huson, D. H., Scholten, T., Jochmann, M., Kappler, A., & Behrens, S. 2016. A metagenomic-based survey of microbial (de)halogenation potential in a German forest soil. *Sci. Rep.* 6:28958.

Welschmeyer, N. A. 1994. Fluorometric analysis of chlorophyll *a* in the presence of chlorophyll *b* and pheopigments. *L&O.* 39(8): 1985-1992.

Wolf, D., Georgic, W., Klaiber, H. A. 2017. Reeling in the damages: Harmful algal blooms' impact on Lake Erie's recreational fishing industry. *J. of Enviro. Manag.* 199:148-157.

Yan, Z., Chen, S., Li, J., Alva, A., Chen, Q. 2016. Manure and nitrogen application enhances soil phosphorus mobility in calcareous soil in greenhouses. *J. Enviro. Manag.* 181:26-35.

8. Appendix A: Timeline of Sampling Days and Unplanned Exposures and Losses

Sunday	Monday	Tuesday	Wednesday	Thursday	Friday	Saturday
12-Aug	13	14	15	16 Day 0 Boxes in Sample 1	17 Day 1	18 Day 2
19 Day 3 All boxes at Slag found down stream. Medium Box exposed to atypical light ≤ 12hrs. Light box broke up and bottles moved to new light box.	20 Day 4 Sample 2	21 Day 5	22 Day 6	23 Day 7	24 Day 8	25 Day 9
26 Day 10	27 Day 11	28 Day 12 Sample 3 Dark Box at Thompson upside down and exposed to atypical ≤72hrs, and bottle 3 lost. Medium box at KOA upside down and exposed to atypical ≤72hrs. Medium box at Slag Canyon lost lids and expsoed to atypical light ≤72hrs. Light and dark box at Santa lost lids and expsoed to atypical light ≤72hrs. Bottle 3 lost in both treaments.	29 Day 13	30 Day 14	31 Day 15 Sample 4	1-Sep Day 16
2 Day 17 Medium box at Thompson bottle 2 lost and recoverd. It was expsoed to exess light ≤ 48 hrs. Dark box at KOA lid off and exposed to extra light ≤ 48 hrs. Medium box upsidedown and exposed to extra light ≤ 48 hrs. Dark box at Slag canyon lid off and exposed to extra light ≤ 48 hrs.	3 Day 18 Sample 5 Thompson medium box lost bottle 2.	4 Day 19 Sample 6	5 Day 20 Sample 7	6 Day 21 Sample 8 Slag Canyon Dark all bottles exposed to extra light ≤ 24 hrs.	7 Day 22	8 Day 23 Boxes out Sample 9 Santa medium box lid off and expsoed to extra light ≤ 24 hrs. Drak box all bottle lost.

Figure 24: Sampling calendar.

9. Appendix B: Raw Data

Table I: Field Parameters

Site	Date (YYMMDD)	Treatment	Latitude (°)	Longitude (°)	pH	pH Error	Temperature (°C)	Temp. Error	Specific Conductivity (µS/cm)	Specific Conductivity Error
Thompson	180816	Initial	45.8727	-112.4560	8.30	0.01	10.9	0.1	220	1
Thompson	180908	Light			8.85	0.01	11.5	0.1		
Thompson	180908	Medium			9.31	0.01	11.5	0.1		
Thompson	180908	Dark			9.33	0.01	11.5	0.1		
KOA	180816	Initial	45.9919	-112.5299	8.04	0.02	15.2	0.1	340	2
KOA	180908	Light			8.67	0.01	14.9	0.1		
KOA	180908	Medium			8.60	0.01	14.9	0.1		
KOA	180908	Dark			8.77	0.01	14.9	0.1		
Slag Canyon	180816	Initial	45.9958	-112.5391	8.10	0.01	12.3	0.1	257	1
Slag Canyon	180908	Light			9.07	0.01	12.5	0.1		
Slag Canyon	180908	Medium			8.62	0.01	12.5	0.1		
Slag Canyon	180908	Dark			9.31	0.01	12.5	0.1		
Slag Canyon	180908	Dark			4.45	0.01	12.5 12.5	0.1		
Slag Canyon	180908	Dark			9.50	0.01		0.1		
Santa	180816	Initial	46.0092	-112.7321	8.20	0.02	17.7	0.1	637	3
Santa	180908	Light			7.80	0.01	13.0	0.1		
Santa	180908	Medium			8.94	0.01	13.0	0.1		
Santa	NA	Dark			NA	NA	NA	NA	NA	NA

Measured by *in situ* meters. Reported error is variability in the reading. NA=sample not taken

All Dark Bottles at Santa were lost.

Table II: Major Anions

Sample Name	Date (YYMMDD)	Treatment	F⁻ (mol kg⁻¹)	F⁻ %Error	Cl⁻ (mol kg⁻¹)	Cl⁻ %Error	Br⁻ (mol kg⁻¹)	Br⁻ %Error	SO₄⁻² (mol kg⁻¹)	SO₄⁻² %Error
Thompson	180816	Initial	9.3E-06	7.6%	1.28E-04	1.3%	BDL	1.8%	9.4E-05	1.6%
Thompson	180908	Light	9.0E-06	7.6%	1.24E-04	1.3%	BDL	1.8%	8.9E-05	1.6%
Thompson	180908	Medium	8.5E-06	7.6%	1.20E-04	1.3%	BDL	1.8%	8.0E-05	1.6%
Thompson	180908	Dark	9.4E-06	7.6%	1.48E-04	1.3%	BDL	1.8%	9.6E-05	1.6%
KOA	180816	Initial	1.3E-05	7.6%	4.91E-04	1.3%	7.9E-07	1.8%	3.2E-04	1.6%
KOA	180908	Light	1.1E-05	7.6%	4.96E-04	1.3%	BDL	1.8%	3.2E-04	1.6%
KOA†	180908	Light	6.0E-05	7.6%	7.58E-04	1.3%	1.37E-05	1.8%	8.5E-04	1.6%
KOA	180908	Medium	1.1E-05	7.6%	4.96E-04	1.3%	BDL	1.8%	3.1E-04	1.6%
KOA	180908	Dark	1.2E-05	7.6%	4.03E-04	1.3%	BDL	1.8%	2.7E-04	1.6%
Slag Canyon	180816	Initial	1.2E-05	7.6%	4.32E-04	1.3%	7.0E-07	1.8%	2.9E-04	1.6%
Slag Canyon	180908	Light	1.3E-05	7.6%	5.56E-04	1.3%	BDL	1.8%	3.3E-04	1.6%
Slag Canyon	180908	Medium	1.2E-05	7.6%	4.51E-04	1.3%	BDL	1.8%	2.7E-04	1.6%
Slag Canyon	180908	Dark 1	1.2E-05	2.1%	5.19E-04	1.8%	BDL	1.5%	3.1E-04	1.7%
Slag Canyon	180908	Dark 2	4.0E-06	7.6%	1.42E-05	1.3%	BDL	1.8%	1.6E-05	1.6%
Slag Canyon*	180909	Dark 2	4.1E-06	7.6%	1.47E-05	1.3%	BDL	1.8%	1.8E-05	1.6%
Slag Canyon	180908	Dark 3	1.2E-05	2.1%	5.19E-04	1.8%	BDL	1.5%	3.2E-04	1.7%
Santa	180816	Initial	2.0E-05	7.6%	1.24E-03	1.3%	1.63E-06	1.8%	1.2E-03	1.6%
Santa	180908	Light	1.8E-05	7.6%	1.25E-03	1.3%	1.18E-06	1.8%	1.2E-03	1.6%
Santa	180908	Medium	1.7E-05	7.6%	1.19E-03	1.3%	1.30E-06	1.8%	1.2E-03	1.6%
Santa	NA	Dark	NA	NA	NA	NA	NA	NA	NA	NA
Detection limit			5.3E-07		2.80E-07		1.25E-07		5.2E-06	

Analyzed by IC. Percent error represents instrumental error. BDL=below detection limit NA=sample not taken

All Dark Bottles at Santa were lost.
*Quality control duplicate
†Quality Control Spike

Table II: Continued – Major Anions.

Sample	PO$_4^{-3}$ (mol kg^{-1})	PO$_4^{-3}$ %Error	NO$_2^-$ (mol kg^{-1})	NO$_2^-$ %Error	NO$_3^-$ (mol kg^{-1})	NO$_3^-$ %Error
Thompson I	2.63E-07	3.2%	BDL	1.7%	7.4E-07	1.5%
Thompson L	BDL	3.2%	BDL	1.7%	1.05E-06	1.5%
Thompson M	BDL	3.2%	BDL	1.7%	BDL	1.5%
Thompson D	2.32E-07	3.2%	BDL	1.7%	6.8E-07	1.5%
KOA I	4.0E-07	3.2%	BDL	1.7%	1.90E-05	1.5%
KOA L	BDL	3.2%	BDL	1.7%	BDL	1.5%
KOA L†	1.02E-05	3.2%	1.37E-05	1.7%	1.70E-05	1.5%
KOA M	BDL	3.2%	BDL	1.7%	BDL	1.5%
KOA D	BDL	3.2%	BDL	1.7%	6.3E-07	1.5%
Slag Canyon I	4.95E-07	3.2%	BDL	1.7%	1.59E-05	1.5%
Slag Canyon L	BDL	3.2%	BDL	1.7%	4.81E-06	1.5%
Slag Canyon M	BDL	3.2%	BDL	1.7%	6.0E-06	1.5%
Slag Canyon D1	BDL	1.3%	3.17E-06	1.1%	1.92E-05	1.1%
Slag Canyon D2	BDL	3.2%	BDL	1.7%	1.41E-05	1.5%
Slag Canyon D2*	BDL	3.2%	BDL	1.7%	1.51E-05	1.5%
Slag Canyon D3	BDL	1.3%	3.33E-06	1.1%	1.92E-05	1.1%
Santa I	3.8E-07	3.2%	BDL	1.7%	2.37E-05	1.5%
Santa L	BDL	3.2%	BDL	1.7%	5.71E-06	1.5%
Santa M	BDL	3.2%	BDL	1.7%	4.27E-06	1.5%
Santa D	NA	NA	NA	NA	NA	NA
Detection limit	2.11E-07		2.17E-07		1.61E-07	

Analyzed by IC. Percent error represents instrumental error. BDL=below detection limit NA=sample not taken

All Dark Bottles at Santa were lost.

*Quality control duplicate

†Quality Control Spike

Table III: Major Cations

Sample Name	Date (YYMMDD)	Treatment	Li⁺ (mol kg⁻¹)	Li⁺ %Error	Na⁺ (mol kg⁻¹)	Na⁺ %Error	K⁺ (mol kg⁻¹)	K⁺ %Error
Thompson	180816	Initial	BDL	2.7%	2.2E-04	5.8%	3.91E-05	1.7%
Thompson†	180816	Initial	1.49E-04	2.7%	2.6E-04	5.8%	2.97E-04	1.7%
Thompson	180908	Light	BDL	2.7%	2.3E-04	5.8%	3.89E-05	1.7%
Thompson	180908	Medium	BDL	2.7%	2.4E-04	5.8%	4.99E-05	1.7%
Thompson*	180908	Medium	BDL	2.7%	2.4E-04	5.8%	4.87E-05	1.7%
Thompson	180908	Dark	BDL	2.7%	2.4E-04	5.8%	5.14E-05	1.7%
Thompson†	180908	Dark	1.44E-04	2.7%	2.8E-04	5.8%	3.07E-04	1.7%
KOA	180816	Initial	BDL	2.7%	5.5E-04	5.8%	7.4E-05	1.7%
KOA	180908	Light	BDL	2.7%	5.5E-04	5.8%	7.1E-05	1.7%
KOA	180908	Medium	BDL	2.7%	5.5E-04	5.8%	7.3E-05	1.7%
KOA	180908	Dark	BDL	2.7%	6.0E-04	5.8%	7.2E-05	1.7%
Slag Canyon	180816	Initial	BDL	2.7%	6.1E-04	5.8%	7.7E-05	1.7%
Slag Canyon*	180816	Initial	BDL	2.7%	6.0E-04	5.8%	7.7E-05	1.7%
Slag Canyon	180908	Light	BDL	2.7%	6.3E-04	5.8%	8.9E-05	1.7%
Slag Canyon	180908	Medium	BDL	2.7%	6.4E-04	5.8%	9.0E-05	1.7%
Slag Canyon*	180908	Medium	BDL	2.7%	6.3E-04	5.8%	8.9E-05	1.7%
Slag Canyon	180908	Dark 1	BDL	3.9%	6.4E-04	3.6%	9.7E-05	2.0%
Slag Canyon	180908	Dark 2	BDL	2.7%	6.7E-04	5.8%	9.5E-05	1.7%
Slag Canyon†	180908	Dark 2	1.45E-04	2.7%	6.5E-04	5.8%	3.48E-04	1.7%
Slag Canyon	180908	Dark 3	BDL	3.9%	2.2E-04	3.6%	1.0E-04	2.0%
Santa	180816	Initial	5.9E-06	2.7%	1.8E-03	5.8%	1.49E-04	1.7%
Santa	180908	Light	5.4E-06	2.7%	1.7E-03	5.8%	1.70E-04	1.7%
Santa	180908	Medium	5.5E-06	2.7%	1.7E-03	5.8%	1.48E-04	1.7%
Santa	NA	Dark	NA	NA	NA	NA	NA	NA
Detection limit			3.14E-06		8.00E-07		9.2E-07	

Analyzed by ICP-OES. Percent error represents instrumental error. BDL=below detection limit NA=sample not taken

All Dark Bottles at Santa were lost.

*Quality control duplicate †Quality Control Spike

Table III: Continued – Major Cations

Sample	Mg^{+2} (mol kg^{-1})	Mg^{+2} %Error	Ca^{+2} (mol kg^{-1})	Ca^{+2} %Error	Si^{+4} (mol kg^{-1})	Si^{+4} %Error
Thompson I	2.89E-04	2.5%	3.9E-04	2.7%	4.13E-07	1.1%
Thompson I†	3.22E-04	2.5%	3.9E-04	2.7%	4.26E-07	1.1%
Thompson L	2.89E-04	2.5%	3.9E-04	2.7%	3.67E-07	1.1%
Thompson M	2.88E-04	2.5%	3.9E-04	2.7%	2.99E-07	1.1%
Thompson M*	2.90E-04	2.5%	3.9E-04	2.7%	2.95E-07	1.1%
Thompson D	2.90E-04	2.5%	4.0E-04	2.7%	3.56E-07	1.1%
Thompson D†	3.23E-04	2.5%	4.0E-04	2.7%	3.66E-07	1.1%
KOA I	6.2E-04	2.5%	5.4E-04	2.7%	4.42E-07	1.1%
KOA L	3.64E-04	2.5%	2.35E-04	2.7%	2.58E-07	1.1%
KOA M	3.67E-04	2.5%	2.20E-04	2.7%	2.22E-07	1.1%
KOA D	3.73E-04	2.5%	2.57E-04	2.7%	1.99E-07	1.1%
Slag Canyon I	3.83E-04	2.5%	5.6E-04	2.7%	4.66E-07	1.1%
Slag Canyon I*	4.0E-04	2.5%	5.7E-04	2.7%	4.66E-07	1.1%
Slag Canyon L	3.79E-04	2.5%	2.21E-04	2.7%	2.15E-07	1.1%
Slag Canyon M	3.78E-04	2.5%	2.47E-04	2.7%	2.19E-07	1.1%
Slag Canyon M*	3.78E-04	2.5%	2.48E-04	2.7%	2.18E-07	1.1%
Slag Canyon D1	4.2E-04	3.7%	5.7E-04	4.6%	4.42E-07	1.7%
Slag Canyon D2	4.0E-04	2.5%	5.6E-04	2.7%	4.27E-07	1.1%
Slag Canyon D2†	4.2E-04	2.5%	5.6E-04	2.7%	4.40E-07	1.1%
Slag Canyon D3	4.3E-04	3.7%	5.7E-04	4.6%	4.45E-07	1.7%
Santa I	6.2E-04	2.5%	8.1E-04	2.7%	3.95E-07	1.1%
Santa L	6.0E-04	2.5%	3.6E-04	2.7%	1.98E-07	1.1%
Santa M	6.0E-04	2.5%	3.6E-04	2.7%	2.23E-07	1.1%
Santa D	NA	NA	NA	NA	NA	NA
Detection limit	2.14E-07		1.26E-07		6.59E-10	

Analyzed by ICP-OES. Percent error represents instrumental error. BDL=below detection limit NA=sample not taken
All Dark Bottles at Santa were lost.
*Quality control duplicate †Quality Control Spike

Table IV: Trace Elements

Sample Name	Date (YYMMDD)	Treatment	Li (mol kg^{-1})	Li % Error	B (mol kg^{-1})	B % Error	Al (mol kg^{-1})	Al % Error
Thompson	180816	Initial	7.1E-07	1.9%	9.1E-07	4.7%	1.27E-06	2.2%
Thompson	180908	Light	6.8E-07	1.9%	8.6E-07	4.7%	2.63E-07	2.2%
Thompson	180908	Medium	7.9E-07	1.9%	1.0E-06	4.7%	2.05E-06	2.2%
Thompson	180908	Dark	7.3E-07	1.9%	9.6E-07	4.7%	2.92E-07	2.2%
KOA	180816	Initial	1.47E-06	1.9%	3.2E-06	4.7%	8.6E-07	2.2%
KOA	180908	Light	1.58E-06	1.9%	4.0E-06	4.7%	4.9E-07	2.2%
KOA	180908	Medium	1.37E-06	1.9%	3.4E-06	4.7%	3.02E-07	2.2%
KOA	180908	Dark	1.54E-06	1.9%	3.7E-06	4.7%	2.31E-07	2.2%
Slag Canyon	180816	Initial	1.54E-06	1.9%	3.9E-06	4.7%	2.53E-07	2.2%
Slag Canyon	180908	Light	1.55E-06	1.9%	4.0E-06	4.7%	7.2E-07	2.2%
Slag Canyon	180908	Medium	1.51E-06	1.9%	4.0E-06	4.7%	1.46E-07	2.2%
Slag Canyon	180908	Dark	1.24E-06	1.9%	2.8E-06	4.7%	1.68E-07	2.2%
Slag Canyon	180908	Dark	1.61E-06	1.9%	3.8E-06	4.7%	3.21E-07	2.2%
Slag Canyon	180908	Dark	1.46E-06	1.9%	3.0E-06	4.7%	1.68E-07	2.2%
Santa	180816	Initial	7.8E-06	1.9%	1.16E-05	4.7%	2.80E-07	2.2%
Santa	180908	Light	7.3E-06	1.9%	1.21E-05	4.7%	2.63E-07	2.2%
Santa*	180908	Light	6.9E-06	1.9%	1.24E-05	4.7%	2.83E-07	2.2%
Santa	180908	Medium	6.7E-06	1.9%	1.21E-05	4.7%	1.92E-07	2.2%
Santa†	180908	Medium	1.19E-05	1.9%	1.41E-05	4.7%	1.76E-06	2.2%
Santa	NA	Dark	NA	NA	NA	NA	NA	NA
Detection limit			7.8E-08		2.3E-08		1.85E-08	

Analyzed by ICP-OES. Percent error represents instrumental error. BDL=below detection limit NA=sample not taken

All Dark Bottles at Santa were lost.

*Quality control duplicate †Quality Control Spike

Table IV: Continued – Trace Elements

Sample	Ti (mol kg⁻¹)	Ti %Error	V (mol kg⁻¹)	V %Error	Cr (mol kg⁻¹)	Cr %Error	Mn (mol kg⁻¹)	Mn %Error	Fe (mol kg⁻¹)	Fe %Error
Thompson I	BDL	1.4%	3.00E-08	1.0%	BDL	1.1%	3.38E-07	2.6%	4.3E-06	4.5%
Thompson L	BDL	1.4%	3.87E-08	1.0%	BDL	1.1%	BDL	2.6%	2.8E-06	4.5%
Thompson M	2.75E-07	1.4%	4.22E-08	1.0%	4.71E-09	1.1%	BDL	2.6%	4.2E-06	4.5%
Thompson D	1.94E-07	1.4%	3.52E-08	1.0%	BDL	1.1%	7.2E-08	2.6%	5.1E-06	4.5%
KOA I	BDL	1.4%	8.21E-08	1.0%	4.71E-09	1.1%	8.6E-07	2.6%	1.48E-06	4.5%
KOA L	2.90E-07	1.4%	9.82E-08	1.0%	7.01E-09	1.1%	BDL	2.6%	4.5E-07	4.5%
KOA M	BDL	1.4%	8.60E-08	1.0%	BDL	1.1%	BDL	2.6%	1.18E-07	4.5%
KOA D	2.56E-07	1.4%	9.38E-08	1.0%	7.10E-09	1.1%	BDL	2.6%	BDL	4.5%
Slag Canyon I	2.48E-07	1.4%	7.73E-08	1.0%	BDL	1.1%	1.04E-06	2.6%	1.58E-06	4.5%
Slag Canyon L	2.44E-07	1.4%	8.71E-08	1.0%	5.70E-09	1.1%	BDL	2.6%	BDL	4.5%
Slag Canyon M	BDL	1.4%	7.09E-08	1.0%	6.03E-09	1.1%	BDL	2.6%	1.07E-07	4.5%
Slag Canyon D1	3.03E-07	1.4%	4.90E-09	1.0%	4.90E-09	1.1%	BDL	2.6%	BDL	4.5%
Slag Canyon D2	3.07E-07	1.4%	8.37E-08	1.0%	5.88E-09	1.1%	7.1E-08	2.6%	BDL	4.5%
Slag Canyon D3	3.04E-07	1.4%	4.63E-09	1.0%	4.63E-09	1.1%	BDL	2.6%	BDL	4.5%
Santa I	6.34E-07	1.4%	6.56E-08	1.0%	4.08E-08	1.1%	1.62E-06	2.6%	BDL	4.5%
Santa L	8.3E-07	1.4%	6.76E-08	1.0%	7.42E-09	1.1%	BDL	2.6%	BDL	4.5%
Santa L*	7.6E-07	1.4%	7.22E-08	1.0%	7.26E-09	1.1%	BDL	2.6%	BDL	4.5%
Santa M	6.58E-07	1.4%	5.73E-08	1.0%	BDL	1.1%	BDL	2.6%	BDL	4.5%
Santa M†	1.92E-05	1.4%	9.62E-07	1.0%	1.08E-06	1.1%	8.7E-07	2.6%	1.03E-06	4.5%
Santa D	NA	NA	NA	NA	NA	NA	NA	NA	NA	NA
Detection limit	2.44E-07		9.84E-09		4.59E-09		3.64E-08		9.76E-08	

Analyzed by ICP-MS. Percent error represents instrumental error. BDL=below detection limit NA=sample not taken

All Dark Bottles at Santa were lost.

*Quality control duplicate †Quality Control Spike

Table IV: Continued – Trace Elements.

Sample	Ni (mol kg⁻¹)	Ni %Error	Cu (mol kg⁻¹)	Cu %Error	Zn (mol kg⁻¹)	Zn %Error	Ga (mol kg⁻¹)	Ga %Error	As (mol kg⁻¹)	As %Error
Thompson I	BDL	2.8%	1.2E-07	9.7%	3.0E-07	3.6%	4.5E-08	3.1%	5.0E-08	3.8%
Thompson L	BDL	2.8%	1.4E-07	9.7%	3.3E-07	3.6%	4.4E-08	3.1%	5.0E-08	3.8%
Thompson M	3.5E-08	2.8%	1.9E-07	9.7%	2.8E-06	3.6%	4.5E-08	3.1%	5.0E-08	3.8%
Thompson D	4.6E-08	2.8%	2.2E-07	9.7%	8.8E-06	3.6%	5.0E-08	3.1%	5.1E-08	3.8%
KOA I	BDL	2.8%	6.0E-08	9.7%	9.5E-07	3.6%	1.44E-07	3.1%	6.3E-08	3.8%
KOA L	4.40E-08	2.8%	9.2E-08	9.7%	1.42E-07	3.6%	8.1E-08	3.1%	6.1E-08	3.8%
KOA M	BDL	2.8%	7.0E-07	9.7%	1.31E-07	3.6%	7.2E-08	3.1%	5.7E-08	3.8%
KOA D	BDL	2.8%	7.4E-08	9.7%	9.9E-08	3.6%	8.3E-08	3.1%	5.7E-08	3.8%
Slag Canyon I	BDL	2.8%	6.9E-08	9.7%	6.1E-07	3.6%	1.49E-07	3.1%	6.9E-08	3.8%
Slag Canyon L	7.1E-08	2.8%	1.9E-07	9.7%	2.09E-07	3.6%	7.9E-08	3.1%	6.4E-08	3.8%
Slag Canyon M	7.1E-08	2.8%	1.9E-07	9.7%	8.4E-08	3.6%	8.4E-08	3.1%	6.2E-08	3.8%
Slag Canyon D1	6.7E-08	2.8%	1.6E-07	9.7%	7.3E-07	3.6%	1.07E-07	3.1%	5.3E-08	3.8%
Slag Canyon D2	8.0E-08	2.8%	2.3E-07	9.7%	1.18E-06	3.6%	1.50E-07	3.1%	6.8E-08	3.8%
Slag Canyon D3	7.6E-08	2.8%	1.6E-07	9.7%	8.9E-07	3.6%	1.15E-07	3.1%	5.2E-08	3.8%
Santa I	BDL	2.8%	1.4E-07	9.7%	2.8E-06	3.6%	1.10E-07	3.1%	7.6E-08	3.8%
Santa L	1.0E-07	2.8%	2.1E-07	9.7%	6.9E-07	3.6%	6.2E-08	3.1%	6.9E-08	3.8%
Santa L*	1.14E-07	2.8%	2.1E-07	9.7%	6.7E-07	3.6%	6.0E-08	3.1%	6.8E-08	3.8%
Santa M	5.8E-08	2.8%	1.8E-07	9.7%	5.2E-07	3.6%	6.4E-08	3.1%	6.4E-08	3.8%
Santa M†	3.4E-06	2.8%	1.3E-06	9.7%	3.3E-06	3.6%	9.1E-07	3.1%	7.5E-07	3.8%
Santa D	NA	NA	NA	NA	NA	NA	NA	NA	NA	NA
Detection limit	3.3E-08		2.3E-08		5.5E-08		1.80E-08		2.7E-08	

Analyzed by ICP-MS. Percent error represents instrumental error. BDL=below detection limit NA=sample not taken

All Dark Bottles at Santa were lost.

*Quality control duplicate †Quality Control Spike

Table IV: Continued – Trace Elements.

Sample	Se (mol kg⁻¹)	Se %Error	Rb (mol kg⁻¹)	Rb %Error	Sr (mol kg⁻¹)	Sr %Error	Zr (mol kg⁻¹)	Zr %Error	Mo (mol kg⁻¹)	Mo %Error
Thompson I	BDL	3.7%	1.65E-08	3.7%	1.62E-06	2.8%	1.16E-08	2.9%	4.0E-07	3.2%
Thompson L	BDL	3.7%	1.74E-08	3.7%	1.71E-06	2.8%	BDL	2.9%	4.1E-07	3.2%
Thompson M	BDL	3.7%	2.46E-08	3.7%	1.68E-06	2.8%	BDL	2.9%	4.2E-07	3.2%
Thompson D	BDL	3.7%	2.8E-08	3.7%	1.82E-06	2.8%	1.31E-08	2.9%	4.6E-07	3.2%
KOA I	6.4E-08	3.7%	1.12E-08	3.7%	3.7E-06	2.8%	1.07E-08	2.9%	4.0E-07	3.2%
KOA L	6.0E-08	3.7%	1.23E-08	3.7%	2.81E-06	2.8%	2.11E-08	2.9%	4.1E-07	3.2%
KOA M	5.9E-08	3.7%	1.06E-08	3.7%	2.64E-06	2.8%	BDL	2.9%	3.8E-07	3.2%
KOA D	6.6E-08	3.7%	1.03E-08	3.7%	2.80E-06	2.8%	BDL	2.9%	3.8E-07	3.2%
Slag Canyon I	7.0E-08	3.7%	1.05E-08	3.7%	3.7E-06	2.8%	1.46E-08	2.9%	4.0E-07	3.2%
Slag Canyon L	BDL	37%	1.77E-08	3.7%	2.88E-06	2.8%	1.37E-08	2.9%	3.9E-07	3.2%
Slag Canyon M	5.9E-08	3.7%	1.83E-08	3.7%	2.96E-06	2.8%	BDL	2.9%	3.9E-07	3.2%
Slag Canyon D1	6.2E-08	3.7%	1.84E-08	3.7%	3.37E-06	2.8%	1.22E-08	2.9%	3.4E-07	3.2%
Slag Canyon D2	7.1E-08	3.7%	2.38E-08	3.7%	4.2E-06	2.8%	BDL	2.9%	4.4E-07	3.2%
Slag Canyon D3	6.5E-08	3.7%	1.91E-08	3.7%	3.4E-06	2.8%	BDL	2.9%	3.3E-07	3.2%
Santa I	8.8E-08	3.7%	6.9E-08	3.7%	7.4E-06	2.8%	BDL	2.9%	3.7E-07	3.2%
Santa L	8.5E-08	3.7%	7.1E-08	3.7%	6.0E-06	2.8%	BDL	2.9%	3.9E-07	3.2%
Santa L*	8.3E-08	3.7%	6.9E-08	3.7%	5.8E-06	2.8%	BDL	2.9%	3.6E-07	3.2%
Santa M	8.1E-08	3.7%	6.1E-08	3.7%	5.6E-06	2.8%	BDL	2.9%	3.3E-07	3.2%
Santa M†	7.2E-06	3.7%	4.3E-07	3.7%	4.9E-06	2.8%	5.29E-07	2.9%	2.50E-06	3.2%
Santa D	NA	NA	NA	NA	NA	NA	NA	NA	NA	NA
Detection limit	2.9E-08		8.1E-09		1.38E-08		1.07E-08		2.14E-08	

Analyzed by ICP-MS. Percent error represents instrumental error. BDL=below detection limit NA=sample not taken

All Dark Bottles at Santa were lost.

*Quality control duplicate †Quality Control Spike

Table IV: Continued – Trace Elements.

Sample	Pd (mol kg⁻¹)	Pd % Error	Sb (mol kg⁻¹)	Sb % Error	Cs (mol kg⁻¹)	Cs % Error	Ba (mol kg⁻¹)	Ba % Error	W (mol kg⁻¹)	W % Error
Thompson I	BDL	3.0%	2.99E-09	1.9%	BDL	2.3%	1.45E-06	2.7%	BDL	0.9%
Thompson L	BDL	3.0%	2.89E-09	1.9%	BDL	2.3%	1.41E-06	2.7%	BDL	0.9%
Thompson M	BDL	3.0%	3.27E-09	1.9%	BDL	2.3%	1.44E-06	2.7%	BDL	0.9%
Thompson D	BDL	3.0%	3.38E-09	1.9%	BDL	2.3%	1.53E-06	2.7%	4.52E-09	0.9%
KOA I	BDL	3.0%	3.51E-09	1.9%	BDL	2.3%	4.5E-06	2.7%	6.07E-09	0.9%
KOA L	BDL	3.0%	4.12E-09	1.9%	BDL	2.3%	2.62E-06	2.7%	1.00E-08	0.9%
KOA M	BDL	3.0%	3.32E-09	1.9%	BDL	2.3%	2.26E-06	2.7%	6.93E-09	0.9%
KOA D	BDL	3.0%	3.63E-09	1.9%	BDL	2.3%	2.69E-06	2.7%	7.53E-09	0.9%
Slag Canyon I	BDL	3.0%	3.77E-09	1.9%	BDL	2.3%	4.7E-06	2.7%	1.15E-08	0.9%
Slag Canyon L	BDL	3.0%	3.85E-09	1.9%	BDL	2.3%	2.47E-06	2.7%	1.06E-08	0.9%
Slag Canyon M	BDL	3.0%	3.86E-09	1.9%	BDL	2.3%	2.66E-06	2.7%	1.05E-08	0.9%
Slag Canyon D1	BDL	3.0%	2.92E-09	1.9%	BDL	2.3%	3.10E-06	2.7%	1.05E-08	0.9%
Slag Canyon D2	BDL	3.0%	4.44E-09	1.9%	BDL	2.3%	4.7E-06	2.7%	1.01E-08	0.9%
Slag Canyon D3	BDL	3.0%	2.93E-09	1.9%	BDL	2.3%	3.41E-06	2.7%	9.52E-09	0.9%
Santa I	3.4E-08	3.0%	7.7E-09	1.9%	4.76E-09	2.3%	3.6E-06	2.7%	2.25E-08	0.9%
Santa L	BDL	3.0%	8.1E-09	1.9%	4.45E-09	2.3%	1.95E-06	2.7%	2.15E-08	0.9%
Santa L*	BDL	3.0%	7.9E-09	1.9%	4.56E-09	2.3%	2.08E-06	2.7%	1.97E-08	0.9%
Santa M	BDL	3.0%	6.9E-09	1.9%	BDL	2.3%	1.94E-06	2.7%	1.65E-08	0.9%
Santa M†	7.3E-07	3.0%	7.8E-07	1.9%	2.00E-07	2.3%	5.2E-06	2.7%	1.97E-08	0.9%
Santa D	NA	NA	NA	NA	NA	NA	NA	NA	NA	NA
Detection limit	2.10E-08		2.87E-09		4.02E-09		6.48E-08		4.11E-09	

Analyzed by ICP-MS. Percent error represents instrumental error. BDL=below detection limit NA=sample not taken

All Dark Bottles at Santa were lost.

*Quality control duplicate †Quality Control Spike

Table IV: Continued – Trace Elements.

Sample	U (mol kg^{-1})	U % Error
Thompson I	6.7E-09	2.8%
Thompson L	7.0E-09	2.8%
Thompson M	6.9E-09	2.8%
Thompson D	7.3E-09	2.8%
KOA I	2.02E-08	2.8%
KOA L	2.24E-08	2.8%
KOA M	2.01E-08	2.8%
KOA D	2.20E-08	2.8%
Slag Canyon I	2.41E-08	2.8%
Slag Canyon L	2.12E-08	2.8%
Slag Canyon M	2.28E-08	2.8%
Slag Canyon D1	1.93E-08	2.8%
Slag Canyon D2	2.55E-08	2.8%
Slag Canyon D3	2.01E-08	2.8%
Santa I	3.38E-08	2.8%
Santa L	3.26E-08	2.8%
Santa L*	3.43E-08	2.8%
Santa M	2.95E-08	2.8%
Santa M[†]	1.32E-07	2.8%
Santa D	NA	NA
Detection limit	8.5E-10	

Analyzed by ICP-MS. Percent error represents instrumental error. BDL=below detection limit NA=sample not taken
All Dark Bottles at Santa were lost.
*Quality control duplicate [†]Quality Control Spike
The following elements were analyzed and concentrations were always below detection (detection limit in mol kg^{-1}): Co (3.32E-09), Nb (5.38E-09), Ag (3.58E-09), Cd (1.39E-08), Sn (1.74E-08), La (1.44E-09), Ce (1.61E-09), Pr (1.42E-09), Nd (8.07E-09), Tl (3.32E-09), Pb (1.84E-09), Th (8.62E-10)

10. Appendix C: Experimental Design: Box Plans, Construction, and Deployment
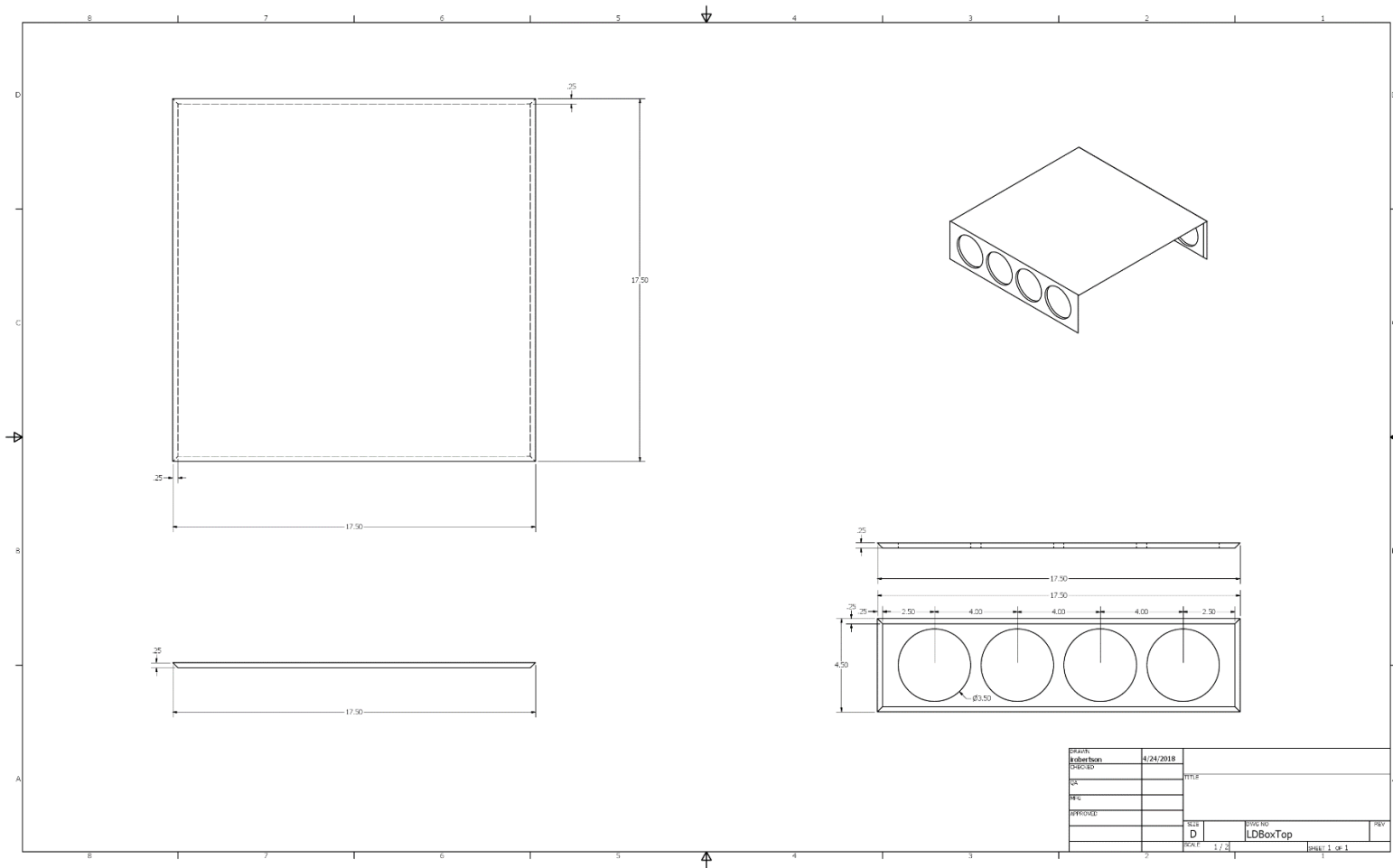
Figure 25: Plans for box lids.
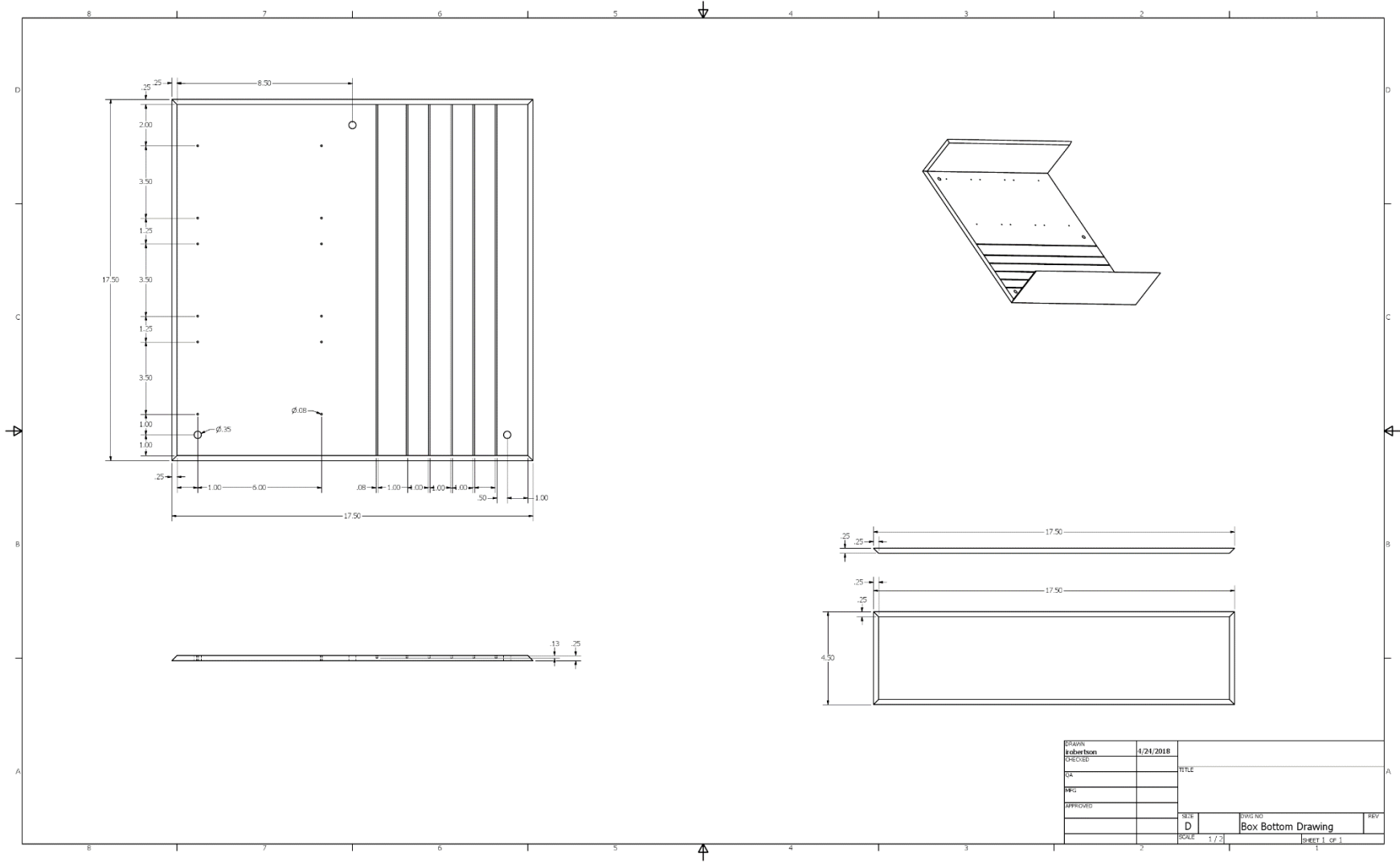
Figure 26: Plans for box base.

Figure 27: Constructed box with bottles and slides.

Figure 28: Tinted boxes.

Figure 29: Deployed boxes. (a) Thompson, (b) KOA, (c) Slag Canyon, and (d) Santa. Photo credit: A. Cox

Figure 30: Microcosm after 12 days of incubation at Santa.

11. Appendix C: *In Vivo* Chlorophyll

11.1. Methods

Throughout the 23-day incubation, eight samples were collected from within the microcosms and analyzed for *in vivo* chlorophyll. These samples were kept chilled in the dark for up to 24 hours before analysis on a TD 700 fluorometer (Turner Designs, Sunnyvale, CA, USA). For samples to be accurate and comparable, they should have been run immediately after collection. Relative fluorescence units (RFU) were calibrated to a sample from the clear box at KOA and set to 200 of 1000 RFU. Upon withdrawal, samples were taken for *in vivo* chlorophyll fluorescence, extracted chlorophyll *a*, major anions, major cations, and metals.

11.2. Results

At Santa, *in vivo* chlorophyll (Fig. 32b) increased most rapidly between days 18 and 22 and lowered slightly on day 23. Santa showed no difference in chlorophyll with light treatments. Upstream, *in vivo* chlorophyll at Slag Canyon (Fig. 32a) also increased most rapidly between days 18 and 22 and decreased slightly into day 23. The light and medium box generally showed the same trends, but the dark box at Slag Canyon had little to no change. In BTC, at KOA *in vivo* chlorophyll (Fig. 31b.) showed no separation between light treatments and increased most rapidly between days 12 and 19 and dropped off rapidly after day 19. *In vivo* chlorophyll at Thompson (Fig. 31a) showed its most rapid increase between days 18 and 20 and declined on days 21 and 23. Thompson generally displayed diminished chlorophyll concentrations with the highest only being 125 RFU.
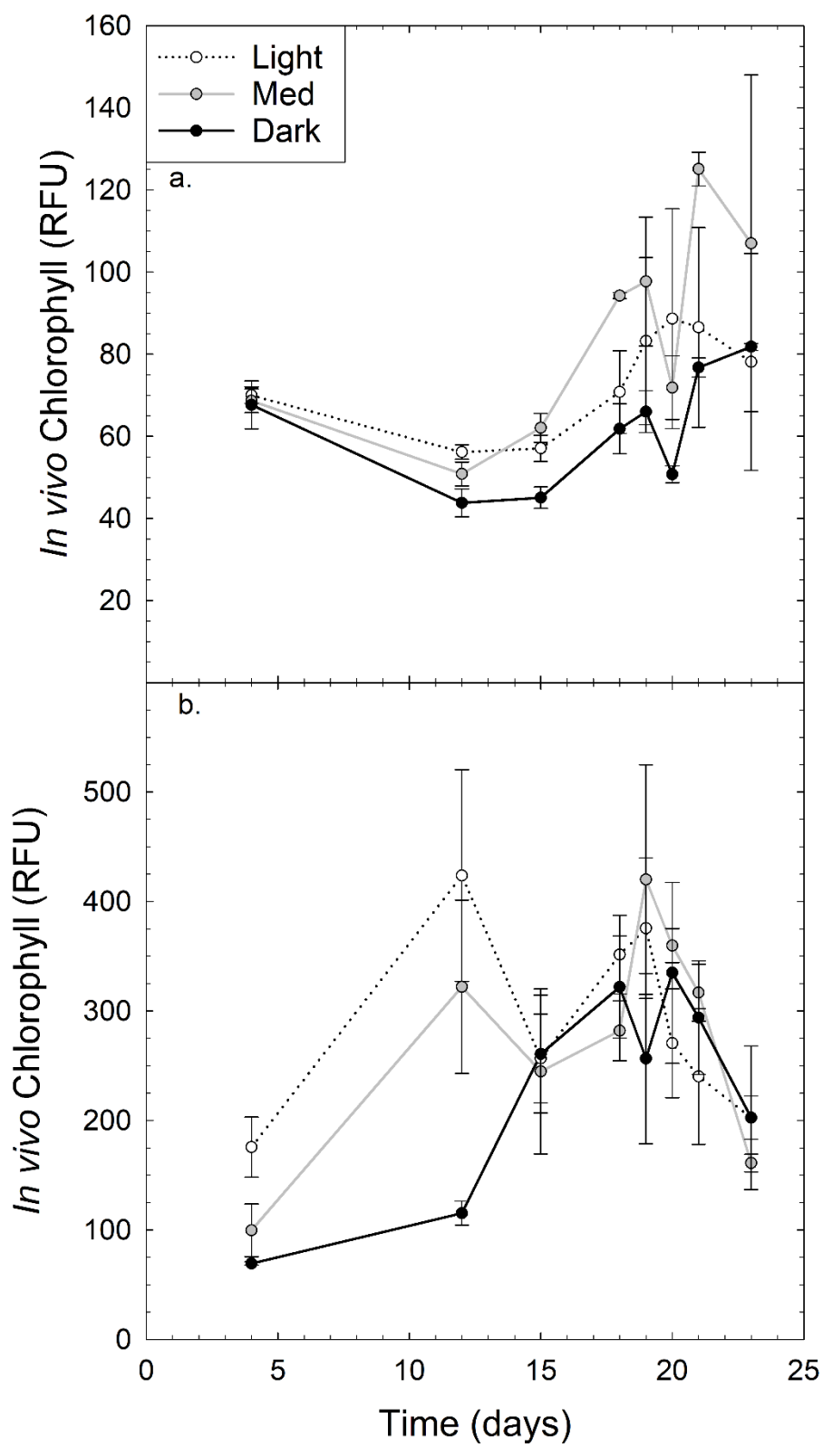
Figure 31: In vivo chlorophyll at (a) Thompson and (b) KOA.
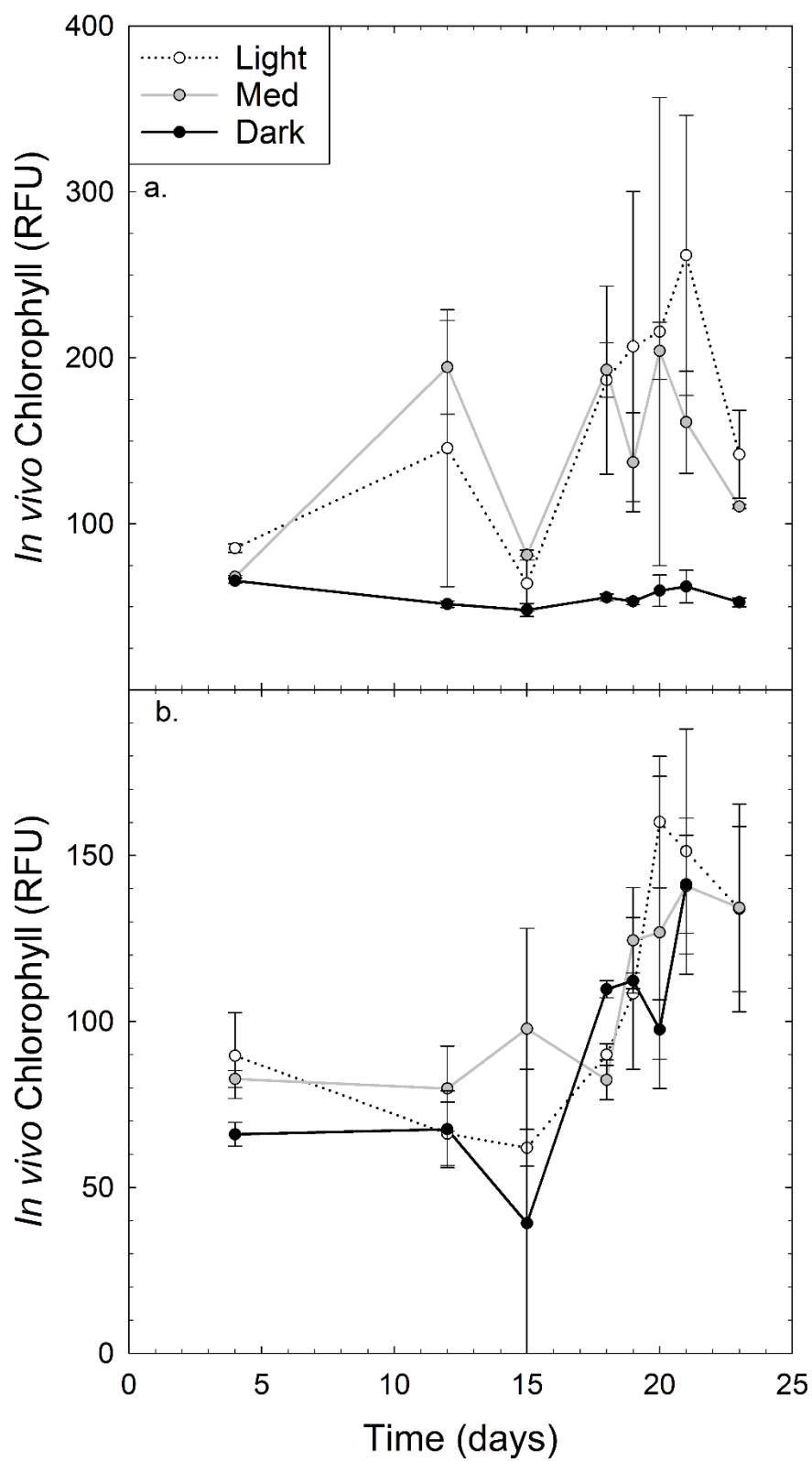
Figure 32: In vivo chlorophyll at (a) Slag Canyon and (b) Santa.

12. Appendix D: Lotic Plant Survey

12.1. Methods

The length of each site was determined. Then transects were established by using a random number generator to select five distances from the most upstream end of the sample site and pacing the randomly generated number of meters. Thompson and Slag Canyon were determined to be less than 12 meters long, and odd number transects between one and nine were used. A tape was then run perpendicular to stream flow two meters into each riparian zone. Within one-meter quadrants, macrophytes and colonial algae were visually identified, and relative percent abundance estimated (Fig. 33). Inverse Simpson Diversity Index (Eq. 1) was calculated for each site and each quadrant. Although zero cannot be calculated from Inverse Simpsons Diversity Index, and a quadrant that does not contain any plants does not have a biodiversity, if a quadrant had no plants, it was assigned a biodiversity of zero for graphical representation.

$$\textbf{Inverse Simpson Diversity Index}$$
$$\frac{1}{\lambda} = \frac{1}{\sum_{i=1}^{R} p_i^2} = \ ^2D \tag{3}$$

12.2. Results

The first and last two points of each transect represent the riparian zone. Each point received a nominal distance along the transect to keep the centers of the transects in line with each other. Generally, the highest biodiversity occurred in the riparian zones (Figs. 34,35,36,37). Thompson had a shallow creek with rapid flow, and low light, therefore, had many quadrants without any plants (Fig. 34). KOA had many plants and the highest biodiversity (Figs. 35,38). Slag Canyon had a rocky streambed and spikes in biodiversity corresponds with fine sediments

(Fig. 34). Santa had relatively homogeneous streamflow and streambed. Therefore, Santa had relatively homogeneous biodiversity (Fig. 37). Overall biodiversity for each site has a strong relationship with the amount of available light (Figs. 3,7).

Figure 33: KOA Transect 1 (a-q) quadrants 1-17. Photo credit: A. Cox
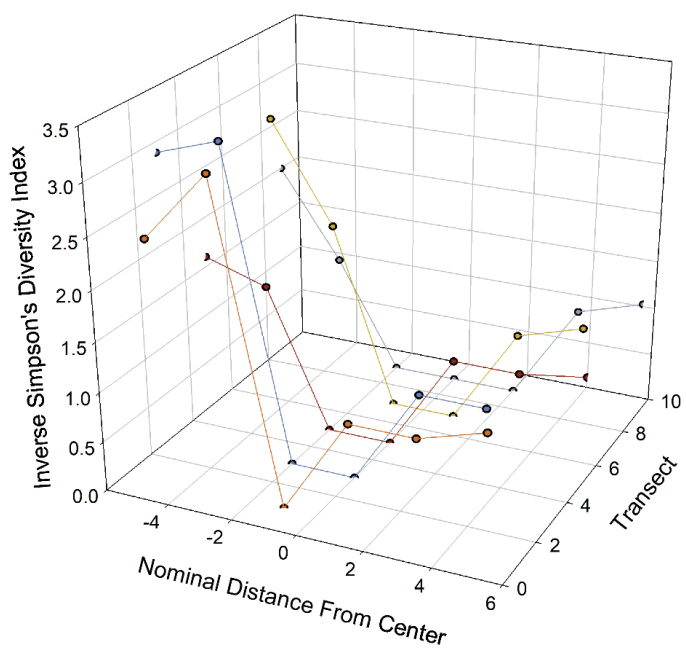
Figure 34: Biodiversity along stream flow at Thompson.
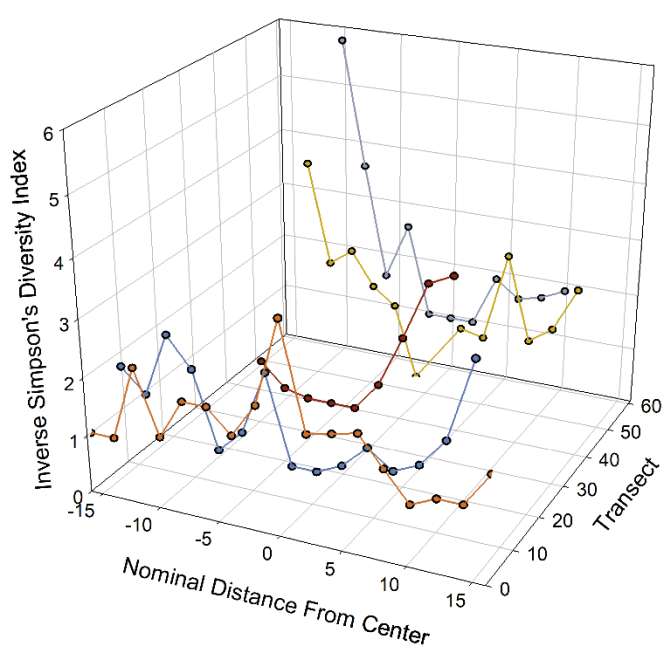
Figure 35: Biodiversity along stream flow at KOA.
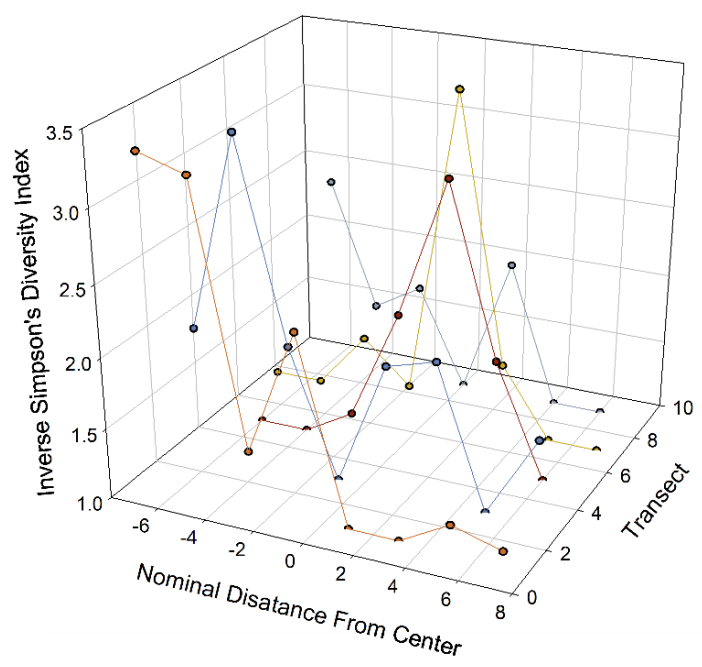
Figure 36: Biodiversity along stream flow at Slag Canyon.
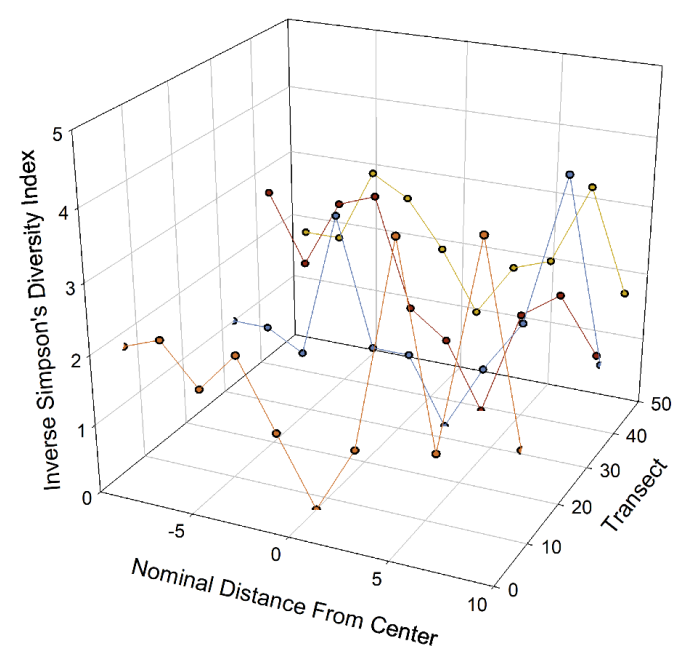
Figure 37: Biodiversity along stream flow at Santa.
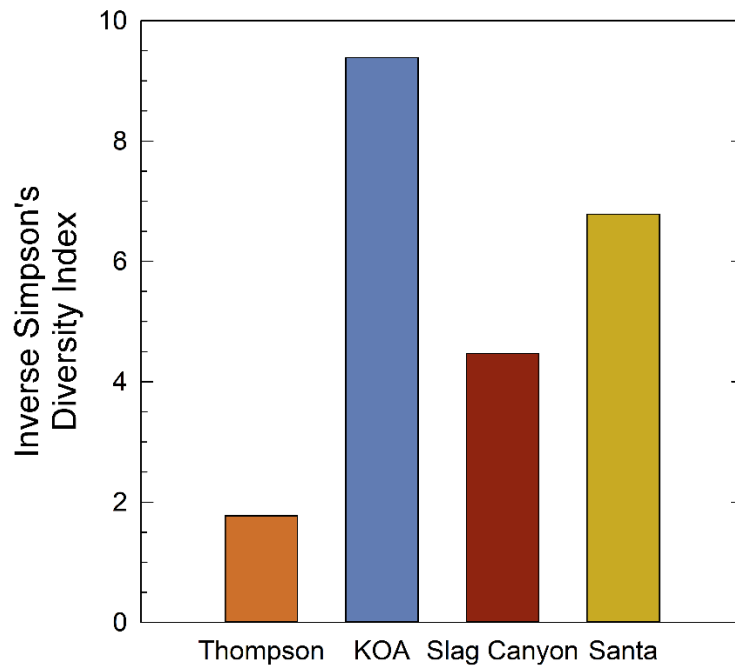
Figure 38: Biodiversity for each sample site.

Table V: Percent macrophyte coverage of each quadrant

Site	Transect	Quadrant	% Macrophyte Coverage	Site	Transect	Quadrant	% Macrophyte Coverage
Thompson	1	1	18	KOA	1	1	80
		2	22			2	70
		3	0			3	24
		4	30			4	16
		5	100			5	78
		6	100			6	31
	3	1	35			7	50
		2	13			8	25
		3	0			9	80
		4	0			10	30
		5	10			11	22
		6	50			12	10
		7	100			13	31
	5	1	65			14	82
		2	12			15	56
		3	0			16	66
		4	0			17	10
		5	10		4	1	30
		6	100			2	90
		7	100			3	34
	7	1	25			4	9
		2	30			5	30
		3	0			6	96
		4	0			7	36
		5	30			8	82
		6	100			9	100
	9	1	20			10	50
		2	31			11	100
		3	0			12	80
		4	0			13	100
		5	0			14	71
		6	100			15	55
		7	100				

Table V: Continued – Percent macrophyte coverage of each quadrant

Site	Transect	Quadrant	% Macrophyte Coverage	Site	Transect	Quadrant	% Macrophyte Coverage
KOA	24	1	100	Slag Canyon	1	1	14
		2	100			2	42
		3	6			3	6
		4	100			4	5
		5	93			5	3
		6	90			6	2
		7	91			7	43
		8	43			8	86
		9	65		3	1	28
		10	57			2	5
	55	1	99			3	5
		2	80			4	5
		3	80			5	5
		4	20			6	10
		5	45			7	72
		6	0			8	100
		7	21		5	1	100
		8	15			2	92
		9	44			3	11
		10	83			4	2
		11	44			5	3
		12	100			6	83
	60	1	100		7	1	100
		2	50			2	100
		3	20			3	51
		4	30			4	45
		5	2			5	23
		6	10			6	50
		7	15			7	100
		8	25			8	100
		9	65				
		10	88				
		11	100				

Table V: Continued – Percent macrophyte coverage of each quadrant

Site	Transect	Quadrant	% Macrophyte Coverage	Site	Transect	Quadrant	% Macrophyte Coverage
Slag Canyon	9	1	100			1	25
		2	100			2	35
		3	100			3	23
		4	50			4	15
		5	20		39	5	6
		6	50			6	4
		7	100			7	0
		1	43			8	27
		2	63			9	75
		3	95	Santa		10	86
		4	16			1	30
		5	1			2	41
	7	6	0			3	35
		7	5			4	52
		8	25		49	5	10
		9	97			6	0
		10	67			7	15
		11	100			8	41
Santa		1	81			9	95
		2	80			10	60
		3	100				
		4	50				
		5	55				
	33	6	10				
		7	0				
		8	1				
		9	15				
		10	40				
		11	61				

Table VI: List of identified plants in Blacktail and Silver Bow Creeks. In order of abundance.

Blacktail Creek		Silver Bow Creek	
Salix geyeriana		*Salix boohtii*	
Potamogeton zosteriformis	*Veronica anagallis-aquatica*	*Alopecurus aequalis*	*Carex nebrascensis*
Salix alba	*Lemna minor*	*Cornus sericea*	*Juncus balticus*
Elodea canadensis	*Epilobium ciliatum*	*Veronica anagallis-aquatica*	*Potamogeton zosteriformis*
Carex rostrata	*Callitriche palustris*	*Zannichellia palustris*	*Lomatium macrophylum*
Zannichellia palustris	*Callitriche hermaphroditica*	*Agrostis stolonifera*	*Artemisia tridentata*
Phalaris arundinacea	*Crisium vulgare*	*Salix ericephala var watsonii*	*Lepidium latifolium*
Agrostis stolonifera	*Rumex crispus*	*Stuckenia pectinata*	*Oenthera biensis*
Lepidium latifolium	*Linaria vulagres*	*Epilobium ciliatum*	*Potentilla anserina*
Salix boothii	*Melilotus officinalis*	*Ranunculus aquatilis*	*Eleocharis palustris*
Mentha arvensis	*Asarum caudatum*	*Agrostis cristatus*	*Erysimum capitatum*
Carex nabrascensis	*Alnus rubra*	*Carex utriculata*	*Ligusticum tenuifolium*
Potentilla anserina	*Rubus ideaus*	*Betula pendula*	*Lemna minor*
Alopecurus aequalis	*Glyceria borealis*	*Elodea canadensis*	*Tragopogon dubius*
Juncus balticus	*Lomatium macrophylum*	*Mentha arvensis*	*Trifolium pratense*
Eleocharis palustris	*Cynoglossum oficinale*	*Agropyron intermedium*	*Melilotus officinalis*
Geum macrophilum	*Taraxacum lyratum*	*Salix exigua*	*Phalaris arundinacea*
Equestium arvense	*Achillea millefolium*	*Achillea millefolium*	*Rumex crispus*
Agrostis cristatus	*Oenthera biensis*	*Crisium vulgare*	*Taraxacum lyratum*
Salix barchlayi	*Nitella acumulata*	*Linaria vulagres*	*Nasturtium officinale*
Centaurea jacea	*Rorippa aquatica*	*Centaurea jacea*	*Fontinalis sp.*

SIGNATURE PAGE

This is to certify that the thesis prepared by Isaiah James Robertson entitled "Limitations to Photosynthesis in Silver Bow and Blacktail Creeks" has been examined and approved for acceptance by the Department of Chemistry and Geochemistry, Montana Technological University, on this 8th day of July, 2019.

Alysia Cox, PhD, Assistant Professor
Department of Chemistry and Geochemistry
Chair, Examination Committee

Katie Hailer, PhD, Associate Professor and Department Head
Department of Chemistry and Geochemistry
Member, Examination Committee
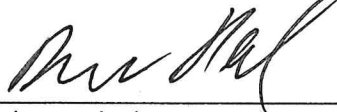
Robert Pal, PhD, Associate Professor and Director of Restoration
Department of Biology
Member, Examination Committee